Alma Mater Studiorum – Università di Bologna

DOTTORATO DI RICERCA IN

SCIENZE MEDICHE GENERALI E SCIENZE DEI SERVIZI

Ciclo XXXIII

Settore Concorsuale: 06/G1- PEDIATRIA GENERALE, SPECIALISTICA E NEUROPSICHIATRIA INFANTILE

Settore Scientifico disciplinare: MED/38 - PEDIATRIA GENERALE E SPECIALISTICA

EXPLORATION OF CARDIOVASCULAR AND CEREBRAL PHYSIOLOGY IN PRETERM INFANTS DURING THE TRANSITIONAL PERIOD WITH CONTINUOUS HAEMODYNAMIC MONITORING

Presentata da: Dott.ssa Silvia Martini

Coordinatore Dottorato	*Supervisore*
Prof. Fabio Piscaglia	Prof. Luigi Tommaso Corvaglia
	Co-supervisore
	Prof. Topun Austin

Per aspera ad astra

TABLE OF CONTENTS

ABSTRACT

The transition from intrauterine to extrauterine life represents a critical phase of physiological adaptation in preterm infants. The validation of comprehensive haemodynamic monitoring, aimed at the assessment of cardiovascular function and end-organ perfusion throughout this challenging phase, would not only improve knowledge of transitional physiology and pathophysiology following preterm birth, but would also support the development of an individualized approach to therapeutic management.

The aim of this research project was to add further knowledge to cardiovascular and cerebrovascular physiology in preterm infants during postnatal transition.

To achieve this aim, transitional haemodynamics were explored in preterm infants <32 weeks' gestation or with a birth weight <1500g using a non-invasive system of integrated multiparametric monitoring, which included electrical velocimetry, near-infrared spectroscopy, pulse oximetry and serial echocardiographic assessments.

Sixty-four preterm infants with a mean (standard deviation) gestational age of 29.6 (2.7) weeks were included in the research analysis. The results are divided into 3 sections:

1. In the first section, the time trends of cardiovascular and cerebrovascular haemodynamics during the transitional period were evaluated, demonstrating a progressive improvement in overall cardiovascular function and cerebrovascular reactivity. The presence of a haemodynamically significant patent ductus arteriosus (hsPDA) was associated with significantly different patterns of cardiac output (CO), stroke volume (SV), heart rate (HR), cardiac contractility and with a greater impairment of cerebral autoregulation. The association between cardiovascular and cerebrovascular parameters and a pool of antenatal, perinatal and postnatal factors was also evaluated, revealing characteristic haemodynamic profiles in relation to gestational age, antenatal Doppler status, ductal status during the transitional

period. In particular, more preterm infants showed significantly increased systemic vascular resistance (SVR) and HR, reduced SV and cardiac contractility, lower cerebral oxygenation and higher cerebral oxygen extraction. Infants with an abnormal umbilical Doppler had significantly higher SVR. Of these, those with antenatal brain sparing also showed an altered cerebral autoregulation, whereas a significant CO reduction was observed in the subgroup with no evidence of cerebral blood flow redistribution. The presence of a hsPDA significantly affected cerebral autoregulation and was also associated with significantly higher CO, SV, HR values, an enhanced cardiac contractility and decreased SVR.

2. In the second part, the relationship existing between CO and its two main determinants, HR and SV, was evaluated. The correlation between CO and HR was not perfectly linear and was significantly influenced by HR ranges, the ductal status and ongoing cardiovascular drugs. A strong relationship between SV and CO was also demonstrated, supporting the role for SV in CO determination even in preterm infants.

3. In the third part, the cardiovascular and cerebrovascular response to brief cardio-respiratory events, which are particularly common during the transitional period, was evaluated. The haemodynamic impact of these events on both cardiovascular and cerebral sides was modulated not only by the event characteristics – with events characterized by combined desaturation and bradycardia <80 bpm showing the greatest effects – but also by the individual neonatal features, namely gestational age, antenatal Doppler status and ductal status.

The results of this project demonstrate how multifaceted the transitional haemodynamic status is in such a heterogenic population as preterm infants and provide valuable hints in support of the development of an individualized haemodynamic management of preterm infants during this delicate phase of life.

LIST OF ABBREVIATIONS

ACA: anterior cerebral artery

AREDF: umbilical absent or reversed end-diastolic flow

BP: blood pressure

CBF: cerebral blood flow

cFTOE: cerebral fraction of tissue oxygen extraction

CO: cardiac output

CO_{ECHO}: cardiac output, measured by echocardiography

CO_{EV}: cardiac output, measured by electrical velocimetry

CPAP: continuous positive airway pressure

CPP: cerebral perfusion pressure

CRE: cardio-respiratory events

CrUSS: cranial ultrasounds

cTOI: cerebral tissue oxygenation index

CW: continuous wave

DA: ductus arteriosus

DAo: descending aorta

DB: combined desaturation and bradycardia

EV: electrical velocimetry

FO: foramen ovale

FTOE: fraction of tissue oxygen extraction

GA: gestational age

GEE: generalized estimating equation

GLMM: generalized linear mixed-effects model

HF: high frequency

HR: heart rate

HR_{EV}: heart rate, detected by electrical velocimetry

HR_{PO}: heart rate, detected by pulse oximeter

hsPDA: haemodynamically significant patent ductus arteriosus

IB: isolated bradycardia

ICON: index of cardiac contractility

ID: isolated desaturation

IUGR: intrauterine growth restriction

IVH: intraventricular haemorrhage

LA:Ao: left atrium to aortic root ratio

LF: low frequency

LVO: left ventricular output

LMM: linear mixed-effects model

MABP: mean arterial blood pressure

MCA: middle cerebral artery

MPE: mean percentage error

MRI: magnetic resonance imaging

NICU: neonatal intensive care unit

NIRS: near-infrared spectroscopy

PDA: patent ductus arteriosus

PFO: patent foramen ovale

PHI: parenchymal haemorrhagic infarction

PVL: periventricular leukomalacia

PVR: pulmonary vascular resistance

PW: pulsed-wave

RVO: right ventricular output

SpO_2: peripheral arterial oxygen saturation

SV: stroke volume

SVIA: self-ventilating in air

SVR: systemic vascular resistance

TOHRx: correlation index between cTOI and HR

TOI: tissue oxygenation index

1. INTRODUCTION

1.1.   Transitional haemodynamics of preterm infants

The transition from intrauterine to extrauterine life represents a critical phase of physiological adaptation which has an important impact on many organs and systems, most notably the cardiovascular system and the lungs. The functional and anatomical immaturity that characterizes premature infants poses a major challenge to their postnatal adaptation. As a result, the haemodynamic status of this population during the transitional phase is typically unstable, with clinically relevant implications. Knowledge of transitional physiology and pathophysiology following preterm birth is core to appropriate interpretation of the haemodynamic changes occurring during this period and to the establishment of optimal therapeutic management.

1.1.1.   Transition of the fetal circulation at birth

The development of an adequate placental circulation, providing a low-resistance vascular bed for efficient exchange of gases and nutrients between maternal and fetal blood, is vital for fetal development. During antenatal life, oxygenated blood enters the fetal circulation through the umbilical vein. Between 50-60% of this blood flow bypasses the hepatic circulation via the ductus venosus and enters the inferior vena cava, where it tends to stream separately from the desaturated systemic return of the lower portions of the body. At the junction between the inferior vena cava and the right atrium, a tissue flap known as the Eustachian valve directs this blood across the foramen ovale into the left atrium, from which it enters the left ventricle and is ejected into the ascending aorta. The majority of this blood is then delivered to the brain and coronary circulation, to ensure the delivery of better oxygenated blood to these vital structures. Desaturated blood from the superior vena cava, the coronary sinus and the inferior vena cava, which comprises the venous return from lower body and hepatic circulation, is collected in the right atrium and then directed into the right ventricle

across the tricuspid valve. This deoxygenated blood is then ejected into the pulmonary artery. However, due to the high pulmonary vascular resistance (PVR) that characterizes the antenatal period, only a small proportion of blood reaches the pulmonary circulation, while 80-90% of this flow is shunted across the ductus arteriosus (DA) into the descending aorta toward the lower half of the body, which is thus supplied with relatively desaturated blood. At the level of the iliac arteries, this deoxygenated blood enters the umbilical arteries and flows back to the low-resistance vascular bed of the placenta for gas and nutrient exchanges. The gradients of oxygen saturation in the fetal circulation gives a picture of the distribution and blending of flows: the highest saturation is found in the umbilical vein, whereas the lowest is observed in the abdominal tract of the inferior vena cava, before its connection with the ductus venous [1].

During pregnancy several pathological conditions may compromise placental circulation, with significant implications on fetal haemodynamics [2]. The placental trophoblast invasion, which begins around 10-12 weeks of gestational age, is responsible for the development of a low-resistance placental circulation. This process is regulated by several biochemical modulators, among which blood oxygen, growth factors, cytokines, and other angiogenic substances [3]. Poor trophoblast invasion or maternal ischaemia increases placental impedance and is associated with a hypoxia-driven cardiovascular fetal adaptation to ensure an adequate oxygen delivery to vital organs, such as the brain. This adaptation, which is characterized by an increase in systemic vascular resistance (SVR) in splanchnic and peripheral vascular beds and by vasodilatation of cerebral vessels [4], results in a raised ventricular afterload, which is also exacerbated by abnormal retrograde diastolic flow in the aortic isthmus secondary to cerebral vasodilatation, with potential failure of coronary perfusion and ensuing myocardial damage [5]. Moreover, the decreased fetal perfusion ensuing from the altered placental circulation and the blood flow redistribution towards the brain further worsen the low blood oxygenation of splanchnic fetal organs, which are thus more prone to hypoxic-ischemic complications after birth [6].

At delivery, clamping the umbilical cord triggers a cascade of major cardiovascular changes that occur within seconds to hours. Disconnection from the low-resistance placental bed results in an instantaneous increase in SVR, whereas the onset of ventilation is followed by a rapid fall in PVR, which drastically increases pulmonary blood flow. Due to the subsequent increase in pulmonary venous return, the left atrial pressure rises rapidly and leads to the functional closure of the septal layers of the foramen ovale [7]. At the same time the shunt across the DA shifts from predominantly right-to-left to predominantly left-to-right; in term neonates, this usually occurs within 10 min after birth, as a consequence of the rapid PVR drop [8]. The increase in arterial oxygen saturation from 60-70% at 1 minute to above 90% within 10 minutes after birth reflects the effective establishment of pulmonary gas exchange resulting from these physiological changes [9]. While the ductus venosus can remain patent for several days with no circulatory consequences [10], the DA usually undergoes a functional closure by 48-72 hours of life in the majority of healthy term neonates [11]. This event cascade is illustrated in Figure 1.1.
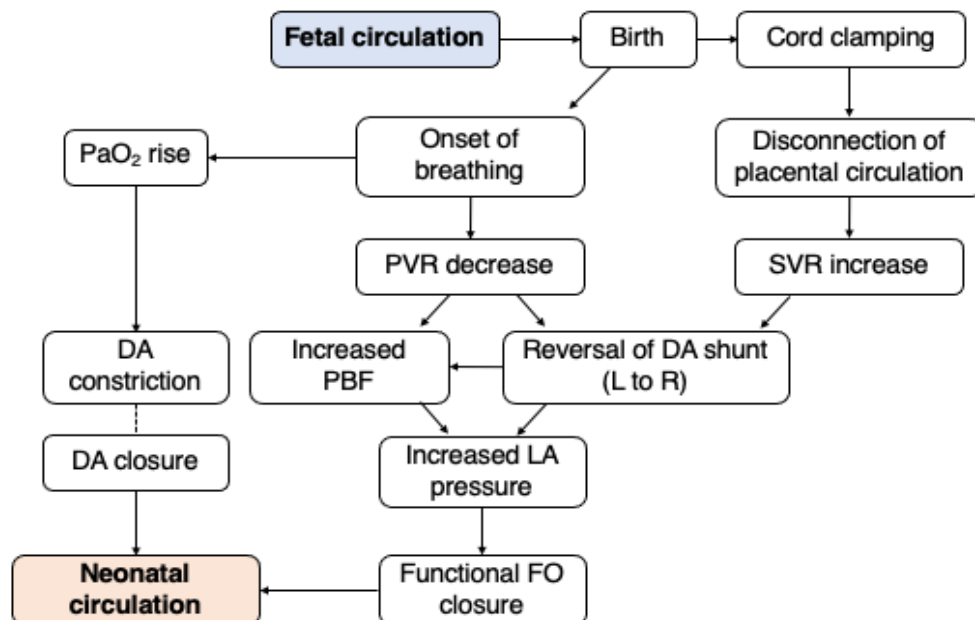
Figure 1.1. Cascade of events during transition from a fetal to a neonatal circulation. Abbreviations: DA, ductus arteriosus; FO, foramen ovale; LA, left atrium; PaO2, arterial O_2 pressure; PBF, pulmonary blood flow; PVR, pulmonary vascular resistance.

The closure of the fetal shunts completes the transition from a parallel into a serial circulation (Figure 1.2). For the above reasons, the first 72 hours of life are commonly defined as the transitional period.
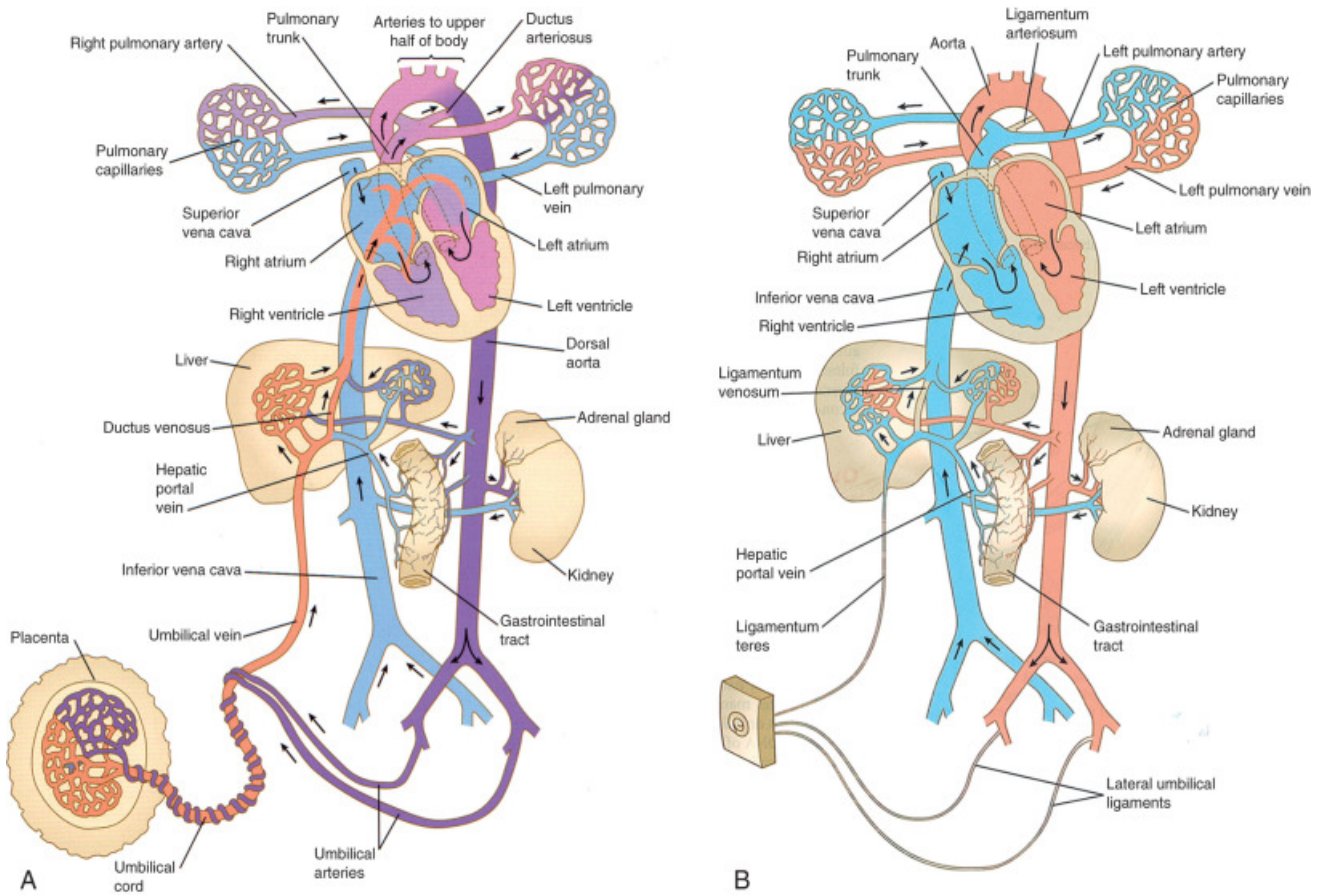
Figure 1.2. *Blood flow circulation before (A) and after birth (B). The paths of oxygenated blood are shown in orange. Antenatal circulation is a parallel circuit, whereas postnatal circulation is a serial circuit. Adapted from Dees and Baldwin, Avery's Diseases of the Newborn: Tenth Edition (2018) [12].*

1.1.2. Cardiovascular adaptation in the transitional period

The heterogeneity of the preterm population in terms of gestational and postnatal ages results in different levels of maturation of the cardiovascular system, with different degrees of functional impairment of preload, diastolic filling, intra-cardiac flow patterns, contractility and afterload [5,13].

The ability of the cardiac muscle fibers to change their force of contraction in response to changes in the volume of venous return is defined as preload. According to the Frank-Starling mechanism (Figure 1.3), as preload increases, sarcomeres stretch and the number of formed actin–myosin bridges augments, thus enhancing cardiac contractile force [5].
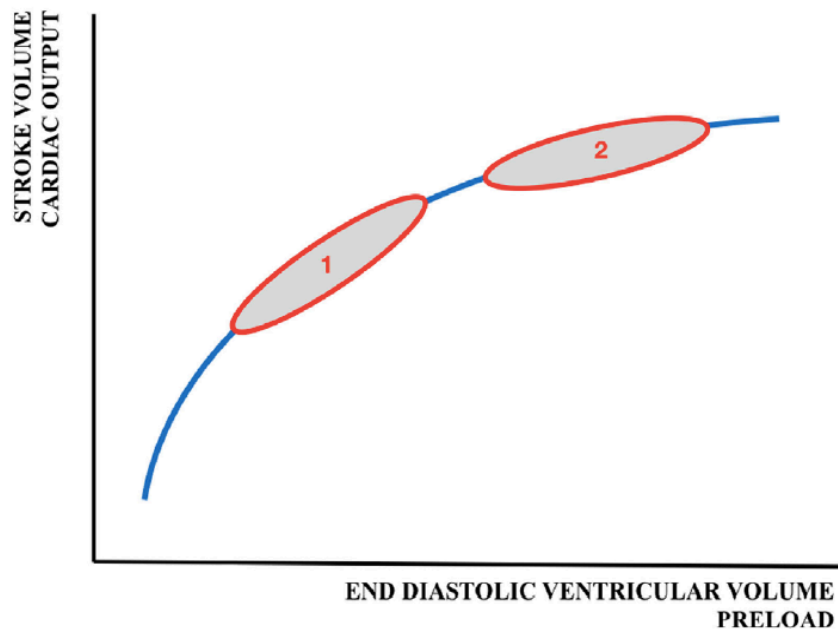
Figure 1.3. *Representation of Frank-Starling curve according to the adult (1) and the neonatal cardiac function (2). Adapted from Vrancken et al. Frontiers in Pediatrics (2018)* [13]

A reduction in preload, resulting from a decreased blood volume from acute blood loss, or extensive insensible water loss or capillary leak associated with sepsis, will result in ventricular dysfunction. However, as shown in Figure 1.3, the functional curve of the Frank-Starling mechanism is different in neonates, with similar changes in preload resulting in a smaller increase in cardiac output compared

to older children and adults. As a result, excessive fluid administration will shift neonatal cardiac function towards the flat part of the curve resulting in impaired ventricular function [13].

Volume changes in response to a change in pressure define compliance. Cardiac compliance depends on the structural properties of the cardiac muscle, with particular reference to connectin, a protein that links the *z*-disk region of the thin filament to the myosin thick filament. Early studies suggested that fetal cardiac compliance is poor and undergoes a developmental increase during gestation [14]. More recently, however, it has been shown that, due to the presence of specific fetal connectin isoforms with high elastic properties that contribute to reduce myocardial stiffness and passive tension, suggesting the fetal heart actually has a higher compliance compared to the adult heart [15].

Ventricular filling is characterized by an early passive phase followed by an active phase, secondary to atrial contraction. Due to its enhanced elastic properties, however, the force that the fetal connectin isoform generates when restoring its resting length after systolic contraction or diastolic distention is decreased [16]. This, in turn, may alter the rotational patterns of intracardiac flow [17], resulting in lower passive filling when the ventricle untwists. As a consequence, neonatal ventricular filling is more dependent on atrial contraction [5,18].

Cardiac contractility is defined by the ability of sarcomeres to change their contractile force. Intracellular calcium is a principal determinant of cardiac contractility; when calcium levels increase, some bind to troponin and alter its shape, allowing the formation of actin–myosin cross-bridges that lead to cardiac contraction, whereas the removal of calcium from troponin restores the tropomyosin blocking action, with subsequent muscle relaxation [19]. The sympathetic autonomic nervous system and catecholamines also play a relevant role on cardiac contractility by regulating the calcium influx within the cardiac myocyte [20].

Due to structural and functional immaturity of the preterm myocardium, which is characterized by a relatively low number of myofibrils with a simplified internal organization, immaturity of the sarcoplasmatic reticulum and T tubules resulting in altered calcium release, lower troponin C levels

and higher troponin T levels, the cardiac contractile function of premature neonates is often reduced [13,14]. Nevertheless, a significant improvement in cardiac contractility has been observed in very-low-birth-weight infants from day 1 to 5 after birth [21], suggesting the occurrence of adaptive mechanisms, such as a progressive improvement of the intracellular calcium influx in the early postnatal period [13].

The ability of the heart to increase its contractile function with increasing heart rates is defined as the Bowditch effect [5]. However, in in-vitro experiments, it has been shown that the force-frequency relationship in the newborn human ventricle is flat and tends to increase with age, possibly because of developmental changes in calcium handling (Figure 1.4) [22]. Furthermore, the sympathetic innervation and the number of β-adrenergic receptors in the immature myocardium are decreased [23]; as a consequence, administration of inotropes has been shown to result in smaller increases of myocardial contractility in a neonatal animal model, compared to adult controls [24].
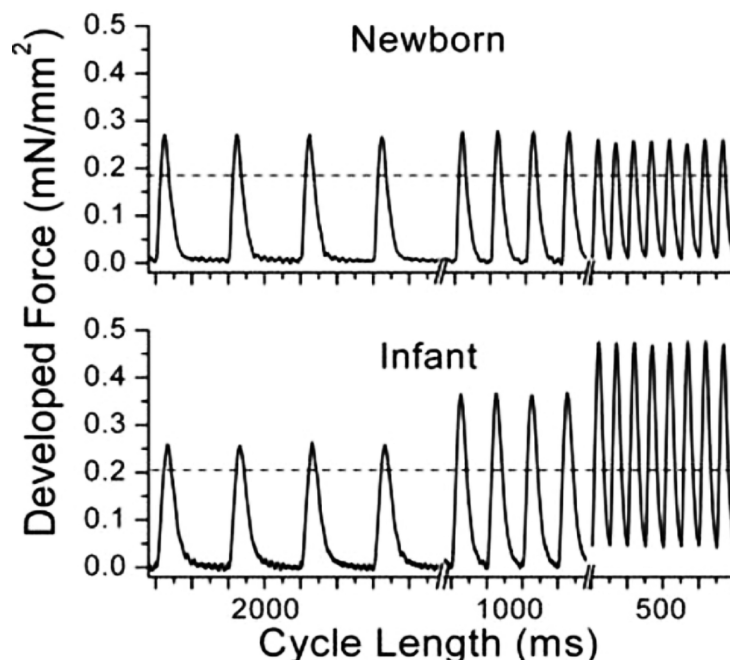

Figure 1.4. Force developed from a newborn and an infant at different cycle lengths, indicating different heart rates. Adapted from Wiegerinck et al. Pediatric Research (2009) [22]

While it had long been assumed that neonates can only increase their cardiac output by increasing their heart rate, with stroke volume remaining relatively fixed [13], more recent evidence has indicated that, in preterm infants, cardiac output changes mainly result from stroke volume changes rather than heart rate increases [25,26]. The preterm circulation is characterized by high resting heart rates, which subsequently reduce the time available for the end-diastolic ventricular filling and may further exacerbate the consequences of the intrinsic diastolic dysfunction previously described. Moreover, the chronotropic effects of the vasopressor-inotropes that are commonly used to support the cardiovascular function in this population may contribute further to shorten the diastolic ventricular filling [20], with potential therapeutic implications.

Afterload is defined as the force against which the heart must work to pump the stroke volume and depends upon ventricular dimensions, SVR, blood pressure (BP) and vascular compliance [5]. Ventricular wall stress and afterload are intrinsically related: with increasing afterload, the ventricular wall stress increases and the velocity of circumferential fiber shortening decreases, resulting in a reduced stroke volume [13]. Echocardiographic data have shown an age-dependent relationship between circumferential fiber shortening and end-systolic wall stress, suggesting that the performance of the neonatal myocardium is more sensitive to afterload [27].

The complex interactions existing between BP, SVR, cardiac output and end-target organ blood flow in the preterm population and their regulating factors are summarized in Figure 1.5. In premature infants, a high resting α-adrenergic tone in the peripheral vasculature maintains the constriction of the capacitance arterioles in many vascular beds, leading to increased SVR [5]. Echocardiographic studies in preterm neonates have shown that the immature myocardium not only has reduced contractility, but also a poor tolerance to high SVR that contributes to increased afterload [21,28]. Among the factors that contribute to further increase afterload in this population are ductal ligation, or the presence of conditions characterized by low cardiac output and increased SVR, such as cold shock. On the other hand, low afterload results from reduced SVR, as in warm shock [13]. Given the

15

substantial difference in the pathophysiological mechanisms of shock presentation, an adequate diagnosis is fundamental in order to undertake the appropriate therapeutic approach (i.e., inotropes versus vasopressors) [29,30].

When OBF regulation exhausted:
1. ↑ capillary recruitment
2. ↑ O_2 extraction

Vital organ blood flow distribution (brain, heart, adrenals)

Systemic Blood Pressure
Dependent Variable

$BP - CVP = CO \times SVR$

Resistance affected by:
1. Autonomic, endocrine, paracrine, autocrine regulators of vascular function
2. GA, PNA, shunts, vascular anatomy
3. pH, $PaCO_2$, PaO_2, electrolytes (Ca^{++})
4. Pathology: cytokines, chemokines

O_2 Delivery to Meet O_2 Demand

Systemic Flow
Independent variable*
(Inotropes)

Systemic Vascular Resistance
Independent Variable
(Vasopressors, Lusitropes)

Systemic blood flow affected by:
1. Autonomic, endocrine, paracrine, autocrine regulators of cardiac function
2. GA, PNA, shunts (PDA, PFO)
3. pH, $PaCO_2$, PaO_2, electrolytes (Ca^{++})
4. Pathology: cytokines, chemokines

Non-vital organ blood flow distribution

Figure 1.5. Modulatory interactions between blood flow, systemic vascular resistance and blood pressure and related influencing factors. Abbreviations: BP, blood pressure; CO, cardiac output; CVP, central venous pressure; GA, gestational age; OBF, organ blood flow; PFO, patent foramen ovale; PNA, postnatal age; PDA, patent ductus arteriosus. Adapted from Noori et al. Neonatology questions and controversies: haemodynamics and cardiology (2012) [31].

The postnatal persistence of the fetal shunt pathways also provides a significant challenge to transitional cardiovascular physiology. The persistence of patent ductus arteriosus (PDA) will be addressed in detail in section 1.1.3. Unlike in term infants, transitional circulation of preterm infants is characterized by the exposure to a unrestrictive PDA in most of the cases [32]. In the vast majority of preterm neonates, PVR drops below systemic levels within a few hours after birth and, as a consequence, the shunting direction of transductal blood reverses to left to right [7]. This causes

significant pulmonary overflow at the expenses of systemic perfusion. The foramen ovale tends to remain patent in many premature infants; in the absence of a PDA, the haemodynamic consequences of this are trivial. However, the large amount of blood returning to the left atrium due to the pulmonary overcirculation caused by the ductal patency may reverse the direction of shunting via the foramen ovale, thus further worsening pulmonary hyperperfusion and low systemic blood flow.

Finally, it should be taken into account that the heart and the lungs are intrinsically connected by complex dynamic physiological interactions. Due to their immaturity, preterm infants have weak thoracic musculature with a high thoracic compliance, while lung compliance is poor and the respiratory drive insufficient. For these reasons, positive pressure ventilation is often needed in the early postnatal phases. While positive pressure ventilation is obviously beneficial to improve alveolar gas exchanges and to reduce the work of breathing, the use of high tidal volumes, peak and end-expiratory pressures can alter the neonatal haemodynamics in several ways [33]. An increased airway pressure decreases the transmural pressure gradient of the alveolar/capillary interface, thus contributing to squeeze blood out of the intra-alveolar capillaries [13]; the ensuing PVR increase results in a reduction of pulmonary perfusion and venous return, decreasing systemic cardiac output. If increased PVR persists, a reversion of the transductal shunt to right-to-left may occur. Furthermore, the reduction in cardiac output observed in association with increased airway pressure can also be ascribed to a direct compressive effect on left ventricular filling [13]. At an end-target organ level, inappropriate ventilation strategies might also affect cerebral blood flow according with several mechanisms. High positive end-expiratory pressures can significantly reduce superior vena cava blood flow, which represents the blood return from the head, neck and upper limbs; moreover, the use of high tidal volumes during the transitional period, when cerebral autoregulation is often impaired, may cause detrimental fluctuations in cerebral blood flow, thus increasing the risk of short- and long-term neurodevelopmental sequelae.

1.1.3. Patent ductus arteriosus: the protagonist of transitional pathophysiology

The role of the DA during postnatal circulatory transition has been object of much research and discussion especially because of its known association with specific prematurity-related complications.

Postnatal DA closure is regulated by the exposure to oxygen and vasodilators. Oxygen induces the release of the potent vasoconstrictor endothelin-1 at the ductal level, whereas vasodilators substances such as prostaglandin E_2, prostacyclin and nitric oxide contribute to DA patency [34]. The immature DA is characterized by a thinner muscular wall compared to the term ductus, with smooth muscle cells that are less sensitive to oxygen-related vasoconstriction and more sensitive to the prostaglandin E_2 and prostacyclin-related vasodilative effects. The increased circulating levels of systemic inflammatory mediators and prostaglandins that are observed in the preterm population further contribute to the failure of spontaneous DA closure in this population [35]. Moreover, it has been observed that platelets are recruited into the DA lumen during closure, probably promoting a thrombotic sealing of the constricted DA [34]. Hence, thrombocytopenia [36], or an impaired platelet function [37] may also play a role in the persistence of the DA.

It has been largely established that PDA prevalence increases with decreasing gestational age (GA). Even when spontaneous closure is achieved, however, it may take up to several days to occur: in a large retrospective study on preterm infants who did not receive active medical or surgical treatment for PDA closure, the median closing time ranged from 6 days in infants ≥30 weeks of gestation to 71 days in those <26 weeks [38]. This observation suggests that, in the absence of targeted interventions, a significant proportion of extremely preterm neonates may be exposed to a prolonged transductal shunting with potential pathophysiological implications [32].

The shunt volume and direction across the PDA strictly depends on PVR, and so do the ensuing haemodynamic effects (Figure 1.6).
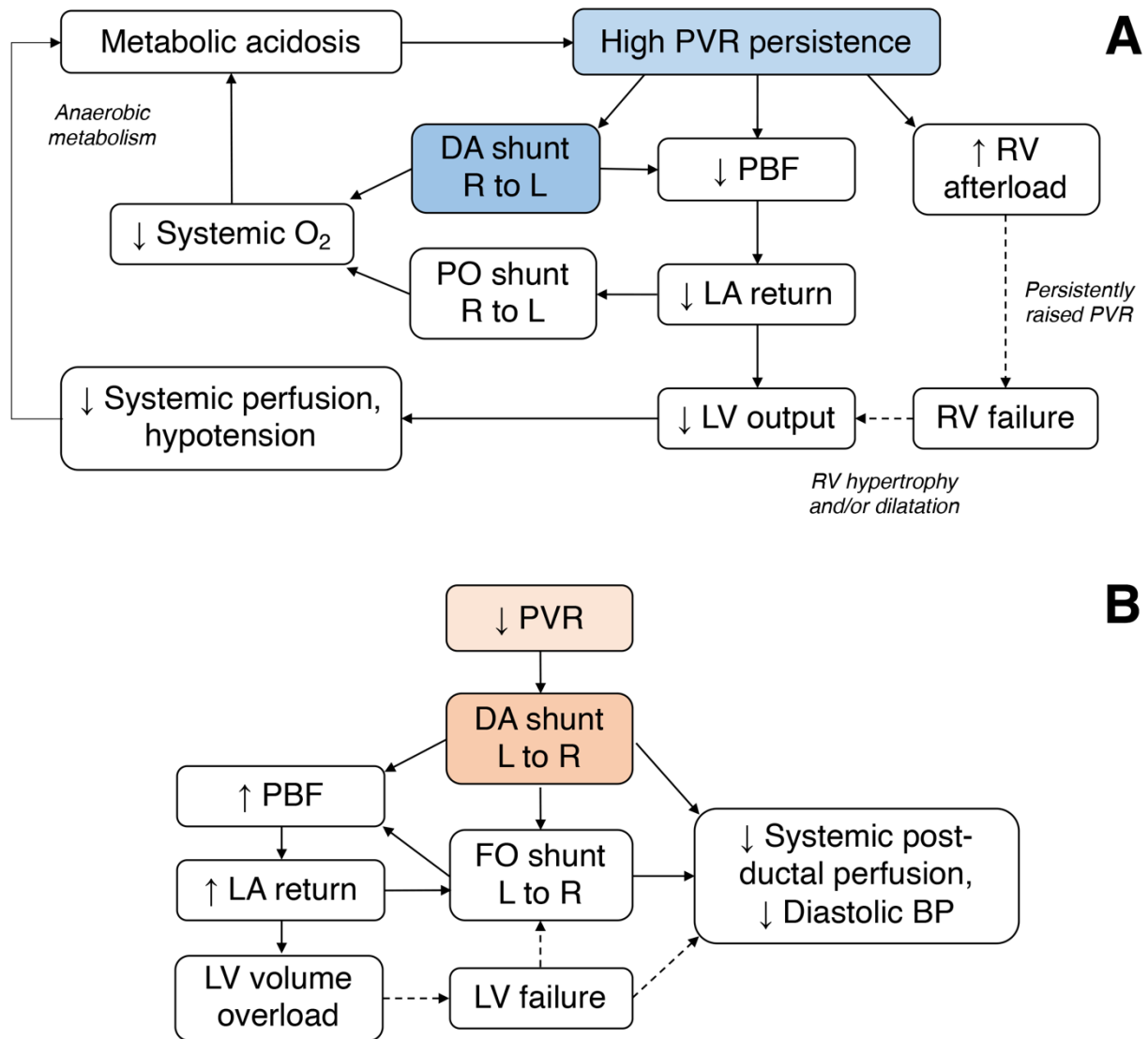
Figure 1.6. *Event cascade associated with different directions of transductal shunt (scenario A and B), depending upon pulmonary vascular resistance (PVR). Abbreviations: BP; blood pressure; DA, ductus arteriosus, LV, left ventricle; L, left; PBF, pulmonary blood flow; R, right; RV, right ventricle.*

In preterm infants, the decrease in PVR may be slower than in term infants, due to the immaturity of the lung parenchyma, respiratory distress and metabolic acidosis frequently seen in the early postnatal phase (Figure 1.6 A). The persistence of high PVR prolongs the right-to-left or bidirectional shunting across the PDA, with subsequent reduction of pulmonary perfusion, low oxygen saturation levels and increased need for supplemental oxygen and invasive respiratory support. If pulmonary blood flow

decreases, the venous return to the left atrium is also decreased, and so are the left ventricle preload and cardiac output, leading to decreased perfusion and oxygenation in end-target organs. As a consequence, a raise in lactate and acidosis, which contribute to increasing PVR, may occur, feeding a detrimental vicious cycle that eventually leads to the development of persistent pulmonary hypertension [39]. Persistently elevated PVR increase the afterload of the right ventricle, which gradually becomes hypertrophic and/or dilated. The resulting bowing of the interventricular septum toward the left ventricle further compromises left ventricular output, leading to biventricular dysfunction. Systemic hypotension requiring cardiovascular support often coexists during these phases.

Conversely, if PVR gradually decreases during the transitional period (Figure 1.6 B), a left-to-right shunt across the PDA may become haemodynamically significant. Pulmonary hyperperfusion, increases pulmonary venous return with volume overload of the left ventricle and systemic hypoperfusion below the ductal level. The increased venous return to the left atrium may raise the left atrial pressure and reverse the direction of shunting through the foramen ovale, thus further worsening pulmonary hyperperfusion and low systemic blood flow. Moreover, due to the diastolic dysfunction that characterizes the preterm myocardium, which has been previously discussed [5], the left ventricle may struggle to adapt to the increased stroke volume, eventually progressing to left ventricular failure in case of wide or prolonged left-to-right transductal shunting.

Hence, the signs and symptoms of PDA depend not only upon the characteristics, the magnitude and the duration of the transductal shunt, but also on the individual adaptive ability of the immature myocardium as well as additional concomitant factors (e.g., fluid intakes, metabolic and ventilatory status).

Persistence of the PDA in preterm neonates has been reported to be associated with increased mortality and several major complications [40–44]; among these, the most relevant that typically occur during the transitional period are intraventricular haemorrhage (IVH) and pulmonary

haemorrhage . Currently available physiological studies, conducted with sequential echocardiography investigations, have provided invaluable insights to better understand the causality and the mechanisms through which the PDA may contribute to these complications [43–47].

A strong association between low superior vena cava flow, considered as a proxy for cerebral blood flow (CBF), during the early hours after preterm birth and subsequent development or progress to higher grade IVH has been reported by Kluckow and Evans [46]. The prevalence of a haemodynamically significant PDA (hsPDA) was significantly higher in infants with this low-flow state. Another prospective physiological study reported lower cardiac output, ventricular function and CBF during the first 12 hours of age in extreme preterm neonates who later developed high-grade IVH [47]. These observations are consistent with the recognized ischaemia–reperfusion theory for the occurrence of IVH and suggest a link with the left-to-right shunt across the DA.

Deshpande et al. [32] have proposed two potential pathophysiological models in which the interaction between the immature preterm myocardium and the exposure to an unrestrictive transductal shunt during postnatal transition are important aetiological contributors to the development of both pulmonary haemorrhage and IVH in preterm neonates with a PDA. In particular, the delayed adaptation of the myocardial function to the volume overload resulting from transductal left-to-right may increase left atrial pressure and pulmonary venous hypertension, placing the infant at risk of pulmonary haemorrhage. The temporal association between this functional disturbance and the typical timing of pulmonary haemorrhage onset (usually at 48 hours after birth) is noteworthy [43]. On the other hand, the myocardial adaptation to the loading changes, which usually occurs within the first 48 hours of life, may result in a sudden increase of CBF, triggering the reperfusion phase of ischaemia-reperfusion predisposing to IVH [47]. The ischaemia-reperfusion theory may be an oversimplification of a complex set of events which challenge the idea of a simple causative relationship between these haemodynamic changes and clinical outcome [32]. As an example, the extent of the transductal shunt may itself be high enough to supersede the autoregulatory capacity of

CBF, and sicker infants may exhibit more prolonged periods of impaired cerebral autoregulation, thus increasing their risk of IVH development in the presence of predisposing conditions [48].

On the above basis, a thorough and integrated clinical and echocardiographic assessment in preterm neonates presenting with a PDA is essential, and the subsequent haemodynamic management should be adapted according to the underlying cardiovascular physiology and the clinical context of each individual patient, with the ultimate goal of preventing unfavourable outcomes and of defining the optimal treatment strategy for PDA closure and/or cardiovascular support [49].

1.2. Cerebral autoregulation

Given the multiple haemodynamic, metabolic and neurogenic factors that influence CBF and the high metabolic demands of the brain tissue, the regulation of cerebral perfusion is of fundamental importance to prevent hypoxic-ischemic brain injury. However, the anatomical and physiological immaturity of the cerebral vasculature that characterizes preterm infants results in incomplete and underdeveloped mechanisms of cerebral autoregulation which, together with the haemodynamic instability often observed during the transition from a fetal to a neonatal circulation, puts this population at high risk of developing noxious CBF fluctuations. The present section will address in detail the several mechanisms involved in the regulation of CBF in infants and neonates, along with the methods currently available for the assessment of cerebral autoregulation. An overview on the characteristics of cerebral autoregulation in preterm infants and its association with the development of neonatal brain injury will be reviewed.

1.2.1. Regulation of cerebral blood flow in infants and neonates

Cerebral blood flow is regulated by several integrated metabolic, biochemical, autonomic and myogenic factors [50]. The main physiological mechanisms that contribute to the regulation of CBF should therefore be taken into consideration when assessing cerebral haemodynamics of preterm infants; these mechanisms are described below.

- *Partial arterial pressure of oxygen (PaO$_2$) and carbon dioxide (PaCO$_2$):* both low PaO$_2$ (hypoxia) and high PaCO$_2$ (hypercapnia) exert a vasodilatory effect on cerebral circulation, leading to an increase in CBF, whereas hypocapnia leads to cerebral vasoconstriction. The mechanisms through which CBF reactivity to PaCO$_2$ is achieved involve H+/K+ homeostasis: the hypercapnia-induced increase in H+ concentration of the perivascular space increases K+ outflow from smooth muscles cells of cerebral arteries and arterioles, leading to their relaxation and subsequent vasodilatation, whereas the hypocapnia-induced decrease in H+

concentration leads to vasoconstriction [51]. The molecular mechanisms underlying O_2-mediated CBF regulation include the nitric oxide pathways and thus require an intact endothelium for its production. By increasing H+ concentration, the tissue lactic acidosis induced by hypoxia can also provide a link between CO_2- and O_2-mediated regulation of CBF. There is evidence that CBF reactivity to $PaCO_2$ and PaO_2 changes is present in preterm neonates: at 34 weeks of gestation, CBF reactivity to 1 kPa of CO_2 is between 10 and 100% with an average of 60%, while the administration of 100% O_2 reduces CBF by approximately 15% [52]. Of interest, it has been observed that the CBF response to increased CO_2 might be absent under certain circumstances, such as in preterm infants who subsequently developed intracranial haemorrhage [53,54], whereas those with normal cerebral ultrasounds showed a gradual increase of $PaCO_2$-CBF reactivity over the first 48 hours of life [53]. Under normal conditions, there is a functional interaction between the reactivity of CBF to $PaCO_2$ and blood pressure: the vasoconstriction occurring with hypocapnia enables the autoregulatory plateau to extend towards higher pressures whereas, conversely, hypercapnia shortens the plateau and increases the slope of the autoregulatory curve. However, $PaCO_2$-CBF reactivity seems to be more robust compared to pressure-flow reactivity: after severe birth asphyxia the first may be preserved while the latter is lost [55].

- *Neurovascular coupling:* this regulatory mechanism links neuronal activity to subsequent changes in CBF. This occurs through a neuronal glutamate signalling pathway upon neuronal activation, with the release of vasoactive substances, such as prostaglandins, nitric oxide and adenosine, from both neurons and the astrocyte glial cells that lead to the relaxation of vascular smooth muscle. This is also known as functional hyperaemia [56]. Although it has long been assumed this regulatory mechanism was associated only with vasodilatory effects, a more complex balance of vasodilation and vasoconstriction, driven by chemical mediators that control CBF in a direct way, has emerged from recent studies [57]. In addition, a role for the pericytes that surround neurons in the local regulation of CBF has also been described

[58]. To date, there is some evidence on CBF fluctuations in response to seizures in the neonatal population [59,60], reporting a significant increase in CBF; however, from an electrical perspective, seizures represent an extreme event and may well result in disturbances of physiological neurovascular coupling. Data on spontaneous neural activity and related changes in cerebral haemodynamics, especially in the preterm population, are few and mainly aimed at exploring new methodologies for neurovascular coupling investigation [57,61].

- *Metabolic coupling:* glucose is the major brain substrate of the neonate, although alternative metabolites may in part support cerebral metabolism. In newborn infants, CBF appears to be actively coupled to the cerebral fuel demands: it has been previously shown that, in preterm infants, the occurrence of hypoglycaemia within 2 hours after birth was found to be associated with a 2.5 fold increase in CBF, as a result of cerebral vasodilation in response to decreased substrate availability [62]. Following the restoration of adequate blood glucose levels, CBF gradually decreased, reaching a steady state after approximately 3 minutes after the end of glucose infusion [63]. Individual reductions in cerebral blood volume were inversely related to the pre-treatment concentration of glucose, while no relation was observed between changes in CBF, mean arterial blood pressure (MABP) and blood gases, suggest the existence of a cerebral glucose sensor that may induce capillary recruitment to maintain the glucose transport to the neural tissue under hypoglycaemic conditions. The evidence of increased plasma epinephrine values during the hypoglycaemic episodes supports the role of the sympathetic nervous system in the observed cerebral hyperperfusion, consistent with evidence from animal studies [64], but a possible effect of vasoactive aminoacids released during hypoglycaemia has also been proposed [65].

- *Autonomic nervous system:* due to its abundance in α1-adrenergic receptors, the cerebral vasculature is a target of the autonomic control. The autonomic system may also influence cerebrovascular responses by counterbalancing release of nitric oxide and catecholamines in response to sympathetic and parasympathetic stimulation [66,67]. By activating α- and β-

receptors, catecholamines modulate the arterial tone. The sympathetic activation shifts the autoregulatory plateau toward higher pressures, thereby protecting the brain against BP increases [68]. In an animal model, the ablation of relevant sympathetic ganglia was associated with a left-shift of the upper limit of the autoregulation range, with subsequent poor adaptation to increased BP [69]. The autonomic regulation of cerebral vasculature is intrinsically integrated with other regulating mechanisms of CBF. As an example, evidence from a neonatal animal model has demonstrated an interaction between the effect of sympathetic activation and $PaCO_2$ reactivity, with sympathetic activation reducing blood flow to specific brain regions during hyperaemic conditions, such as hypercapnia [70]. A role for the sympathetic system has also been proposed for the CBF changes in response to the fluctuations in blood glucose levels described above [62]. Moreover, the sympathetic system plays an important role in the perinatal period during hypoxic-ischemic events, as it favours a diversion of cardiac output to the brain, heart and adrenals [71].

- *Myogenic mechanisms:* the regulation of the vascular tone in relation to changes in intraluminal pressure is a leading mechanism of CBF regulation. This mechanism results from a primitive reflex mediated by smooth muscle cells lining the cerebral arteries. In response to increased intraluminal pressure, depolarization of smooth muscle cell membranes and calcium-dependent vasoconstriction occur with the aim of preventing cerebral hyperperfusion, while the opposite occurs at low intraluminal pressure, resulting in vasodilation and increased cerebral perfusion [72]. In addition to calcium, endothelium-derived nitric oxide is also involved in the vasodilation response of this mechanism; however, since the contribution of endothelial nitric oxide increases with age, it may be less efficient in the preterm infant, where other factors may possibly dominate [73]. The myogenic mechanism is the basis for cerebral autoregulation, which will be discussed in detail in the next paragraph.

1.2.2. Cerebral autoregulation: definition and methods of assessment

The ability of cerebral vasculature to maintain stable brain perfusion across a broad range of cerebral perfusion pressure (CPP) is defined as cerebral autoregulation. This mechanism results from the myogenic reflex described in the previous paragraph, which, in response to changes in intravascular pressure, determines either vasoconstriction or vasodilation to preserve a stable cerebral perfusion. CPP is the product of MABP and intracranial pressure. Since the latter is assumed to be relatively constant in the neonatal population and in healthy adults, MABP is thus the main determinant of CPP.

The classic depiction of this system is a sigmoidal curve (Figure 1.7) with stable CBF over a range of normal MABP and unstable CBF when MABP is outside of this range.
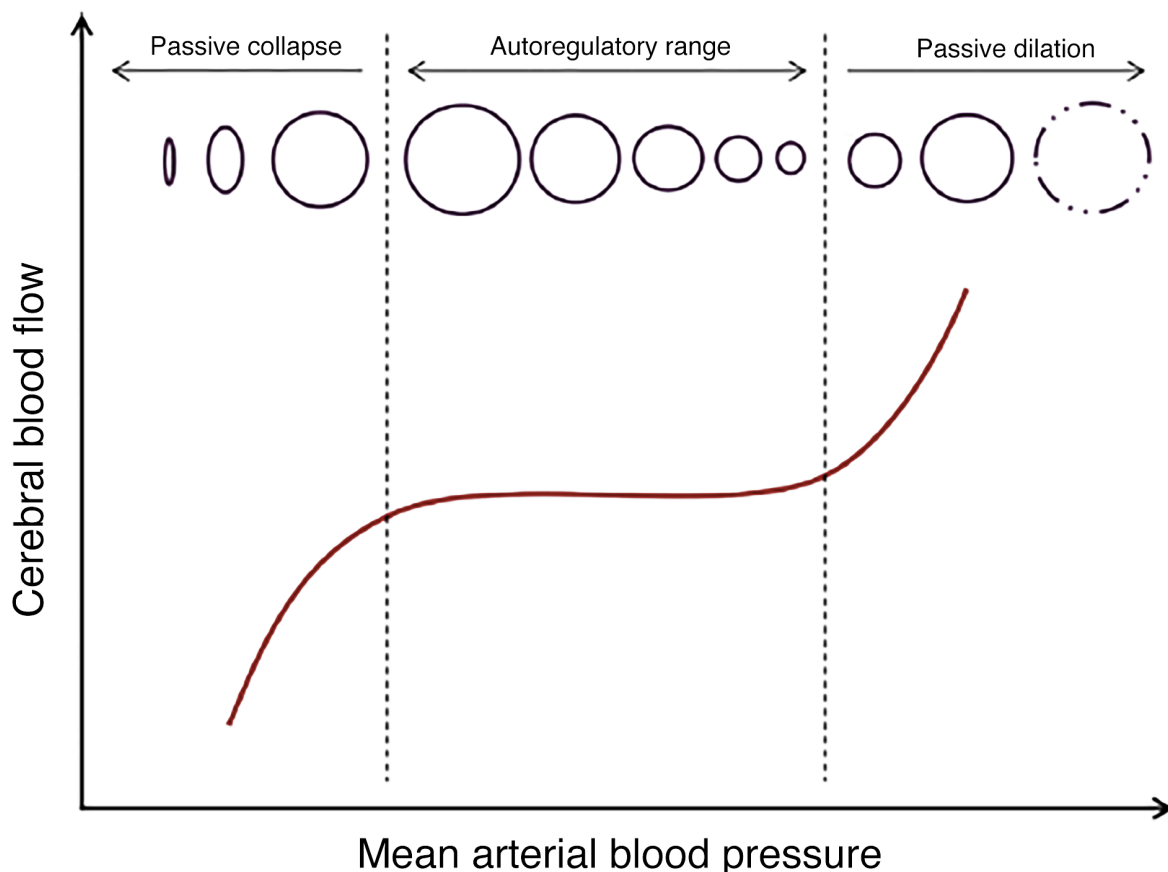

Figure 1.7. *The cerebral autoregulatory curve. Circles represent the schematic arterial diameter. Vertical dotted lines indicate the lower and the upper pressure-dependent limit of the autoregulatory range. Modified from Kooi and Richter, Clin Perinatol (2020)* [74]*.*

If MABP falls below the lower limit of autoregulatory capacity, arteries tend to collapse and CBF decreases, whereas if MABP rises above the upper limit, arteries are forcedly dilated and may snap, causing haemorrhagic complications [74]. The failure of the preterm cerebral vasculature to maintain uniform cerebral perfusion over a range of systemic blood pressures results in the so-called pressure-passive circulation [75].

A complementary view of blood flow regulation was initially proposed in the nineteenth century by the physiologist Siegmund Mayer, who observed spontaneous rhythmic oscillations in the blood vessel diameter, with a periodicity of 10 s (0.1 Hz), in the wings of bats. Based on their periodicity, BP oscillations can be divided into three groups: high frequency (HF, >0.5 Hz), driven by the respiratory cycle and therefore relatively fixed, low frequency (LF, 0.05–0.5 Hz) and very-low frequency (<0.05 Hz), which are regulated by neurogenic, myogenic and metabolic mechanisms [67,76,77]. The development of advanced computational techniques has allowed greater exploration of cerebral autoregulation, with data suggesting that this autoregulatory mechanism attenuates the effects of LF fluctuations of BP, functioning as a high-pass filter [78,79].

It is possible to assess the function of the autoregulatory system by measuring how an input signal (i.e., MABP) is shaped and altered into the output (i.e., CBF) [75,80]. However, CBF cannot be measured directly in the newborn population, therefore, non-invasive methods for CBF estimation and for quantifying the state of cerebral autoregulation have evolved over time in conjunction with advances in technology.

The methods aimed at assessing cerebral autoregulation can be classified according two different approaches: static and dynamic. Quantitative methods that measure CBF over a minute or more ignore the time course of blood flow fluctuations in response to dynamic MABP changes, therefore the pressure-flow reactivity described by these methods is static. The earliest approaches for CBF measurement that used ^{133}Xe clearance had a static approach to CBF estimation. In fact, these methods provide only semiquantitative information about ongoing autoregulation, and their clinical

application is not feasible for longitudinal monitoring due to concerns about the use of invasive delivery of radioactive isotopes [75]. Conversely, by monitoring CBF and MABP with sampling frequencies of less than few seconds, the dynamic approach allows to describe how MABP fluctuations are followed immediately by parallel changes in CBF.

Positron emission tomography has been previously used to evaluate dynamic cerebral autoregulation in human studies. However, the exposure to radiation that this technique entails makes its use unsuitable in neonatal settings.

Transcranial Doppler sonography measures the blood flow velocity within a specific vessel. It is commonly assumed that the perfusion of a given cerebral territory can be inferred from blood flow velocity measurements in the corresponding stem artery. Hence, upon the calculation of the diameter of the insonated vessel, this technique can be used to obtain a non-invasive estimation of CBF and to evaluate the immediate effect of MABP changes on cerebral haemodynamics [81]. Since the estimation of absolute CBF values would require the knowledge of the brain mass perfused by the sampled artery, transcranial Doppler provides a relative index of CBF [80]. While in adults transcranial Doppler monitoring is largely used for the continuous estimation of CBF by measuring the flow velocities in large cerebral arteries, the application of this monitoring technique in the neonatal population, and especially in preterm infants, is hindered by specific technical issues. The small size of the neonatal vessels hinders an accurate assessment of their diameter, which is required to estimate CBF from Doppler measurements of blood flow velocity. Furthermore, due to the small vessel dimension, signal loss is very frequent unless the probe is manually hold in position for the whole monitoring time. Eventually, ultrasound is associated with a time-dependent heating effect, therefore a prolonged transcranial Doppler monitoring may induce a temperature increase within such a delicate target tissue as the developing brain [82]. For these reasons, transcranial Doppler evaluation in neonatal studies aimed at assessing the dynamic features of cerebral autoregulation are often intermittent and performed over limited time periods [60,83,84]. Computerized coherent averaging

of Doppler flow velocity in the middle cerebral arteries in response to spontaneous MABP fluctuations has proved to provide a reliable non-invasive assessment of non-stationary cerebral autoregulation in neonates undergoing intensive care [84].

Cerebral tissue oxygenation, measured continuously and non-invasively using near-infrared spectroscopy (NIRS), can be used as a surrogate for cerebral perfusion and allows a dynamic approach to cerebral autoregulation assessment. NIRS technique will be discussed in detail in section 1.3.2. Since the vast majority of oxygen in blood is bound to haemoglobin, which is confined to the red blood cells, assuming a stable cerebral metabolism, changes in cerebral oxygenation will likely reflect changes in CBF. Despite several technical limitations, such as the assumption of a stable haemoglobin level and of a fixed arterial–venous volume ratio, or the use of diverse algorithms within the various devices and sensors currently available which may hinder the precision of this method for CBF assessment, its capability to provide a beside continuous monitoring has made this technique widely adopted to study brain haemodynamics in the context of cerebral autoregulation [74,85]. To date, the following mathematical models, based on the assumption that autoregulation is a simple linear process, have been developed for the dynamic assessment of the autoregulatory system in preterm neonates using cerebral NIRS monitoring. These methods can be summarized by the following approaches, which are also graphically summarized in Figure 1.8:

- *Time-domain analysis*: this approach examines the moving correlation between CBF, derived from NIRS parameters, and the measured values of MABP over short segments of data (Figure 1.8 A). A number of different correlation methods have been proposed. Correlations can be examined in predefined time epochs, with or without a predefined threshold [86–89]. The method used in the present research for the evaluation of cerebral autoregulation relies on this type of analysis. The mean correlation for each possible MABP value is then calculated and sorted into bins: the resulting output is reminiscent of the autoregulation curve and allows evaluating the MABP range within which this mechanism is effective [90–93]. Some groups

have also used linear regression to analyse cerebral autoregulation. Tyszczuk et al. used correlation coefficients and multiple linear regression to study CBF, MABP and other variables, indicating the MABP range of 23.7 to 39.3 mmHg for the maintenance of an adequate cerebral perfusion [94]. Moreover, using linear regression to quantify the relationship between MABP and CBF, Munro et al constructed curves for cerebral autoregulation and concluded that a breakpoint exists at 30 mmHg [95].

- *Frequency-domain analysis*: this approach examines the correlation between MABP and cerebral oxygenation within specific frequency bands (i.e., LF). The advantage of this approach is that it allows a dynamic assessment of the autoregulatory system and it takes into account the effect of time lag between changes in cerebral oxygenation and BP [75]. However, different parameter settings, like the length of the epochs or the frequency band, have an important influence on this type of approach [96]. Frequency-domain analyses enables calculation of coherence, phase and gain of transfer function.

The coherence function describes the linear relationship existing between two signals in the frequency domain and can be used as a measure to indicate if a linear relationship exists between the input and the output signal (i.e., CBF), with resulting values ranging between 0 (no coherence) and 1 (perfect coherence) (Figure 1.8 B). A threshold of 0.5 has been proposed to define an impaired cerebral autoregulation and to calculate the proportion of time spent with pressure-passive cerebral perfusion [75]. However, this analysis requires a high degree of precision in time synchronization of data capture [97], and may necessitate of several hours of monitoring to provide reliably measures. Moreover, in some studies, a high coherence was observed when MABP was either below or above the lower limit of autoregulation, and it has thus been suggested that coherence may be most useful as a filter to outline adequate slow wave power to measure autoregulation with either correlation or the time shift between the signals [98].
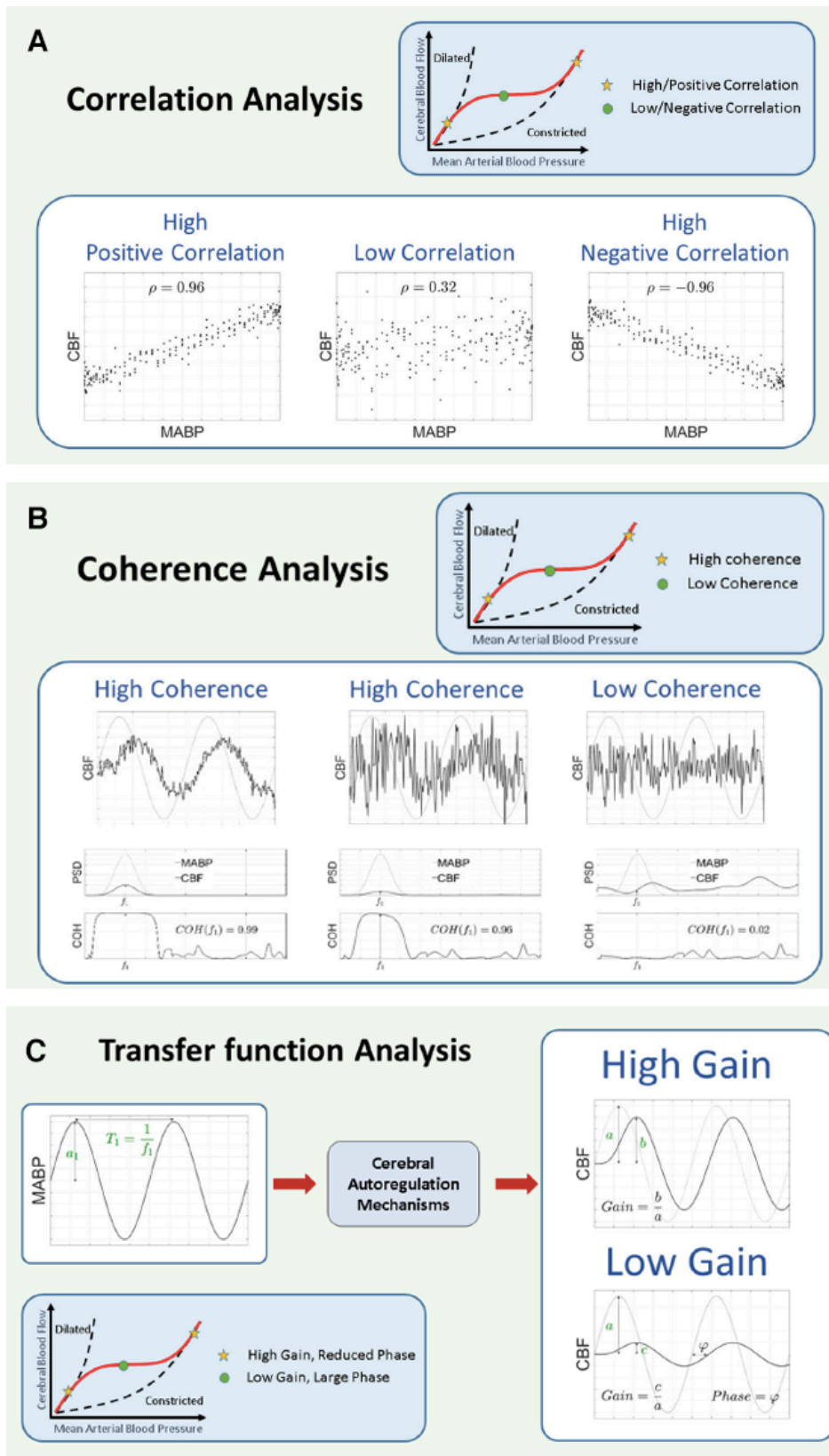
Figure 1.8. *Representation of the different analytical models (A-C) currently available for the assessment of cerebral autoregulation. Adapted from Thewissen et al. Frontiers in Pediatrics (2018)* [78]

Transfer function analysis examines natural LF fluctuations in both BP and CBF to assess how well the autoregulatory system is able to dampen pressure oscillations (Figure 1.8 C). This approach entails the computation of the signal power spectral density, which indicates how much each particular frequency component contributes to form a given signal [78]. By measuring the spectral density ant the cross-power spectral density of MABP and CBF, the phase and the gain can be computed. The phase represents the time shift between the two signals, while the gain represents the relationship in magnitude between BP and CBF and provides a measure of the severity of pressure passivity [78]. A low gain would indicate that, even in the presence of a non-intact cerebral autoregulation, the magnitude of changes in CBF are small or moderate, whereas in the presence of a high gain even moderate changes in MABP are associated with large CBF fluctuations. When using TF phase as a measure for cerebral autoregulation effectiveness, a high gain with a reduced phase has been associated to impaired autoregulation [99].

The evaluation of cerebral autoregulation according to the abovementioned methods requires an invasive continuous monitoring of arterial BP, which is usually performed by an indwelling arterial catheter in the umbilical artery or in a small peripheral artery. As such, it is not exempt from adverse effects, such as thrombosis, vasospasm, air embolism and breaks or transections of the catheter [100], and may not be universally feasible or practical. Moreover, in the presence of a hsPDA, post-ductal blood pressure may not be representative of that in the carotid arteries, due to the haemodynamic effects of trans-ductal shunting [74]. Hence, the moving correlation index between heart rate (HR) and cerebral oxygenation has been recently proposed for non-invasive, yet continuous evaluation of cerebrovascular reactivity in preterm infants [101], based on the fact that HR is a direct cardiac output determinant. When this correlation index turns positive, CBF is dependent on total blood flow, indicating an impaired regulation of CBF.

A shift towards the validation of non-invasive monitoring models for the estimation of cerebrovascular reactivity would support a more extensive evaluation of this physiological parameter in neonates at high-risk of haemodynamic instability and brain injury.

Achieving a reliable evaluation of cerebral autoregulation in the preterm population has proven to be a complex task, largely due to the technical challenges associated with capturing data, the lack of a clear definition for hypotension and the broad range of immaturity in neurovascular development [75]. However, the development of a software able to assess cerebral autoregulation in real time, processing multi-monitoring signals at the infants' cot, would help the clinician to identify infants with pressure-passive CBF and to individualize care by finding each infant's own optimal BP range [102], in order to prevent the development of cerebral complications related to the failure of autoregulation.

1.2.3. Cerebral autoregulation in preterm infants

Under healthy conditions, the mechanisms of cerebral autoregulation mature together with arterial smooth muscle differentiation, starting before mid-pregnancy [103]. However, due to cardiovascular and cerebrovascular immaturity related to premature birth, cerebral autoregulation is often impaired in preterm infants [104], especially under conditions that cause loss of contractile capacity in the immature cerebral arteries, such as hypoxia-ischaemia.

It has been observed that cerebral autoregulation is positively correlated with GA [105,106], suggesting an increased efficacy of this mechanism with advancing functional and anatomical maturation. Moreover, a paradoxical drop of cerebral oxygen extraction has been reported by Vesoulis et al. in preterm neonates ≤25 weeks' gestation during low BP states, which imply a drop in CBF, compared to a physiological increase of this parameter observed in infants aged 26-28 weeks' gestation, suggesting a GA-dependent maturation of the autoregulatory response [107].

Intrauterine growth restriction (IUGR) due to placental insufficiency is a common cause of preterm birth. This condition results from a chronic state of fetal hypoxia which, in turn, determines cardiovascular remodelling aimed preserving cerebral perfusion and oxygenation at the expenses of the splanchnic circulation, characterized by left ventricular predominance, peripheral vasoconstriction and cerebral vasodilation. Recent studies have described altered cerebral autoregulation and an increased cerebral oxygenation in IUGR infants within the first 72-96 hours after birth [108–110], suggesting the postnatal persistence of this vascular redistribution. In addition to GA and IUGR, several conditions and complications that are typically associated with preterm birth further contribute to affect cerebral autoregulation in this delicate population.

Hypotension is common in preterm neonates, especially in the most preterm infants and during the transition from a fetal to a postnatal circulation, which is characterized by a significant haemodynamic instability. By reducing MABP below the lower limit of cerebral autoregulation, hypotension significantly affects this physiological mechanism [93]. Of interest, da Costa et al. aimed to determine the individual optimal MABP at which cerebral autoregulation is most effective using the same software adopted in the present research. They observed that the optimal MABP threshold increased with increasing GA and that a deviation by 4 mmHg or more below the optimal value was associated with higher mortality, whereas an analogous deviation above this value was associated with severe IVH [102].

Dopamine is widely used for the treatment of neonatal hypotension due to its vasopressor properties resulting from the stimulation of the α- and β-adrenergic and dopaminergic receptors. Although a possible role of this medication on cerebral autoregulation has been hypothesized, due to its effects on the vascular tone, current evidence is controversial. Recently, increased time periods with impaired cerebral autoregulation have been observed during the first 96 hours of life in preterm infants exposed to dopamine, in a dose-dependent fashion peaking at a concentration of 11-15 μg/kg/min [111]. A higher correlation between MABP and cerebral oxygenation was reported by Eriksen in preterm

neonates treated with dopamine compared to controls [91], thus suggesting a steeper slope of the autoregulation curve in association with the dopamine-related α-adrenergic vasoconstriction. However, when the same group investigated dopamine effects in newborn piglets during BP fluctuations, they observed a dose-related improvement of cerebral autoregulation at low BP in association with this treatment [112], although an increased dopamine plasma clearance during continuous infusion in piglets compared with neonates may have played a role in these conflicting results [113]. Furthermore, it should be considered that the indication for dopamine treatment is hypotension itself, therefore establishing the individual role of each of these two factors on cerebral autoregulation is a challenging issue.

The association between cerebral autoregulation and the presence of a hsPDA, which may result in a diastolic run-off flow in the cerebral vessels, has been previously investigated in small studies. Chock et al. described a higher, although not significant, burden of pressure-passive cerebral oxygenation in infants with a hsPDA compared to controls. Moreover, comparing infants who had undergone pharmacological PDA closure with those requiring surgical PDA ligation the latter had a transient increase in pressure passivity brain perfusion up to 6 hours after surgical intervention, which resulted in a sudden increase in CBF [88].

A possible correlation between impaired cerebral autoregulation and respiratory distress syndrome has been reported by Lemmers and colleagues [114]. Although $PaCO_2$ levels were similar in infants with respiratory distress syndrome and controls, the former had significantly lower MABP with increased requirement of inotropic drug; therefore, it may be that the observed results were not directly linked to respiratory distress itself, but rather represented an expression of illness severity.

Endotracheal surfactant administration is a first-line treatment in infants with respiratory distress syndrome. Both brief intubation and a less-invasive procedure for surfactant administration (i.e., use of a thinner catheter) have shown transient effects on cerebral autoregulation in preterm infants: the latter was associated with a milder impairment and a quicker recovery compared with brief intubation,

suggesting that autoregulation is affected by the method of surfactant administration [115]. However, the use of a different sedation protocol in association with the two techniques and acute $PaCO_2$ changes associated with the intubation procedure rather than blood pressure changes may have primarily contributed to the observed transient CBF changes [116,117].

In summary, several interrelated conditions may contribute to alter the effectiveness of cerebral autoregulation in preterm neonates; as a result of this constellation of factors, maintaining a stable CBF in this vulnerable population is tenuous, with subsequent clinical implications in terms of brain injury.

1.2.4. Role of cerebral autoregulation in neonatal brain injury

The failure of the cerebrovascular autoregulatory system results in unstable CBF which, by determining repeated cycles of hypoxia–ischaemia–reperfusion, drives the pathogenesis of preterm brain injury, characterized by the development of IVH or of white matter injury.

IVH is a major complication of prematurity, with a highest prevalence during the first 72 hours after preterm birth, suggesting that brain circulation is especially vulnerable in this period [118]. Its aetiology is multifactorial, but primarily lies in the intrinsic fragility of the germinal matrix vasculature and in the disturbances of CBF. In particular, the microvasculature of the germinal matrix is characterized by an abundance of angiogenic blood vessels with an immature basal lamina, decreased pericytes, and deficient glial fibrillary acidic protein in the ensheathing astrocytes endfeet [119]. The exposure of this frail tissue to hypoxia-ischaemia induces a surge in vascular endothelial growth factor and angiopoietin-2 levels, activating rapid angiogenesis within the germinal matrix. In this context, the repeated episodes of ischaemia and reperfusion that often occur as a consequence of CBF fluctuations in the early postnatal period likely contribute to the rupture of the fragile germinal matrix vessels, which represents the *primum movens* for IVH development. Accordingly, CBF fluctuations characterized by a transient phase of hyperperfusion [47,120] and a greater burden of

impaired autoregulation, detected using different techniques [48,104,121–123], have been documented in preterm infants who developed IVH during the transitional period. Moreover, it has also been observed that, in mechanically ventilated neonates, severe IVH was preceded by a global abolishment of CBF reactivity to both $PaCO_2$ and BP, whereas milder IVH did not [54]. As such, the maintenance of a stable CBF since the early postnatal period and the prevention of hypoxic and hypotensive states represent fundamental neuroprotective strategies in the preterm population.

The bleeding in the germinal matrix may disrupt the ependymal lining and extend into the ventricles, causing progressing degrees of IVH, detailed in Table 1.1. Although the Papile criteria [124] are still largely used in clinical and research settings, a more descriptive and precise nomenclature has been proposed by Volpe [125].

Table 1.1. *Grading of intraventricular haemorrhage (IVH) according to Papile and Volpe.*

Papile's grading	Volpe's grading
Grade 1: subependymal haemorrhage	Grade 1: IVH confined to the germinal matrix region
Grade 2: IVH without ventricular dilatation	Grade 2: IVH filling ≤ 50% of the lateral ventricle and/or without ventricular dilatation
Grade 3: IVH causing ventricular distension and dilatation	Grade 3: IVH filling >50% of the lateral ventricle and/or resulting in ventricular dilatation
Grade 4: IVH with parenchymal haemorrhage	IVH with periventricular haemorrhagic infarction (PHI) in the surrounding parenchyma

The destruction of the germinal matrix resulting from IVH and the damage to the glial precursors located in this area may lead to long-term neurodevelopmental sequelae. Moreover, as shown in Figure 1.9 A, severe IVH may be complicated by the development of a parenchymal haemorrhagic infarction (PHI) in the periventricular white matter. PHI was formerly believed to represent a parenchymal extension of the IVH; however, evidence from microscopic studies has revealed that perivascular haemorrhage follows the distribution of the medullary veins in the periventricular white

matter and tend to be concentrated near the ventricular angle, where these veins become confluent, leading to a venous infarction.

PHI frequently results in a large porencephalic cyst that can be isolated or accompanied by smaller cysts. An additional common complication of severe IVH is post-haemorrhagic ventricular dilatation, a consequence of obstruction of cerebrospinal fluid flow caused by the formation of a clot at any level among basilar cisterns in the posterior fossa, the aqueduct of Sylvius or the arachnoid villi.
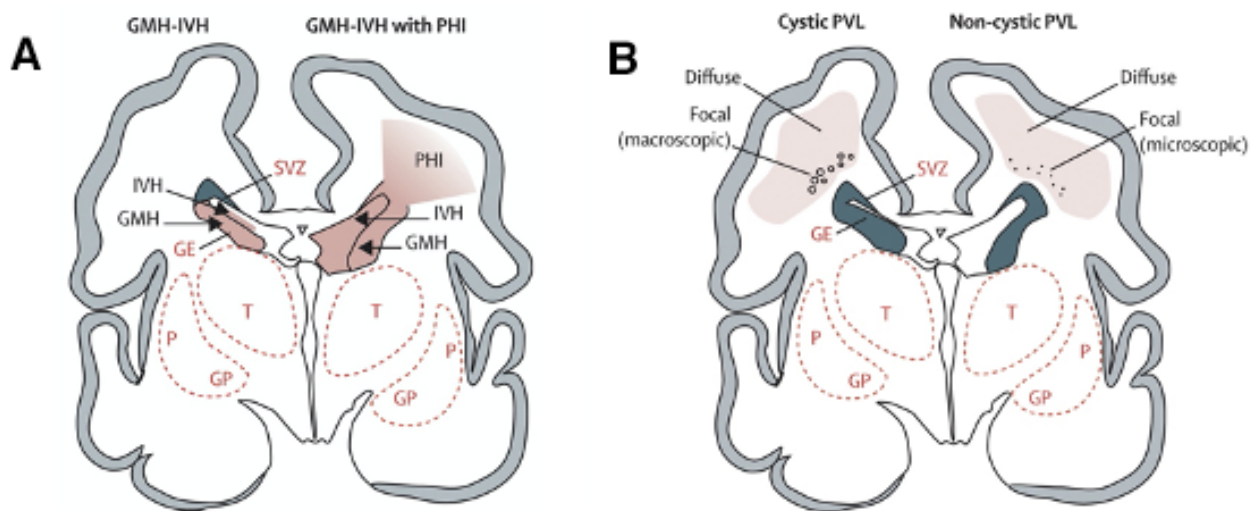
Figure 1.9. *Coronal sections of a premature brain. The dorsal cerebral subventricular zone (SVZ), the germinative epithelium of the ganglionic eminence (GE), thalamus (T), putamen (P) and globus pallidus (GP) are shown.* ***A:*** *a bleeding into the GE results in germinal matrix haemorrhage (GMH), which could burst through the ependyma to cause an intraventricular haemorrhage (IVH) and further progress to periventricular haemorrhagic infarction (PHI).* ***B:*** *cystic and non-cystic periventricular leukomalacia (PVL). The focal necrotic lesions in cystic PVL (small circles) are macroscopic and evolve to cysts, whereas in non-cystic PVL (black dots) are microscopic and evolve to glial scars. The diffuse component is characterised by microscopic cellular changes. Adapted from Volpe J. Lancet Neurology (2009)* [125].

The typical patterns of white matter injury observed in preterm infants mainly consist in periventricular leukomalacia (PVL) and diffuse white matter gliosis.

PVL is a form of white matter injury characterised by loss of pre-myelinating oligodendrocytes and determines a high risk of neurodevelopmental impairment. The principal initiating pathogenetic factors in PVL appear to be cerebral ischaemia-reperfusion and systemic inflammation which, by activating excitotoxicity and free radical damage, lead to death of the vulnerable pre-oligodendrocytes. The cerebrovascular anatomy and physiology of premature infants, namely the presence of arterial border- and end-zones and impaired CBF regulation, underlies the peculiar sensitivity of white matter to ischemic insults, resulting in PVL. This type of injury typically involves the periventricular white matter and, as shown in Figure 1.9 B, can be characterised by macroscopic or microscopic lesions.

The focal white matter damage observed in PVL is caused by a deep necrosis of the periventricular white matter with loss of all cellular elements. The typical areas involved are the arterial watershed zones that lay between the penetrating branches of the middle, anterior and posterior cerebral arteries. The resulting focal necrotic lesions may be either macroscopic or microscopic in size. While macroscopic lesions tend to evolve to the formation of confluent cystic cavities, which are visible on cranial ultrasonography, microscopic necrosis alternatively evolves in whit matter scars characterised by marked astrogliosis and microgliosis. It has estimated that this latter form accounts for the majority of PVL cases; however, it is not easily diagnosed by cranial ultrasound, and only rarely visualized with brain magnetic resonance imaging (MRI), and as such it is underdiagnosed [125].

Diffuse white matter injury is characterized by a diffuse gliosis of pre-oligodendrocytes without focal necroses. The first step leading to this type of injury is a decrease in pre-myelinating oligodendrocytes, which is counteracted by an increase in oligodendroglial progenitors. These progenitors, however, are unable to undergo an appropriate maturation and are exquisitely vulnerable to hypoxic–ischaemic insults. Although it has not yet been conclusively established, it is likely that diffuse white matter gliosis represents the mildest form of injury in a spectrum that includes cystic PVL as the most severe form [126].

Cerebral autoregulation disturbances play also a relevant role in the development of hypoxic-ischemic brain damage following perinatal asphyxia. Experimental studies in newborn animals have shown that, during asphyxia, CBF is diverted towards the brainstem, while it decreases or remains constant in the cerebral hemispheres; this brainstem-sparing phenomenon is named caudal-to-rostral priority and is aimed at protecting the respiratory and vasomotor centres to improve the chances of survival. The second pattern is a parasagittal distribution of cortical and subcortical injury that matches the watershed areas between the anterior, posterior and middle cerebral arteries, and ensues from MABP drops below the regional autoregulatory plateau of these vulnerable areas [71].

Hypoxia, hypercapnia, acidosis and the depressed myocardial function that are typically associated with this condition significantly challenge the mechanisms of cerebral autoregulation [127]. After the initial hypoxic-ischemic hit, a diffuse increase in CBF, starting as early as three hours after the insult and lasting for several days, has been documented in Doppler and NIRS studies [128,129]. This luxury perfusion is the result of an abolishment of the physiological mechanisms of cerebrovascular reactivity, ensuing from the vasoparalysis of cerebral arterioles [129]. Using arterial spin labelling MRI it has been confirmed that primary low CBF followed by hyperperfusion is true for cortex, white matter, central ganglia and is associated with a more severe pattern of brain injury [130,131]. The evidence of impaired cerebral autoregulation in neonates with hypoxic-ischemic encephalopathy correlates with a poorer neurological and neuroradiological outcome and with increased rates of mortality [92,129,132,133]. Hence, the hyperperfusive state that results from the impairment of cerebrovascular reactivity after a hypoxic-ischemic insult has a prognostic value, and may serve as a point of entry for neuroprotective strategies aimed at blocking the sequence of events that leads to the related brain damage [134].

1.3. Non-invasive monitoring of neonatal haemodynamics

1.3.1. Towards comprehensive haemodynamic monitoring

The significant improvements in neonatal intensive care over the past decades have led to a substantial reduction in neonatal mortality, but have also increased the survival of sick neonates, such as extremely preterm infants [135]. Due to the immaturity of the cardiovascular system combined with impaired compensatory mechanisms, these infants are at high risk for significant multisystem complications and haemodynamic instability. Moreover, multiple pathologies may further contribute to challenge the cardiovascular function of the preterm population: among these, are encountered perinatal asphyxia, necrotizing enterocolitis, sepsis, intrauterine growth retardation and congenital heart defects. In addition, it should also be considered that well-intended therapeutic interventions could also result in potentially adverse haemodynamic effects. For example, iatrogenic tachycardia secondary to chronotropic cardiovascular drugs may limit the cardiac preload, whereas invasive ventilation with high mean airway pressure could hinder the venous return, and analgesia, sedation and muscle relaxation have been associated with drug-induced systemic vasodilation [49].

Clinical assessment of the haemodynamic status relies upon the evaluation of HR, BP, urine output, blood gas analysis and capillary refill time [136]; however, it has been demonstrated that, irrespective of the experience of the health care professional, even a severe compromise of systemic perfusion could remain clinically undetected [137]. Moreover, these clinical parameters may not provide enough information to guide the cardiovascular therapeutic management. For instance, low BP can reflect either a high or low cardiac output (depending on SVR) or myocardial impairment, requiring totally different cardiovascular interventions; moreover, oxygen delivery might be impaired despite normal BP in the phase of compensated shock. Hence, a standardized approach in which BP evaluation is used to estimate end-target organ perfusion, with hypotension being the main criterium for interventions (Figure 1.10 A) does not fit all the possible pathophysiological scenarios that can underlie hypotensive symptoms (Figure 1.10 B) and may contribute to underestimate the occurrence

of early haemodynamic disturbances. Moreover, since vasopressors and inotropes have different mechanisms of action and cardiovascular effects [138], the choice of treatment in the presence of hypotension can only be determined when additional information on cardiac function and end-target organ perfusion is gathered [49].

Comprehensive haemodynamic monitoring, integrated with clinical assessment, could help clinicians to build a better picture of the status of the circulation and end organ perfusion. It would also provide useful insights on the underlying pathophysiology, support haemodynamic management of the infants and monitor the effects of the interventions, with the ultimate goal of developing an individualized haemodynamic approach optimized for the patient's specific pathophysiology and clinical situation (Figure 1.10 C) [13,49].
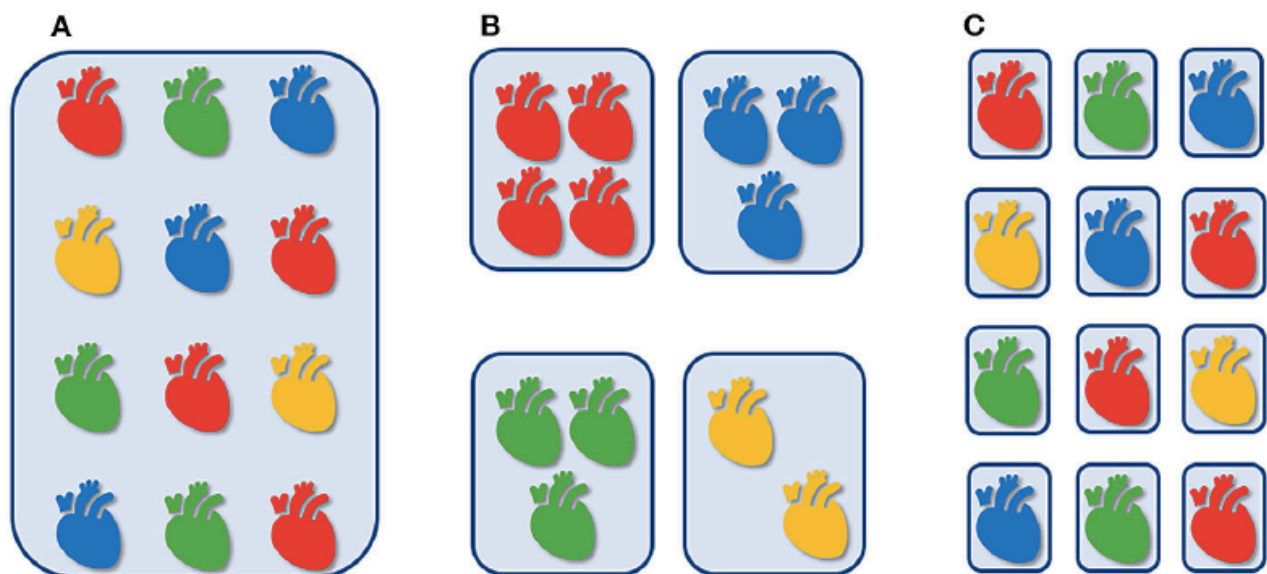
***Figure 1.10.*** *Empirical "one-size-fits-all" approach, irrespective of underlying physiology (A); haemodynamic management stratified according to presumed underlying pathophysiology (B); individualized haemodynamic management tailored to the underlying pathophysiology and to the specific clinical characteristics of each neonate (C). Adapted from De Boode 2020, Frontiers in Pediatrics)* [49].

Nevertheless, the development of a personalized haemodynamic management requires more complex algorithms than standard protocol, as it takes into account the specific characteristics and cardiovascular physiology of each individual neonate at a specific time with the use of adaptive target values for different haemodynamic variables [49].

The ideal technique for neonatal haemodynamic assessment is expected to fulfil the following conditions: to be non-invasive, easily applicable, practical and inexpensive; to be validated against a gold-standard reference method; to be accurate and precise, even under conditions typical of the transitional circulation, such as the presence of shunts; and, eventually, to provide continuous information [139]. Although a monitoring system that fits all these requirements into one device is not available yet, the following techniques meet at least part of these criteria, and all together contribute to depict a comprehensive overview of cardiac function, cardiovascular status and end-target organ perfusion: functional echocardiography, non-invasive cardiovascular monitoring and NIRS. These techniques are reviewed in the next section.

1.3.2. Non-invasive monitoring techniques

Colour-Doppler echocardiography

Since its introduction in the medical field, the diagnostic use of ultrasound has spread universally, and Doppler assessment has enabled to examine blood flow velocity within vessels and cardiac structures. The Doppler technique is the basis of functional echocardiography, which has achieved an important role in neonatal haemodynamic assessment and currently represents the method of choice for the non-invasive evaluation of cardiac output in the neonatal population.

A practical example of the Doppler phenomenon is given by the change in the pitch of sound when a vehicle with a siren passes by. When traveling towards, the pitch of the sound is increases as the vehicle becomes closer, so the sound appears to have a higher frequency; conversely, the frequency appears lower when the vehicle is traveling away. In ultrasound, the shifting reflectors that produce the returning signal echoes are red blood cells, and similar shifts in ultrasound frequency occur as the blood cells move away from or towards the probe. The extent of the difference between the emitted and the received ultrasound frequencies depends primarily on blood flow velocity. The angle of insonation of the ultrasound beam also has a great influence on the extent of Doppler shift; hence, minimizing this angle is a key step in Doppler measurements. An insonation angle <20° produces only a 6% reduction in velocity estimation, and is therefore considered acceptable; for higher angles, correction can be made, but for values >60° this process becomes inaccurate. If the blood flow direction is orthogonal to the imaging plane, no shift is produced [140].

Two different types of spectral Doppler can be used to assess the velocity of blood flow: continuous-wave (CW) and pulsed-wave (PW). PW Doppler emits a single pulse and then pauses to detect received signals. By selecting a timeframe for receiving the data, only velocities from a specific spatial range of interest can be measured; therefore, at any given sampling rate there is a maximal velocity that can be detected, which is called the Nyquist limit. Above this limit, which is usually set a 2 m/s, the Doppler signal aliases and shows an apparent opposite direction of motion; decreasing

the imaging depth to increase the sampling frequency, or decreasing the frequency of the ultrasound beam can be useful to overcome aliasing [140]. In CW Doppler, two separate crystals simultaneously emit and receive signal, and continuous signal transmission detects a wide range of velocities anywhere in the line of the ultrasound beam; hence, CW Doppler has no upper limit for velocity detection.

Colour Doppler allows visualisation of the velocity of blood within an image plane, superimposing blood flow velocities on a colour scale on the corresponding B-mode image. Velocities moving towards the transducer are by convention colour-coded as red, whereas velocities moving away are coded as blue. A turbulent flow is characterized by the addition of yellow or green to the pixels, while colour reversal represents aliasing at the Nyquist limit. PW Doppler is employed for the computation of a colour flow map; given the complexity of the calculation and the high sampling requirement, the temporal resolution of colour flow imaging is limited, but this technique remains extremely useful for the evaluation of shunts and blood flow in regions of interest. Choosing the proper gain settings is the key; for low-velocity signals (e.g., venous returns) it is important to reduce the velocity scale to enable proper visualization [140].

For the estimation of blood flow, the cross-sectional area of the vessel or structure of interest and the velocity of flow by Doppler are needed. The velocity-time integral (VTI) is the area under the Doppler spectral curve and represents the distance that a column of blood will travel during 1 heart cycle. When the cross-sectional area of the great vessels is known, the stroke volume can be calculated. In the case of pulsatile flow pattern, the VTI of the corresponding PW Doppler waveform is the area under a velocity time curve and is equivalent to the stroke distance. Multiplying this value for the cross-sectional area of interest gives an estimate of stroke volume, from which it is then possible to derive cardiac output by multiplying the stroke volume with the heart frequency. Left ventricular output (LVO) and right ventricular output (RVO) can be estimated by measuring cross-sectional area and Doppler flow velocity in the outflow tract of the left and right ventricle, respectively. In neonates,

the estimation of flow volume is subject to significant variability, which mainly derives from the estimation of vessel diameters which are squared to estimate area, with the effect that any associated errors are also squared. In order to minimize this variability, for longitudinal follow-up of ventricular output, if one assumes a constant outflow tract diameter, the minute distance (VTI x heart rate) is less prone to error.

The accuracy of these measurements is subject to a beat-to-beat variability and also depends on the angle of insonation and on the quality of the 2D imaging; the optimization of image quality and data averaging upon multiple measurements help to minimize errors. When compared to accurate invasive reference methods for the determination of cardiac output, such as the Fick method, thermodilution technology or phase contrast MRI, the precision of the echocardiographic assessment of LVO shows an error around 30%, and is also burdened by relatively high interindividual and intraindividual variability [141]. Moreover, it should be taken into consideration that, in the presence of intracardiac (e.g., PFO) and transductal shunting, LVO and RVO are not interchangeable: a left-to-right transductal shunt will increase LVO, whereas interatrial left-to-right shunting will affect RVO. Hence, the discrepancy between the two ventricular outputs can provide additional information on the shunt entity. Since the estimation of systemic blood flow towards end-target organs is of most interest, LVO always needs to be interpreted in the context of potential shunts across fetal channels.

In addition to LVO determination, following a set sequence of views with definite anatomic features illustrated in Figure 1.11, echocardiography allows a longitudinal assessment of systemic and pulmonary blood flow, the ductal status (e.g., patent with a haemodynamically significant or a restrictive transductal shunt), the presence of an interatrial shunt and it allows to rule out any significant structural congenital heart defects which typically present in the neonatal period.
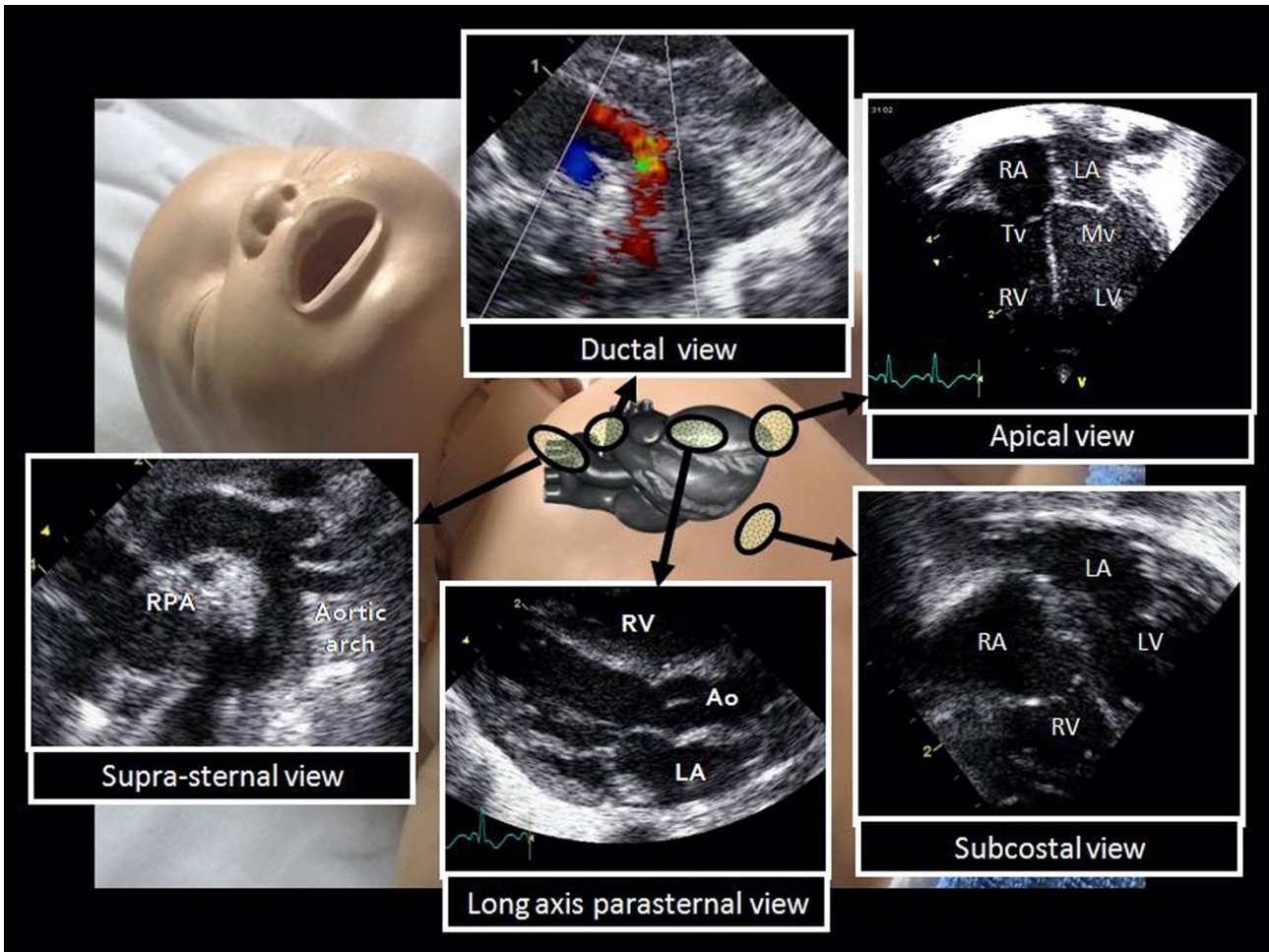
Figure 1.11. *Common echocardiographic windows and views used in neonatal functional echocardiography. Abbreviations: LA, left atrium; Mv, mitral valve; RA, right atrium; Tv, tricuspid valve; LV, left ventricle; RV, right ventricle; Ao, aorta; RPA, right pulmonary artery; Desc Ao, descending aorta; PDA, patent ductus arteriosus. Adapted from El-Khuffash and McNamara, Semin Fetal Neonatal Med (2011)* [142]*.*

The list of anatomic structures and haemodynamic measurements that can be obtained from each of these echocardiographic views is detailed in Table 1.2.

Table 1.2. *Checklist of anatomic features and haemodynamic measurements from each view using different echocardiographic windows. Edited from Groves et al. Ped Res (2018)* [140]

View	Structure	Function
Subcostal situs view	Normal abdominal situs Pulsatile descending aorta Inferior vena cava/right atrium	Inferior vena cava filling and respiratory variation Diastolic flow in descending aorta
Subcostal atrial view	Intra-atrial septum Superior vena cava into right atrium Pulmonary veins into left atrium	Filling of cardiac chambers Direction of interatrial shunt
Apical and subcostal four-chamber view	Both ventricles and intraventricular septum Opening mitral and tricuspid valves Atrioventricular concordance	Mitral and tricuspid inflow pattern, tricuspid regurgitation Tissue Doppler and speckle tracking Ejection fraction from area length
Apical and subcostal five-chamber view	Pulmomary artery crossing over aorta (to exclude transposition)	Aortic stroke distance (LVO)
Parasternal long axis view	Normal motion of mitral and aortic valves Interventricular septum Tricuspid and pulmonary valves	Aortic and pulmonary valve annulus Pulmonary stroke distance (RVO) M-mode for LA:Ao ratio and for fractional shortening
Parasternal short axis view	Aortic valve morphology and coronary origin Pulmonary valve morphology Intraventricular septum Main pulmonary artery with right and left branches Ductal patency and size Drainage of pulmonary veins into left atrium (high parasternal view or "crab view")	Septum morphology (flattening) Pulmonary stroke distance (RVO) Direction, pattern and velocity of transductal shunt
Ductal view	Ductal patency and size	Direction, pattern and velocity of transductal shunt
Suprasternal view	Arch morphology and Doppler profile	Diastolic flow in descending aorta

In addition to the relatively limited precision in cardiac output assessment, especially in the presence of transductal and interatrial shunting, echocardiography requires an intensive operator training and does not allow a continuous monitoring of LVO. Despite of the above limitations, however, it provides fundamental information on the pathophysiologic causes underlying haemodynamic instability, and the integration of functional echocardiography with the clinical picture of the sick neonate is of great support in the development of an individualized therapeutic approach and allows to monitor the effectiveness of such intervention.

Electrical velocimetry

Electrical velocimetry (EV), or electrical cardiometry, is a non-invasive monitoring technique of the haemodynamic status based on the variations of thoracic electrical conductivity.

The monitoring of trans-thoracic bioimpedance for the evaluation of haemodynamic parameters had been first published in 1949 by Kedrov and Liberman [143] and further developed by Kubicek et al. in 1966 [144]. The algorithm has been further modified over the following years, and several electrical biosensing monitors are now available that differ in the methodology used to analyse changes in electrical impedance. This thesis will focus on EV, which has been developed following the modification of the transthoracic bioimpedance algorithm by Bernstein and Osypka in 2003 [145]. This technique measures the changes of transthoracic electrical bioimpedance related to the cardiac cycle using a set of 4 surface sensors, applied as shown in Figure 1.12.

A harmless electrical alternating current of constant amplitude is applied via the pair of outer sensors to the thorax. As blood is the most conducting tissue in the thorax, there will be a voltage change resulting from the movement of blood that occurs during the cardiac cycle, measured using an inner pair of surface ECG sensors. The ratio of applied current and measured voltage equals the conductivity, which is recorded over time.

The measured bioimpedance over time can be expressed as the superposition of three components:

$$Z(t) = Z_0 + \Delta Z_C + \Delta Z_R$$

where Z_0 is the quasi-static portion of the impedance (also referred to as the base impedance), mostly determined by thoracic fluids including the thoracic blood volume, ΔZ_R are the changes of impedance related to respiration, and ΔZ_C are the changes of impedance related to the cardiac cycle. ΔZ_R is considered an artifact to the estimation of stroke volume and, as such, is suppressed.
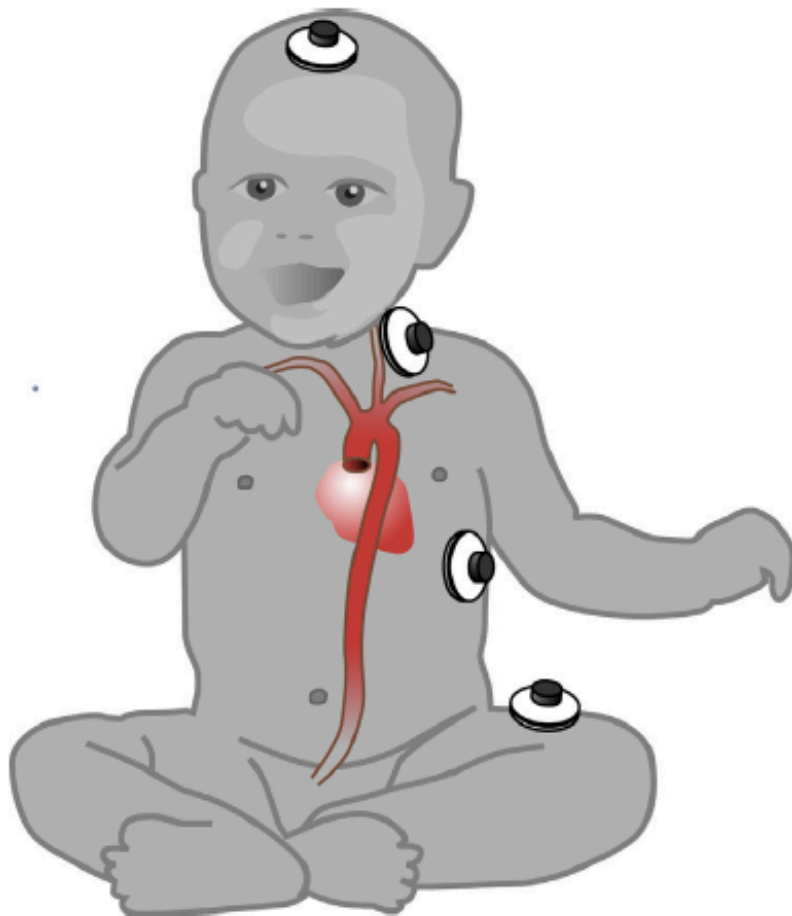
**Figure 1.12.** *Placement sites for electrical velocimetry sensors in infants and neonates, as per the manufacturer's recommendations. Adapted from Narula et al. J Cardiothor Vasc An (2017)* [146].

EV is based on the fact that the conductivity of blood flow in the aorta changes during the cardiac cycle and ascribes the significant bioimpedance changes occurring shortly after aortic valve opening

to the alignment of the erythrocytes at the aortic level (Figure 1.13). When the valve is closed, the electrical current applied circumferences the red blood cells, resulting in a higher voltage measurement and lower conductivity. Very shortly after aortic valve opening, due to their mechanical properties, the disc-shaped red blood cells are forced to align in parallel with the blood flow: now the electrical current passes through red blood cells more easily, resulting in a lower voltage measurement and thus higher conductivity. The change from a random orientation of red blood cells to their alignment upon opening of the aortic valve determines a characteristic increase of conductivity, which corresponds to a steep decrease of impedance (see red arrows pointing to the two states in Figure 1.13).
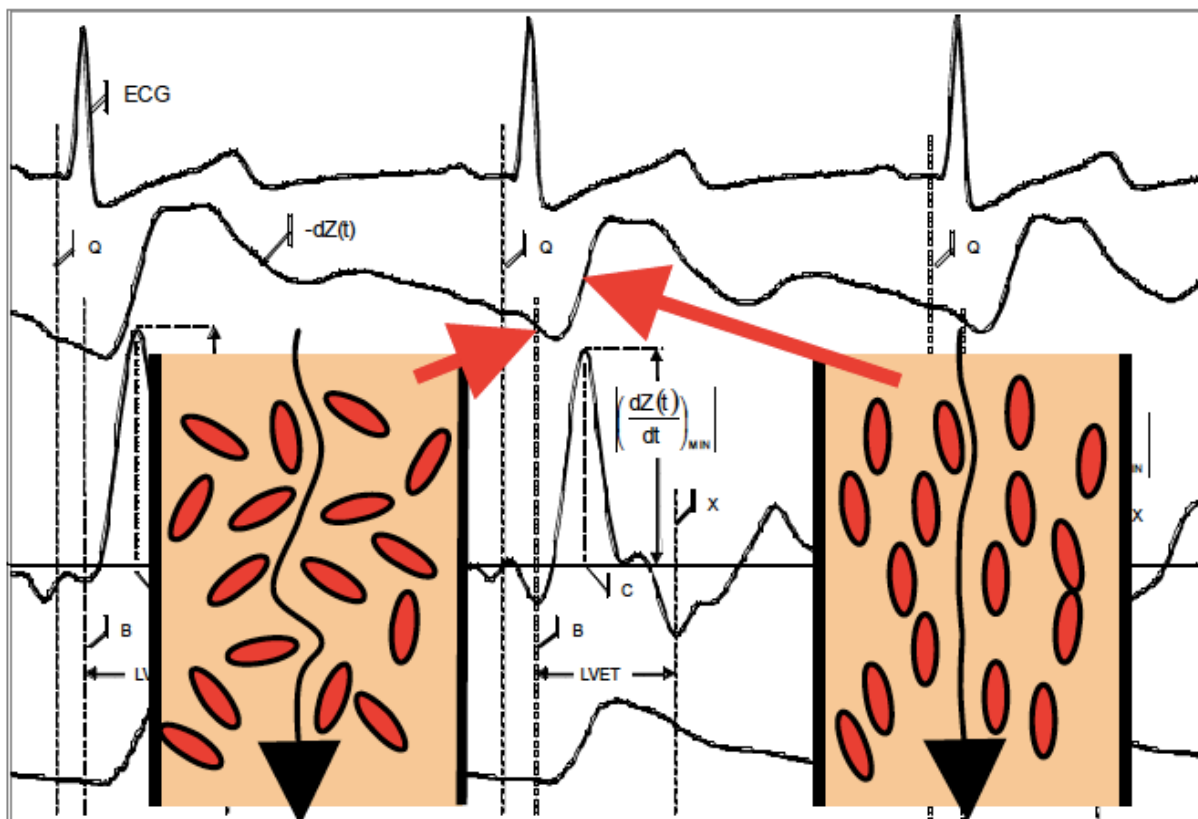

Figure 1.13. Electrical velocimetry analysis of the rate of change in conductivity and ECG signals before and after aortic valve opening. Abbreviations: AoV, aortic valve; dZ(t), conductivity; ECG, electrocardiogram; LVET, left ventricular ejection time. Adapted from Narula et al. J Cardiothor Vasc An (2017) [146].

The beginning of flow time (left ventricular ejection time) and the peak acceleration of the aortic flow and the end of flow time, which corresponds to the closure of the aortic valve, are then identified and used to derive stroke volume (SV), HR and additional haemodynamic parameters, including left cardiac output (CO). Moreover, the steeper the slope of the conductivity, the quicker the alignment process and, thus, the higher the heart contractility. A full list of EV-derived haemodynamic parameters is shown below. If non-invasive MABP and central venous pressure values are inputted into the device, it is also possible to derive SVR.

The agreement between CO measured by transthoracic echocardiography and by EV has been previously evaluated by Noori et al. in healthy term neonates during the transitional period, who reported an acceptable agreement and precision between the two techniques [147]. Similar results have been reported by Grollmuss et al. in term neonates after an arterial switch operation [148]. The same authors also compared the agreement between CO measured with the two techniques in low and very-low-birth-weight preterm infants, indexing SV and CO for the body weight; according to their findings, the limits of agreement fell within the 30% criterion for method interchangeability [149]. Despite of an overall good agreement, a trend towards a CO overestimation by EV at high CO values in the preterm population has been documented in two studies [150,151]; consistent with these findings, van Laere et al. reported increased EV measurements of CO in preterm infants with a haemodynamically significant PDA, compared to those with small or no PDA [152].

However, when evaluating this literature, it should be taken into account that transthoracic echocardiography does not represent the absolute gold-standard for CO calculation, due to the previously mentioned inter- and intraobserver variability and its suboptimal precision compared to real gold-standards for CO assessment (i.e., Fick principle-based or indicator dilution technologies). These, however, are invasive procedures and are thus rarely performed in neonatal settings [139].

Near-infrared spectroscopy

Adequate oxygenation can be defined as a balanced equilibrium between oxygen delivery and consumption at systemic and regional levels. The impairment of blood flow and of subsequent oxygen delivery in vital organs is among the major causes underlying morbidity and mortality in critically ill patients of all ages. Accurate circulatory assessment, monitoring both the macro- and microcirculation, could prevent clinical complications related to ischaemia and hypoxia [153]. NIRS allows to estimate regional tissue oxygenation, which is a proxy of regional blood flow, and tissue oxygen extraction, if simultaneous monitoring of arterial oxygen saturation is performed.

In the 1940s, infrared light started to be used for the development of pulse oximeter, which, by providing a non-invasive assessment of arterial oxygenation and allowing the detection of global hypoxic states, marked a turning point in the history of intensive care [154]. Nevertheless, it was only in the late 1970s that the same physical principle was refined into a monitoring technique able to assess the regional concentration of oxygenated and deoxygenated haemoglobin within different tissues and to examine its changes over time, thus providing an estimate of local oxygen delivery and consumption [155].

NIRS is a spectroscopic technique which exploits the optical properties of biological tissues, namely the wavelength-dependent absorption and scattering coefficients (defined as the mean number of absorption and/or scattering events per unit length a photon travels), in order to obtain clinically relevant information such as regional oxygen saturation, extrapolated from the concentration of oxygenated (HbO_2) and deoxygenated haemoglobin (dHb).

The physical principle on which NIRS is based is the modified Beer–Lambert law [156]. This principle relates the attenuation of light to the properties of the tissue through which the light is traveling according to the following equation:

$$A = \log_{10}(I_0/I) = \mu_a * c * \rho * x + K$$

where A is the attenuation, I_0 the incident photon wavelength, I the detected photon wavelength, μ_a the wavelength-dependent absorption coefficient, c the chromophore concentration, ρ the source-detector separation distance, x the path-length factor (length travelled by I_0, tissue-specific value), and K the photon absorption constant. Since K is assumed constant during the measurement period, it is possible to determine the changes in concentration of the chromophore from the measured changes in attenuation.

NIRS uses light in the near infrared range (wavelength 700–1000nm). Unlike visible light, which is strongly absorbed by haemoglobin, and infrared light, strongly absorbed by water, near-infrared light is relatively 'transparent' in biological tissues; while the concentration of the chromophores such as myoglobin, melanin and bilirubin remain constant, haemoglobin absorbs near infrared light in a manner dependent on its oxygenation state [157,158] (Figure 1.14). In order to optimize the wavelength-dependent absorption characteristics of haemoglobin, current commercial NIRS devices are commonly set between 700-850nm. At 800 nm, HbO_2 and dHb absorption coefficients are overlapping; hence, the photons emitted at this wavelength allow the assessment of total haemoglobin concentration within the tissue examined, from which it is possible to estimate the local blood volume [159]. Because of the larger proportion of blood contained in the lumen of venous vessels, venous haemoglobin accounts for the greatest degree of photon absorption (80-85%), whereas arteries and capillaries account for 15-20% and 5%, respectively [160].

Within biological tissues, photons can be absorbed or scattered; multiple scattering events results in a 'diffuse' path taken by the photons. Relative to absorption, scattering is the main event when light enters tissue and so diffusion (quantified by the tissue-specific scattering coefficient μ_s) is the main determinant for the photon path and for the time the photon takes to be detected. While passing through a few centimetres of biological tissue, photons can be subjected to thousands of scattering events that stochastically govern their trajectory; as a consequence, the photon path is irregular and travels an overall length that is much longer than the source-detector separation (Figure 1.15) [159].
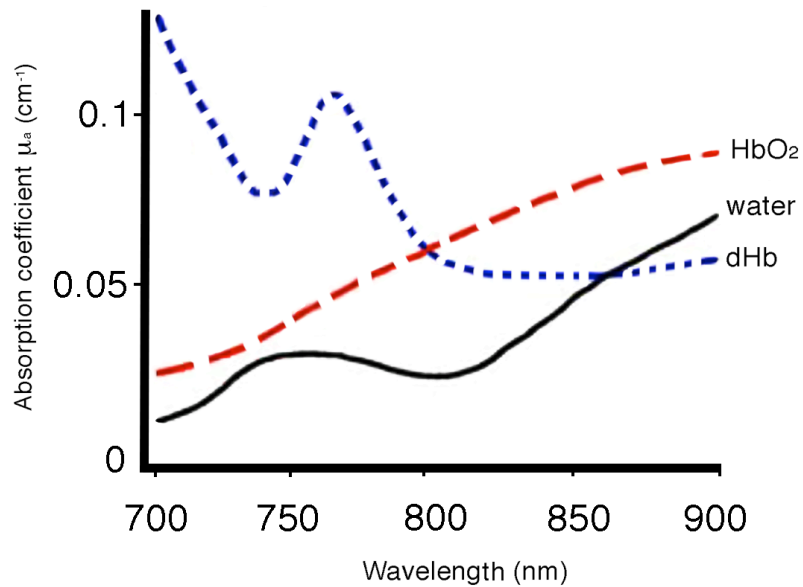
Figure 1.14. *Absorption spectra for oxygenated haemoglobin (HbO₂), deoxygenated haemoglobin (dHb), and water. As highlighted in the square, at 800 nm HbO2 and dHb absorption coefficients are overlapping. Adapted from Martini and Corvaglia, J Perinatol (2018)* [161].
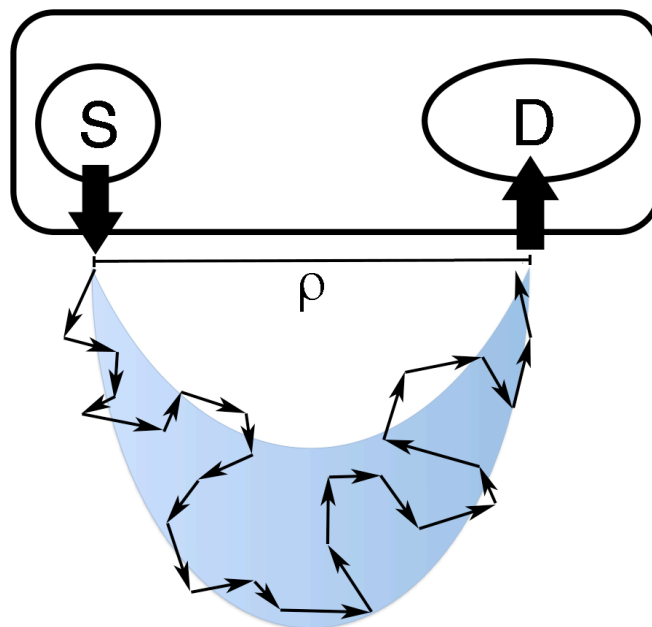
Figure 1.15. *Example of photon trajectory through biological tissue. S=source; D = detector; ρ = source-detector distance. The shaded part highlights the "banana-shaped" area crossed by the photon. Adapted from Martini and Corvaglia J Perinatol (2018)* [161].

There are several approaches to the measurement of light in biological tissues, two of which are described below:

- Time-resolved: the system measures the flight time of transmitted photons from the source to the detector. There are a number of theoretical advantages of this technique over other approaches: it is less susceptible to movement artefact, it is possible to obtain absolute quantitation of chromophore concentration and by obtaining data of photon flight times across the head it is possible using multiple sources and detectors it is possible to reconstruct 3D images of blood volume and oxygenation (optical tomography) [162]. Using optical tomography it has been possible to obtain images of IVH in a preterm infant and functional response to passive motor movement in a newborn infant [163,164].

- Spatially-resolved: by using a single light source and multiple closely spaced detectors, spatially-resolved NIRS is able to resolve scattering to a fixed constant enabling an absolute assessment of the ratio of HbO_2 to total haemoglobin, expressed as the percentage of oxygen saturation [165]. The commercial NIRS oximeters most commonly used in current clinical practice belong to this category, included that used in the present research project (NIRO 200NX, Hamamatsu Photonics K.K., Japan). The light source of this oximeter emits near-infrared light at three different wavelengths and is coupled with a set of two detectors and, as a general rule, the photons emitted cross a so-called "banana-shaped" area and their depth of penetration directly correlates with the source-detector distance *rho* (Figure 1.15) [166].

  The NIRO 200NX provides a percentage value of mixed cerebral oxygen saturation, known as the tissue oxygenation index (TOI), and a normalised value for total haemoglobin concentration (normalized tissue haemoglobin index (nTHI) as well as conventional spectroscopic measurements of change in HbO_2, Hb and total haemoglobin. However, different oximeters use different nomenclatures for mixed tissue oxygenation, and also different algorithms for deriving the values. As an example, the percentage of mixed tissue oxygenation is defined as regional oxygen saturation (rSO_2) by INVOS oximeters (Somanetics/Covidien, Mansfield, MA, USA).

TOI calculation is derived from a modification of the radiative transfer equation for photon diffusion in biological tissue. By estimating the local gradient of attenuation with respect to each source-detector separation and then differentiating $A(\rho)$ with respect to ρ, yields the relation:

$$\frac{\partial A}{\partial \rho} = \frac{1}{ln10} \times \left(\sqrt{3\mu a \times \mu s'} + \frac{2}{\rho} \right)$$

In the first order approximation the scatter coefficient ($\mu s'$) can be treated as a constant (k) with respect to the wavelength, therefore the relative concentrations of oxygenated (HbO_2) and deoxygenated haemoglobin (dHb) can be obtained ($k \cdot HbO_2$ and $k \cdot dHb$, respectively) and resolved to the desired depth. As a result, TOI can be calculated as the ratio of $[HbO_2]$ to total haemoglobin:

$$TOI\ (\%) = \frac{[HbO_2]}{[HbO_2]+[Hb]} \cdot 100$$

When NIRS monitoring is combined with simultaneous monitoring of peripheral arterial oxygen saturation (SpO_2), it is possible to calculate the fractional tissue oxygen extraction (FTOE) of the investigated tissue according to the following formula [167]:

$$FTOE\ (a.u.) = \frac{[SpO_2 - TOI]}{[SpO_2]} \cdot 100$$

FTOE reflects the balance between oxygen delivery and oxygen consumption at a tissue level. Increased values may indicate a higher level of oxygen consumption than oxygen delivery or, if the tissue oxygen consumption is assumed to be constant, may indicate a reduced tissue oxygen delivery. Decreased FTOE values may, on the other hand, reflect a reduction in tissue oxygen extraction due either to a decrease of tissue oxygen consumption, an increased oxygen delivery to the tissue or both.

The first report on the use of NIRS to investigate cerebral haemodynamics and oxygenation in neonates with perinatal asphyxia dates back to 1985 [168]. The brain has been the organ most extensively explored by NIRS in infants and neonates, especially in conditions at risk of hypoxic brain damage and related neurological sequelae, such as cardiac surgery [169,170], perinatal asphyxia [133,171] or during the enhanced haemodynamic instability that characterizes the first days of life [172,173]. The interest in the use of cerebral NIRS monitoring in the context of postnatal transition the has led to the proposal of reference curves for cerebral oxygenation and FTOE during the first 72 hours, specific for different gestational ages [174]. These curves depict the dynamic features of cerebral haemodynamics during this postnatal transition. However, a limitation to the applicability of these curves is related to the use of single-brand devices (INVOS oximeters) and of small adult sensors for cerebral NIRS monitoring. A comparison with neonatal sensors, performed within the same study on a small number of infants (n=16), has revealed that the measurement discrepancy between the two sensor types can be as high as 15%. As discussed later in this section, different oximeters are associated with significant reading discrepancies.

NIRS provides continuous real-time information and is easily applicable even in the smallest preterm infants, where its use has shed light on the cerebral haemodynamic fluctuations involved in the pathophysiology of neurological complications of preterm birth. For example, specific CBF changes characterized by a preliminary ischemic-hypoxic phase, followed by a transient hyperperfusion, have been described as likely haemodynamic antecedents of IVH development [120,175]. Moreover, a greater burden of cerebral hypoxia during the first 48-72 hours after preterm birth have been observed in preterm infants who developed IVH during the transitional period [176,177]. The change between hypoxia-ischaemia and reperfusion is also thought to be involved in the development of PVL [126].

Early NIRS monitoring has also provided important findings also in relation to neurodevelopmental outcomes in at-risk neonates. In particular, the haemodynamic changes documented with the intraoperative use of NIRS in infants undergoing cardiac surgery were found to be associated with

poor neurodevelopment at 12 months [178]. Similarly, preterm infants with low cerebral oxygenation during the transitional period or over the first weeks of life showed a poorer psychomotor outcome within their first 3 years of life [179–181].

The introduction of NIRS in neonatal care to investigate cerebral haemodynamics has been an essential landmark to obtain longitudinal haemodynamic information in the investigation of the physiological mechanism of cerebral autoregulation. The mixed tissue oxygenation measured by NIRS is highly advantageous to the study of cerebral tissue oxygenation, as it reflects the amount of oxygen in the arterial, capillary and venous bed. As venous blood is the largest component, the cerebral tissue oxygen saturation equates most with mixed venous saturation. This is determined by cerebral oxygen delivery (a product of CBF, SaO_2 and Hb) and cerebral oxygen metabolism [75]. Assuming stable cerebral metabolism, SaO_2 and [Hb], the changes occurring in cerebral oxygenation likely result from fluctuations of CBF [182]; hence, cerebral oxygenation can be considered a proxy for CBF and accordingly used for the evaluation of cerebral autoregulation and cerebrovascular reactivity. Details on the mathematical models adopted to assess these parameters and the related findings are provided in section no. 1.2.1.

However, when interpreting NIRS data, the following possible limitations should also be considered.

1. The accuracy and precision of NIRS measurements is questionable: although parts of the body are affected by a greater variability, cerebral oxygenation is not exempt of a noticeable within-subject variability [183,184], and slight shifts of the sensor placement may result in significant cTOI variations.

2. Comparability and reproducibility of measurements between different NIRS monitors represent an additional weakness of this technology. A 3-10% difference between the NIRO and INVOS instruments, with the NIRO reading lower, has been previously reported in several studies [185,186], whereas the Fore-Sight (CAS Med.Medical Systems, Brandord, Connecticut, USA) and SenSmart X-100 (NONIN Medical, Plymouth, Minnesota, USA) have

shown significantly higher values of cerebral oxygenation than the NIRO and INVOS [186], with increasing discrepancies at low cerebral oxygenation levels, suggesting an oxygen-level-dependency of the reading sensibility [186]. One of the leading reasons that underlies these discrepancies is the use of different mathematical algorithms of signal processing by different manufacturers to calculate oxygen saturation, and the lack of a calibration standard. Furthermore, different technical calibrations likely underlie the significant differences observed between adult and neonatal NIRS sensors [174,187].

It is possible that, despite the long use of cerebral NIRS monitoring in neonatal research, this large technical and methodological heterogeneity has hindered the ability to draw definite conclusions about its role in routine clinical practice. In order to be truly effective, a monitoring system must not only alert the clinician about a potential clinical deterioration, but the availability of effective intervention, which would ideally improve short-term and long-term outcomes, is also required [188].

In this regard, the European collaborative group named SafeBoosC (Safeguarding the Brains of our smallest Children) designed a set of randomized control trials aimed to evaluate the effective usefulness of cerebral NIRS in extremely preterm infants during the transitional period. The principal hypothesis being tested is whether continuous cerebral oximetry measurements with NIRS can reduce the burden of cerebral hypoxia and hyperoxia in these infants, and an evidence-based treatment guideline was developed to be applied if cerebral oxygenation was out of range. This group has completed a phase II randomized controlled trial of continuous cerebral NIRS monitoring during the first 72 h of life (experimental), compared with blinded NIRS monitoring with standard care (control) [189]. In the experimental group, the mean burden of hypoxia was significantly reduced compared with controls, demonstrating that cerebral oxygenation can be stabilized by the routine application of cerebral NIRS monitoring in combination with a dedicated treatment guideline [190]. Although an association between the early burden of cerebral hypoxia, but not of hyperoxia, and severe intracranial haemorrhage has been observed at an explorative analysis [177], the ultimate goal would be to

demonstrate improved survivals without neurological impairment in association with this approach. In this regard, a randomized multicentric clinical phase III trial with a primary outcome of death or severe brain injury and secondary outcome of death or moderate-severe neurodevelopmental impairment at 2 years of age is currently ongoing [191].

1.3.3. Values and pitfalls of currently available techniques

Theoretically, the validation of a monitoring system that matches together multiple techniques aimed at investigating different aspects of neonatal haemodynamics would provide valuable information for a better understanding of the underlying physiology in sick and at-risk neonates. In particular, functional echocardiography, by evaluating cardiac function and anatomy, enables assessment of normal cardiac structure, ruling out possible heart defects, is able to assess the effectiveness of cardiac contractility, confirm the presence of a PDA and its haemodynamic impact and to assess the entity of potential shunts at different levels. By providing continuous assessment of CO, cardiac contractility and SVR, EV may be useful to identify an early impairment of the haemodynamic status and the possible underlying cause. Since normal cardiac output does not necessarily imply adequate end-organ perfusion, the inclusion of NIRS in this comprehensive monitoring system contributes to the detection of perfusion impairment at a regional level, that may occur before or even without a concomitant reduction of global blood flow. When cardiac output is impaired, the evaluation of end-target perfusion also provides valuable information in regard of the severity of this impairment and of its effects at a regional level.

If used simultaneously and in an integrated manner, the combination of NIRS, EV and functional echocardiography may help to shed light on the haemodynamic mechanisms underlying specific pathophysiological conditions typically associated with preterm birth, such as IVH or PVL development, or on the haemodynamic consequences of perinatal hypoxia-ischaemia at different levels. Besides, a more extensive use of this comprehensive system to monitor the effects of cardiovascular therapies may aid to assess its potential usefulness in the therapeutic haemodynamic management.

This system, however, is not exempt of a number of potential biases. As stated before, the techniques that are currently available for a continuous haemodynamic monitoring in infants and neonates are

burdened by specific limitations; in particular, the accuracy and reproducibility issues of the provided measurements contribute to hinder the applicability of these techniques in clinical decision making.

When the current literature based on the combination of NIRS and echocardiography is evaluated, the following considerations needs to be made. The use of data averaging over prolonged time intervals for the evaluation of continuous parameters might overlook time and frequency fluctuations of potential clinical relevance. Although functional echocardiography is considered by many the current gold-standard methodology for the non-invasive evaluation of cardiac output in neonatal settings, it does not allow a continuous assessment of dynamic cardiovascular parameters [192] and, as such, it may be blind to relevant haemodynamic fluctuations occurring between one evaluation and the next. In this regard, the translation of non-invasive cardiac output monitoring techniques into neonatal settings represents a landmark towards the development of a continuous monitoring system that matches together cardiovascular and regional haemodynamics, monitored with NIRS.

However, it should be borne in mind that the approach of validating EV against echocardiographic-derived estimations of CO is questionable, due to the imprecision of transthoracic echocardiography. CO using echocardiography is derived by the assumption of a perfect round shape of the outflow tract which hinder the exact measurement of the cross-sectional area, the variability related to the angle of insonation, the inaccuracy of tracking the Doppler velocity envelope for VTI assessment and the effects of potential shunts [13]. Hence, targeted studies evaluating the agreement between non-invasive techniques for continuous haemodynamic monitoring and invasive gold-standard methods are warranted to adequately define their effective accuracy in the determination of central blood flow. While waiting for such evidence, EV represents a helpful tool for continuous trend monitor over time and its data can be matched with NIRS-derived trends to correlate ongoing haemodynamic changes. Furthermore, the cardiovascular parameters obtained by EV are not limited to CO, but also include an estimate of SV, cardiac contractily and SVR, which are very important to obtain a broader evaluation of the neonatal haemodynamic status, especially during the transitional period. Despite the

potential of these measurements, these additional parameters have not been largely explored in neonatal settings [193–197] and thus warrants to be the objective of further targeted research.

It has been recently shown that a comprehensive haemodynamic approach, integrated with clinical assessment, reduced the clinical recovery time in preterm infants with a compromised haemodynamic status [198,199]. However, it must be underscored that it is not the sole monitoring that will improve outcome, but it is rather the appropriateness of the interpretation of the obtained haemodynamic parameters and subsequent therapeutic interventions [13,200].

2. AIMS AND HYPOTHESES

This present research project was developed with the aim to add further knowledge on the cardiovascular and cerebrovascular physiology of preterm infants during postnatal transitional, explored using a non-invasive system of integrated multiparametric monitoring.

The preterm infant is exposed to a number of antenatal, perinatal and postnatal factors (the exposome) which interact with transitional haemodynamics. A better understanding of these interactions will facilitate the development of individualized haemodynamic approaches that are based on specific characteristics of each infant, with possible implications for the outcomes of this delicate population.

A core hypothesis for the present research was that the haemodynamic status of preterm infants during the transitional period varies dynamically over time, and that the early exposome may exert a significant influence on cardiovascular and cerebrovascular haemodynamic parameters and on their interactions during this phase. This hypothesis was developed at 3 levels (discussed in more detail below): haemodynamic cardiovascular and cerebrovascular parameters; dynamic interactions existing between two different haemodynamic parameters (i.e., cardiac output determinants); dynamic fluctuations of the haemodynamic parameters in response to brief and brisk variations of vital parameters (i.e., the so-called cardio-respiratory events).

Two innovative methodological elements were introduced in this research project. First, the combination of a totally non-invasive and continuous haemodynamic monitoring system with echocardiography, which is largely validated for the evaluation of neonatal haemodynamic but allows only intermittent evaluation. Second, the use of a sophisticated bedside software tool, described in detail in paragraph 3.3, which ensured simultaneous recording and integrated analysis of the multiple parameters obtained with the different devices. The perfect signal synchronization guaranteed by this software allowed the calculation of complex inter-parametric correlations, such as a non-invasive biomarker of cerebrovascular reactivity.

Using this methodological approach, the present dissertation aimed to test the following hypotheses:

Hypothesis I: Cardiovascular and cerebrovascular parameters of preterm infants during postntatal transition are subjected to parameter-specific variations over time. Moreover, the antenatal, perinatal and postnatal factors to which preterm infants have been exposed exert factor-specific influences on cardiovascular and cerebrovascular haemodynamics during the transitional phase (*Chapter 4*).

Hypothesis II: The relationship between CO and its two direct determinants (namely, SV and HR) is not linear, but varies at different SV and HR ranges and according to relevant haemodynamic characteristics of the preterm infant during the transitional period (*Chapter 5*).

Hypothesis III: The cardiovascular and cerebrovascular haemodynamic response to cardio-respiratory events during the first 72 hours of life is determined not only by the event features, but also by relevant antenatal, perinatal and postnatal factors to which preterm infants have been exposed (*Chapter 6*).

3. METHODS

3.1. Ethics, Patients and Settings

This research project was conducted in conformity with principles and regulations of the Helsinki Declaration. The study protocol was approved by the Ethics Committee of St. Orsola-Malpighi Hospital, Bologna, Italy (protocol no. 328/2017/O/Oss). Written informed consent was obtained from the parents/legal guardians of each infant. The infants' enrolment was performed between March 2018 and September 2020.

Infants with a GA <32 weeks and/or a birth weight <1500 g, admitted to the Neonatal Intensive Care Unit (NICU) of S. Orsola-Malpighi were consecutively enrolled in this observational prospective research within the first 12 hours of life. Major congenital malformations, including congenital heart disease, and antenatal diagnosis of genetical abnormalities were exclusion criteria. Infants with conditions that may have had influenced cerebral oxygen saturation, such as anaemia [201] (defined as haematocrit <30%) or persistent pulmonary hypertension requiring inhaled nitric oxide [202] were also excluded from the study.

For each infant, the following antenatal and perinatal data were collected:

- GA;
- weight, length and head circumference at birth;
- antenatal steroids (complete course vs. incomplete course or not given);
- antenatal status of Doppler velocimetry (normal vs. evidence of absent or reversed end-diastolic flow [AREDF] in the umbilical artery and/or ductus venosus) and pulsatility index in the middle cerebral artery (MCA-PI, normal vs. below the 5th percentile, which indicates the occurrence of the brain sparing phenomenon) [203];
- Apgar score at 1 and 5 minutes;

During the study period, the following clinical data were also recorded:

- status of ductus arteriosus (see "Echocardiographic evaluation" paragraph for the used definitions);

- development of IVH and related timing (see "Cranial ultrasound evaluation" paragraph for the used definitions);

- type of respiratory support (mechanical ventilation, continuous positive airway pressure [CPAP], nasal cannula or self-ventilating in air [SVIA]) and related modifications;

- systolic, diastolic and mean arterial blood pressure values, measured at regular intervals (i.e., from 30' to 6-hourly) throughout the study period using the oscillometric technique;

- need for cardiovascular drugs (dopamine and/or dobutamine), dosage and treatment duration;

- haemoglobin levels from the blood exams routinely performed during the study period;

- development of sepsis and/or necrotizing enterocolitis during the study period.

3.2. Ultrasound evaluation

Cranial ultrasound

A cranial ultrasound scan (CrUSS) was performed using an ultrasound scanner CX50 (Philips Healthcare) and a convex 8-5 MHz transducer through the anterior, mastoid and posterior fontanelle. The first CrUSS evaluation was carried out at the time of enrolment and repeated 6-12 hourly in the presence of PDA or if an incipient IVH was noted, otherwise 12-24 hourly. CrUSS was mainly aimed to rule out ultrasonographic brain abnormalities and to detect IVH development as well as its localization (mono/bilateral) and severity (classified according to Volpe's grading) [118]. In the presence of a PDA, the blood flow velocity in the anterior cerebral artery (ACA), accessed from the anterior fontanel window, was also evaluated using the PW Doppler.

Colour-Doppler echocardiography

A screening echocardiogram aimed at ruling out cardiac defects and at evaluating cardiac contractility, LVO and the ductal status was routinely performed at the time of enrolment using an ultrasound scanner CX50 (Philips Healthcare) with a linear 12-MHz probe, and repeated 6-12 hourly in the presence of a PDA, or 12-24 hourly if there was no evidence of PDA. The ductal diameter was measured from the high parasternal view at the point of maximum constriction, caring to avoid colour-Doppler interference outside the vessel wall. The ductal flow pattern was evaluated from the parasternal short axis using continuous-wave Doppler and, based on the ratio of end-diastolic to peak-systolic velocity, was defined as pulsatile ($\geq$0.5) or restrictive (<0.5) [204]. The left atrium to aortic root (LA:Ao) ratio was measured on M-Mode scans from the parasternal long axis view, using the leading-edge-to-leading-edge technique. Flow velocity in the descending aorta (DAo) was measured using pulsed-wave Doppler from low subcostal sagittal view. Flow velocity in the ACA was measured as previously described.

Based on these echocardiographic features, the ductal status was classified as follows: hsPDA (pulsatile shunt pattern and LA:Ao ratio $\geq$1.5 and/or evidence of reversed end-diastolic flow in the DAo or ACA) [152]; restrictive PDA (restrictive shunt pattern and LA:Ao ratio <1.5); no evidence of a PDA.

LVO was also calculated according to the formula [(left ventricular outflow VTI) x (HR) x (left ventricular outflow cross-sectional area)] and indexed to body weight [205]. The left ventricular outflow diameter was measured from the parasternal long axis view using the leading-edge technique between the hinges of the aortic valve, whereas VTI was estimated sampling the left ventricular outflow tract from an apical five-chamber view with pulse-waved Doppler, applying the insonation angle correction as appropriate in order to optimize LVO calculation.

3.3. Non-invasive multiparametric monitoring and ICM+ software

Non-invasive multiparametric monitoring

The enrolled infants underwent a continuous, non-invasive multiparametric monitoring using near infrared spectroscopy, pulse oximetry and electrical cardiometry. The monitoring was commenced within 12 hours after birth and continued up to 72 hours of life. In the case of persistence of haemodynamic instability or of echocardiographic evidence of a hsPDA after 72 hours of life, the monitoring was carried on until the achievement of a stable haemodynamic condition or until a restrictive PDA pattern or ductal closure were obtained.

The list of the devices used for the multiparametric monitoring and of the parameters that were continuously recorded from each device is detailed below:

- Near-infrared spectroscopy: cerebral tissue oxygenation index (cTOI) was detected using a NIRO-200NX oximeter (Hamamatsu Photonics K.K, Japan), set on a 1Hz sampling rate, with disposable neonatal sensors placed on the central forehead.
  Using the ICM+ software (see paragraph below), continuous values of cerebral fractional oxygen extraction (cFTOE) were calculated from peripheral arterial oxygen saturation (SpO_2) and cTOI values according to the following formula: $cFTOE = (SpO_2 - cTOI)/SpO_2$ [167].

- Electrical velocimetry: an ICON® device (Osypka Medical Inc., Berlin, Germany), whose sampling frequency was set on the beat-to-beat option, was used for non-invasive haemodynamic monitoring of the following cardiovascular parameters: heart rate (HR_{EV}, bpm), stroke volume (SV, ml/kg), cardiac output (CO_{EV}, ml/kg/min), index of contractility (ICON), systemic vascular resistance (SVR, $dyn \cdot s/cm^5/m^2$). Neonatal Cardiotronic Sensors™ (Cardiotronic, Osypka Medical Inc., Berlin, Germany) were placed as in Figure 1.12, according with the manufacturer's recommendations [146].

- Pulse oximeter: heart rate (HR_{PO}) and SpO_2 were detected using a pulse oximeter Masimo Radical-7 (Masimo Corporation, Irvine, CA, USA), whose averaging time was set at 2-sec.

Masimo neonatal disposable sensors (Masimo Corporation, Irvine, CA, USA) were placed in the right hand.

ICM+ software

ICM+® (*https://icmplus.neurosurg.cam.ac.uk*, Cambridge Enterprise, UK) is a pioneering clinical research software solution that offers high-resolution data collection and real time analysis from multiple bedside monitoring sources, facilitating personalised medicine. This software have been used for over 25 years of clinical research in intracranial dynamics and intensive care of traumatic brain injury [206], becoming a hub for a worldwide scientific network in brain monitoring.

During this period, the application of the ICM+ software has been successfully extended to neonatal haemodynamic research. In particular, by calculating the correlation between MABP and CBF, this software enables real time information on cerebral autoregulation to be displayed at the bedside. In recent research using ICM+, a non-invasive index of cerebrovascular reactivity (TOHRx) has also been described [101]. TOHRx is known as the tissue oxygenation-heart rate reactivity index, and describes cerebral vascular reactivity using the correlation coefficient between slow waves of cerebral oxygenation and the heart rate, with positive TOHRx values indicating impaired cerebrovascular reactivity. Using this software, the MABP range where cerebrovascular reactivity is strongest has been calculated [207]; the authors observed that preterm infants who died or had worse IVH presented with a higher mean absolute deviation from optimal MABP than those who survived.

In the context of this research project, a collaboration agreement was made with the Brain Physics Laboratory, Department of Neuroscience of the Cambridge University (Cambridge, UK) for the licenced use of the ICM+ software for data collection and analysis. The period between November 2017 and February 2018 was dedicated to the technical set-up of the electronic interfaces needed to connect the ICM+ software with the previously listed devices used for the research project.

The monitoring devices of the enrolled infants were connected via a RS232 cable to a laptop running the ICM+ software which, as illustrated in the laptop screenshot of Figure 2.1. recorded all the obtained parameters continuously and simultaneously throughout the whole monitoring duration.

Figure 2.1. Example screenshot of a real-time ICM+ recording during one of the monitoring periods.

After the recording was completed, the ICM+ traces were retrospectively inspected. Time periods showing signal interruptions or a HR discrepancy >20% between pulse oximeter and electrical velocimetry were considered as likely artefacts and, as such, were ruled out from data analysis. Moreover, during the monitoring the nursing staff was provided with a diary where to annotate dates and times of handling, cares or invasive procedures. The monitoring epochs associated with the periods indicated in the diary were marked as possibly artefactual and were not included in the data analyses.

3.4. Statistical analysis

Statistical analysis was performed using IBM SPSS, version 26 (IBM Corp. Released 2019. *IBM SPSS Statistics for Windows, Version 26.0.* Armonk, NY: IBM Corp) and Stata software, version 15 (StataCorp, 2017, *Stata Statistical Software: Release 15,* College Station, Texas, USA: StataCorp LP).

Data distribution was evaluated using the Shapiro-Wilk test for normality. Depending on the distribution, either parametric or non-parametric tests were used. Continuous variables were expressed as median (interquartile range [IQR]) or mean (standard deviation [SD]) as appropriate, whereas categorical variables were summarized as frequencies and percentages. A statistical test was considered significant if P value was < 0.05 (two-tailed) for all the data included in this dissertation.

The specific statistical methods used in each study included in this thesis are described in detail in the respective chapters.

4. TEMPORAL PATTERNS AND CLINICAL DETERMINANTS OF CARDIOVASCULAR AND CEREBROVASCULAR HAEMODYNAMICS DURING THE TRANSITIONAL PERIOD

4.1. Introduction and aim

The transition from intrauterine to extrauterine life represents a critical phase of physiological adaptation, which impacts on several organs and systems. Due to the cardiovascular and respiratory immaturity of premature infants, the first 72 hours of life are often characterized by significant haemodynamic instability [208,209] and by impaired cerebral autoregulation [210], which have been implicated in the pathophysiology of brain injury [47,120,121,175,211].

A deeper knowledge of *in-vivo* cardiac and brain haemodynamics during the post-natal transition, and in particular how cardiovascular and cerebrovascular parameters change over time would bring valuable information for the management of the preterm population during this delicate phase. Moreover, whether specific conditions that characterize the clinical status of each individual infant exert a relevant influence on these parameters will help inform the ultimate goal of developing individualized approaches for monitoring, treatment and care.

Much of the physiological data currently available on transitional haemodynamics are based on pre-clinical or in-vitro experiments, whereas clinical evidence mainly relies upon intermittent techniques of haemodynamic assessment (e.g., functional echocardiography) or require invasive monitoring approaches (e.g., cerebral autoregulation assessment using continuous BP monitoring). We developed an integrated multiparametric monitoring system to investigate the haemodynamic changes occurring at a cardiovascular and cerebral level, including the evaluation of cerebrovascular reactivity, over the first 72 hours of life. As this monitoring is totally non-invasive, it was possible to extend this comprehensive evaluation to preterm infants.

The research objective addressed in this section aimed at defining the temporal patterns and main clinical determinants of cardiovascular and cerebrovascular parameters, measured non-invasively and continuously during the first 72 hours of life.

4.2. Methods and Statistics

Methods

Patient recruitment, ultrasound evaluation and data collection, including the multiple parameters obtained by non-invasive multiparametric monitoring, are described in detail in Chapter 3.

Using the ICM+ software, after the removal of time intervals with evidence of major artifacts, values of cTOI, cFTOE, CO_{EV}, HR_{EV}, ICON and SVR were averaged over 24-h periods (i.e., one value per each day of life) and used for statistical analysis.

For periods where the proportion of missing data <50%, the moving correlation coefficient between cerebral oxygenation and heart rate (TOHRx) was retrospectively calculated with the ICM+ software using 5-min time windows between 10-s average values of cTOI and HR (Figure 4.1), as previously described [101]. The ICM+ traces of each enrolled neonate were visually inspected, and the best quality signal among HR_{EV} and HR_{PO} was used for the calculation.

The physiological rationale of TOHRx is based on fact that in premature neonates HR is the main determinant of cardiac output, whereas the use of a 5-min window for TOHRx calculation has its rationale in the physiology of slow brain waves detected by NIRS. Zero or negative TOHRx indicate that CBF does not depend on total blood flow, which means that brain vasculature is able to self-regulate CBF. Positive TOHRx values, on the other hand, indicate that CBF is dependent on total blood flow, and therefore cerebrovascular reactivity may be impaired. This marker has been previously used to investigate the individual optimal values of MABP at which cerebral autoregulation is most effective.[212]
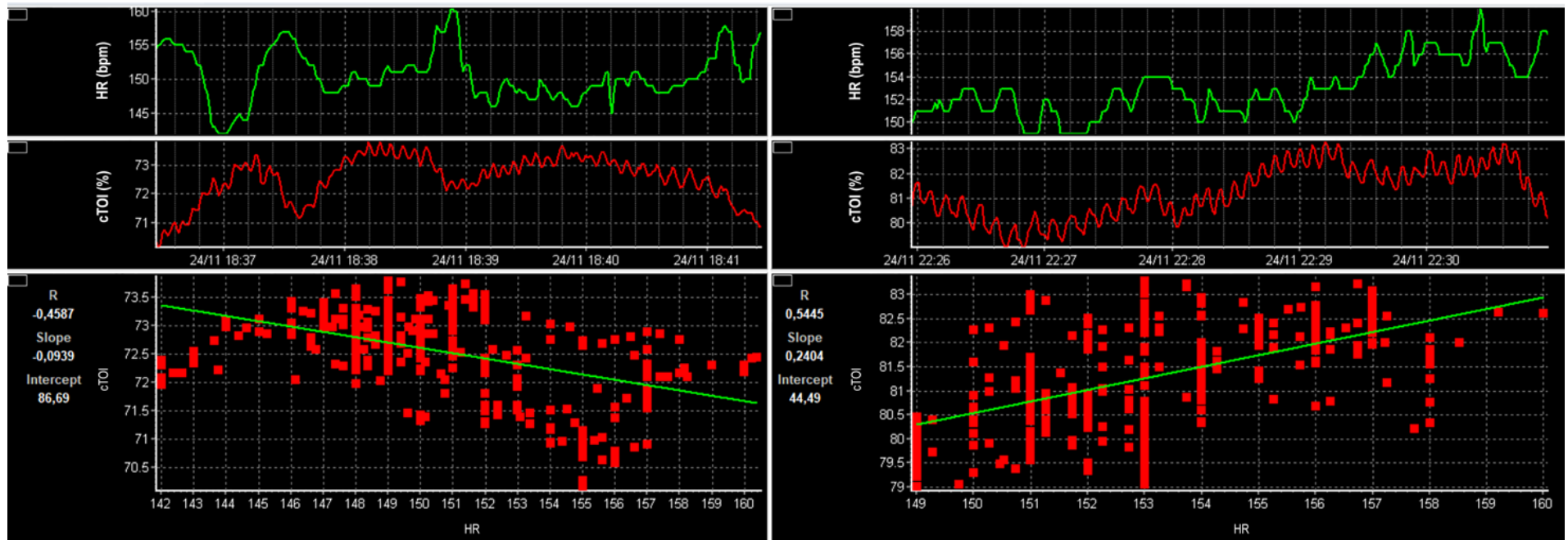
Figure 4.1. *ICM+ screenshot illustrating the calculation of the moving correlation coefficient (R) between cerebral oxygenation (cTOI) and the heart rate (HR), defined as TOHRx.*

Statistical analysis

Data distribution was evaluated using the Shapiro-Wilk test for normality. Continuous variables were expressed as median (IQR) or mean (SD) as appropriate, whereas categorical variables were summarized as frequencies and percentages.

Since cTOI, cFTOE, CO_{EV}, HR_{EV}, ICON and SVR did not follow a normal distribution, to account for repeated measurements on each subject, generalized linear mixed-effects models (GLMMs) using the days of life (day 1, 2 and 3) as within-subject repeated measures were used to evaluate time trends and the effect of relevant clinical factors on each outcome parameter. Fixed-effects hypothesis was tested using Satterthwaite's small-sample adjustment. Sequential Bonferroni adjustment was applied for multiple comparisons. Intercepts at the patient level constituted the random part of model, assuming equal variances and null covariances (scaled identity).

TOHRx followed a normal distribution; therefore, to account for repeated measurements on each subject, a linear mixed-effects model (LMM) was developed to analyse its time trends and the effect of relevant clinical factors. Fixed-effects hypothesis testing, multiple comparisons adjustment methods, random-component specification and covariance structure were the same as those of the previously described GLMM models.

To improve the LMM and GLMMs sensitivity, those variables whose status changed over time, such as MABP values, the ductal status (closed, restrictive or haemodynamically significant), dopamine (ongoing or not), dobutamine (ongoing or not) and the mode of respiratory support were handled as time-dependent covariates. Since both LMMs and GLMMs allow for unbalanced repeated measures, no imputation of missing data was performed. For each model, the magnitude of multicollinearity of model terms was analysed using the variance inflation factor; no collinearity issues were found. The list of the fixed effects included in the GLMMs and LMMs is detailed below:

- *Evaluation of time trends:* days of life, GA, ductal status, days of life by ductal status (all models); treatment with dopamine and/or dobutamine (CO, SV, HR, ICON and SVR models); umbilical Doppler status (cTOI, cFTOE and TOHRx models).

- *Evaluation of clinical determinants:* GA, Apgar score at 5 minutes, antenatal steroids administration, umbilical Doppler status, ductal status, dopamine administration, dobutamine administration, respiratory support modality. MABP was also included in SVR, cTOI, cFTOE and TOHRx models, whereas CO was added to cTOI and cFTOE models.

4.3. Results

As shown in the enrolment flow chart (Figure 4.2), a total of 72 preterm neonates fulfilling the inclusion criteria were enrolled between March 2018 and September 2020. Eight infants underwent sole NIRS and pulse oximeter monitoring, since EV was not available during the time window of the study monitoring. For the sake of data homogeneity, these infants were ruled out and only those with complete NIRS, EV and pulse oximetry data (*n=*64) were included in the data analysis.
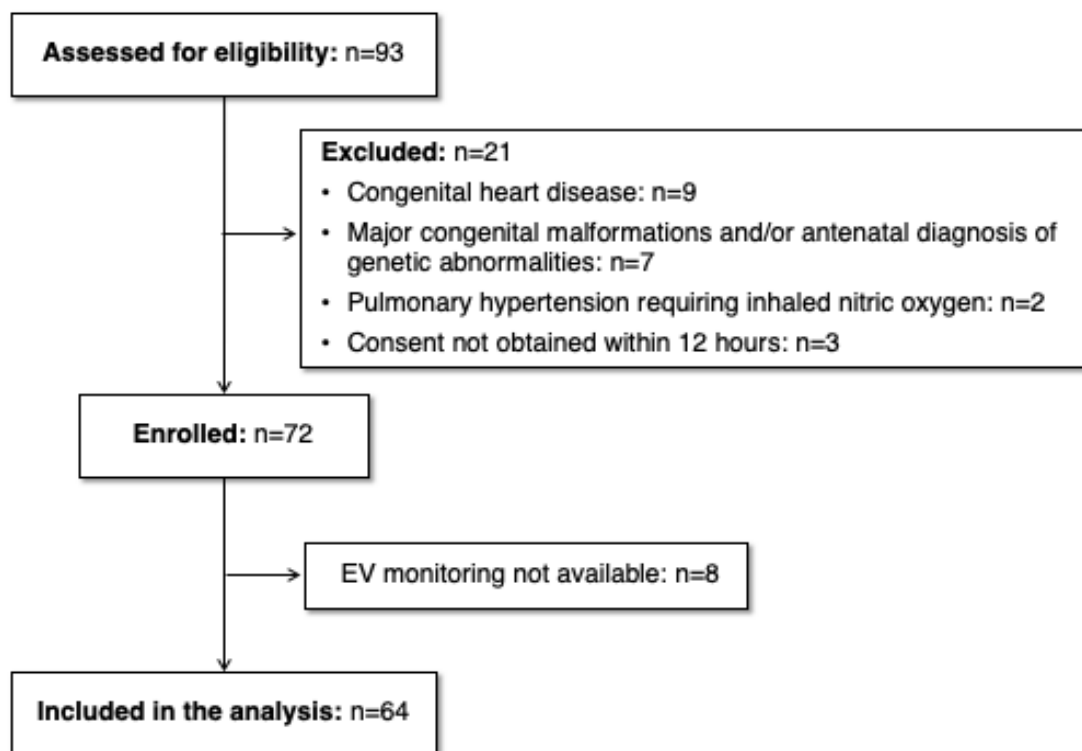
Figure 4.2. Flow chart of the infants' enrolment and inclusion. EV, electrical velocimetry.

The neonatal characteristics of the population included in this research are summarized in Table 4.1, while their clinical and haemodynamic features on day 1, 2 and 3 are provided in Table 4.2.

Table 4.1. *Neonatal characteristics of the study population.*

Neonatal characteristics	*n* = 64
Gestational age (weeks), mean (standard deviation, SD)	29.6 (2.7)
Birth weight (g), mean (SD)	1182 (345)
Length at birth (cm), mean (SD)	37 (3.7)
Head circumference at birth (cm), mean (SD)	26.8 (2.7)
Antenatal corticosteroids, n (%)	
Complete course	47 (73.4)
Incomplete course	12 (18.8)
Not given	5 (7.8)
Intrauterine growth restriction, n (%)	21 (32.8)
Umbilical artery Doppler status, n (%)	
AREDF w/ brain sparing	6 (9.4)
AREDF w/o brain sparing	12 (12.8)
Small for gestational age, n (%)	18 (28.1)
Caesarean section, n (%)	55 (86)
Male gender, n (%)	33 (51.6)
Twinhood, n (%)	18 (28.1)
Apgar score at 1 min, median (interquartile range [IQR])	7 (5-8)
Apgar score at 5 min, median (IQR)	9 (8-9)

Table 4.2. *Clinical and haemodynamic features of the study population during the transitional period.*

Monitoring period (days of life)	Day 1	Day 2	Day 3
Weight (g), mean (standard deviation, SD)	1176 (351)	1131 (344)	1078 (339)
Haemoglobin (g/dl), mean (SD)	15.9 (2.1)	15.4 (2.6)	15.3 (2.9)
Status of ductus arteriosus, n (%)			
Haemodynamically significant	35 (54.7)	17 (26.6)	12 (18.8)
Restrictive	19 (29.7)	19 (29.7)	5 (7.8)
Closed	10 (15.6)	28 (43.8)	47 (73.4)
Blood pressure (mmHg), mean (SD)			
Systolic	47 (6)	51 (7)	54 (6)
Diastolic	26 (5)	30 (6)	30 (5)
Mean	34 (5)	39 (6)	40 (5)
Respiratory support, n (%)			
Mechanical ventilation	16 (25)	15 (23.4)	14 (21.9)
Continuous Positive Airway Pressure	43 (67.2)	40 (62.5)	32 (50)
Nasal cannulas or self-ventilating in air	5 (7.8)	9 (14.1)	18 (28.1)
Surfactant administration, n (%)	35 (54.7)	38 (59.4)	38 (59.4)
Ongoing cardiovascular drugs, n (%)			
Dopamine	9 (14)	8 (12.5)	8 (12.5)
Dobutamine	15 (23.4)	13 (20.3)	12 (18.8)
Intraventricular haemorrhage, n (%) °			
Grade I	0 (0)	1 (1.6)	5 (7.8)
Grade II	1 (1.6)	2 (3.2)	2 (3.2)
Grade III	0 (0)	2 (3.2)	3 (4.7)

° classified accordingly to the maximum severity achieved.

According to our local NICU protocol, dobutamine was administered in the presence of hypotension (defined as a MABP lower than GA associated with any among steady tachycardia, capillary refill time >3 sec, decreased urine output or metabolic acidosis) [213,214] and echocardiographic evidence of impaired cardiac contractility, whereas dopamine was commenced in hypotensive infants without evidence of impaired cardiac contractility or who did not respond to dobutamine and/or volume expansion. The starting dosage of dopamine and dobutamine was 5 mcg/kg/min; none of the treated infants required higher doses. Based on the infant's haemodynamic response, dopamine was gradually tapered to 3 mcg/kg/min before suspension.

Daily echocardiographic features in the presence of a hsPDA are detailed in Table 4.3; a concomitant PFO was evident in all the infant. Of the 35 infants who initially presented with a hsPDA, 21 (60%) underwent spontaneous ductal closure. Pharmacological PDA treatment was required in 14 neonates (40%); of these, 8 were treated with a single paracetamol course, 3 with a single ibuprofen course and 3 with paracetamol followed by ibuprofen, due to lack of effectiveness to the first treatment course. Of the 14 infants requiring pharmacological PDA closure, 4 did not respond to pharmacological treatment and required surgical PDA ligation.

Of note, the number of infants who developed IVH within this group was 1 (grade II, 2.9%) on day 1, 4 (23.5%) on day 2 (of which: grade II, n=2; grade III, n=2), and 3 (25%) on day 3 (of which: grade 1, n=2; grade III, n=1). All the infants who developed a grade III IVH had evidence of diastolic reflow in the ACA at the ultrasound scans that preceded IVH detection.

Table 4.3. *Daily echocardiographic features of infants with a haemodynamically significant patent ductus arteriosus (hsPDA) during the transitional period.*

Monitoring period (days of life)	Day 1 (n=35)	Day 2 (n=17)	Day 3 (n=12)
Ductal size, median (interquartile range [IQR])			
Absolute diameter (mm)	2.1 (1.8-2.4)	2 (1.9-2.4)	2.4 (1.9-2.7)
Weight-indexed diameter(mm/kg)	2 (1.7-2.5)	2.2 (1.8-3)	2.9 (1.7-3.2)
Direction of transductal shunt, n (%)			
Predominantly or entirely right-to-left	1 (2.9)	0 (0)	0 (0)
Bidirectional	6 (17.1)	1 (5.9)	0 (0)
Predominantly or entirely left-to-right	28 (80)	16 (94.1)	12 (100)
Direction of shunt across the foramen ovale			
Predominantly or entirely right-to-left	1 (2.9)	0 (0)	0 (0)
Bidirectional	7 (20)	1 (5.9)	0 (0)
Predominantly or entirely left-to-right	27 (77.1)	16 (94.1)	12 (100)
LA:Ao ratio, median (IQR)	1.3 (1.2-1.6)	1.6 (1.5-1.7)	1.6 (1.4-1.8)
Diastolic reflow, n (%)			
Anterior cerebral artery	7 (20)	5 (29)	1 (8.3)
Descending aorta	4 (11.4)	2 (11.8)	1 (8.3)

Time trends of cardiovascular and cerebrovascular parameters during the transitional period

For each of the haemodynamic parameters, time trends over the first 72 hours after birth were evaluated using the models previously described; the list of the fixed effects included in each model has been listed in the Methods section of this chapter.

CO_{EV} time trends over the first 3 days of life are illustrated in Figure 4.3. CO_{EV} changed significantly over this period (p=0.024); in particular, the pairwise comparison revealed a significant CO_{EV} increase between day 1 and day 2 (β 20.094, 95% confidence interval [CI] 2.410-37.778; p=0.020), whereas a slight, non-significant decrease to intermediate values was observed between day 2 and 3.
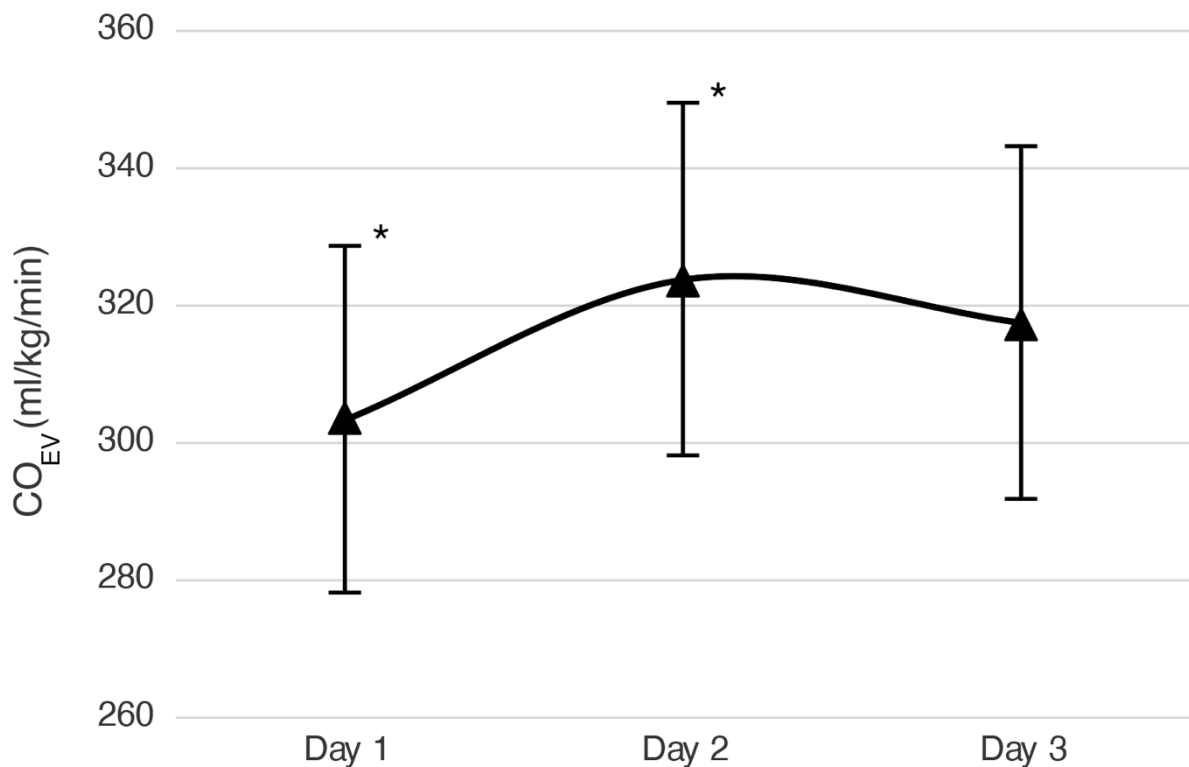

Figure 4.3. *Estimated means of cardiac output (CO_{EV}) during the first 3 days of life. The bars indicate the 95% confidence interval. Predictors are fixed at a gestational age of 29.6 weeks. The asterisks indicate contrasts significant at the 5% (*).*

Time trends of SV depicted a parabolic curve, with a tendence towards an increase between day 1 and day 2, followed by a parallel decrease between day 2 and day 3 (Figure 4.4). However, according to the results of the GLMM, these fluctuations were not statistically significant.
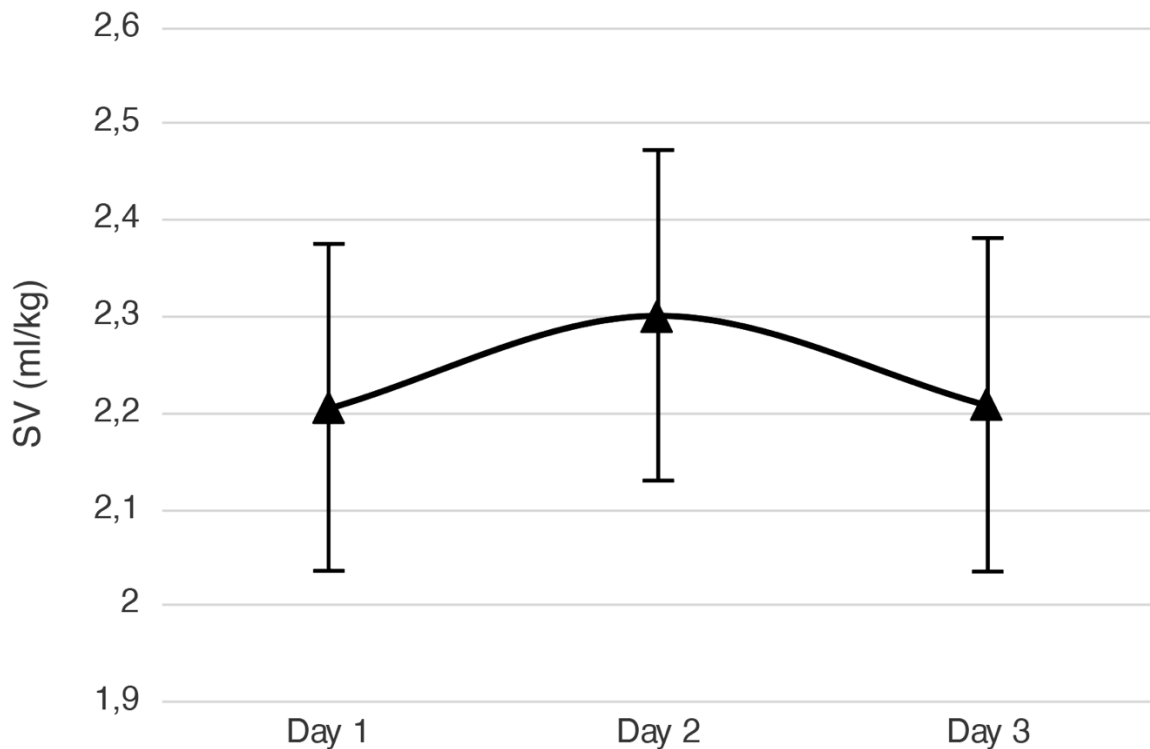
Figure 4.4. *Estimated means of stroke volume (SV) during the first 3 days of life. The bars indicate the 95% confidence interval. Predictors are fixed at a gestational age of 29.6 weeks.*

Time trends of HR, illustrated in Figure 4.5, showed significant changes over the first 3 days of life ($p<0.001$). After the first 24 hours, HR outlined a slight but significant increase, which was maintained until 72 hours of life (day 2 vs. day 1: β 3.505, 95% CI 1.367-5.643, p=0.001; day 3 vs. day 1: β 4.195, 95% CI: 1.810-6.580, p<0.001). No significant HR difference was observed between day 2 and day 3 at pairwise comparison.
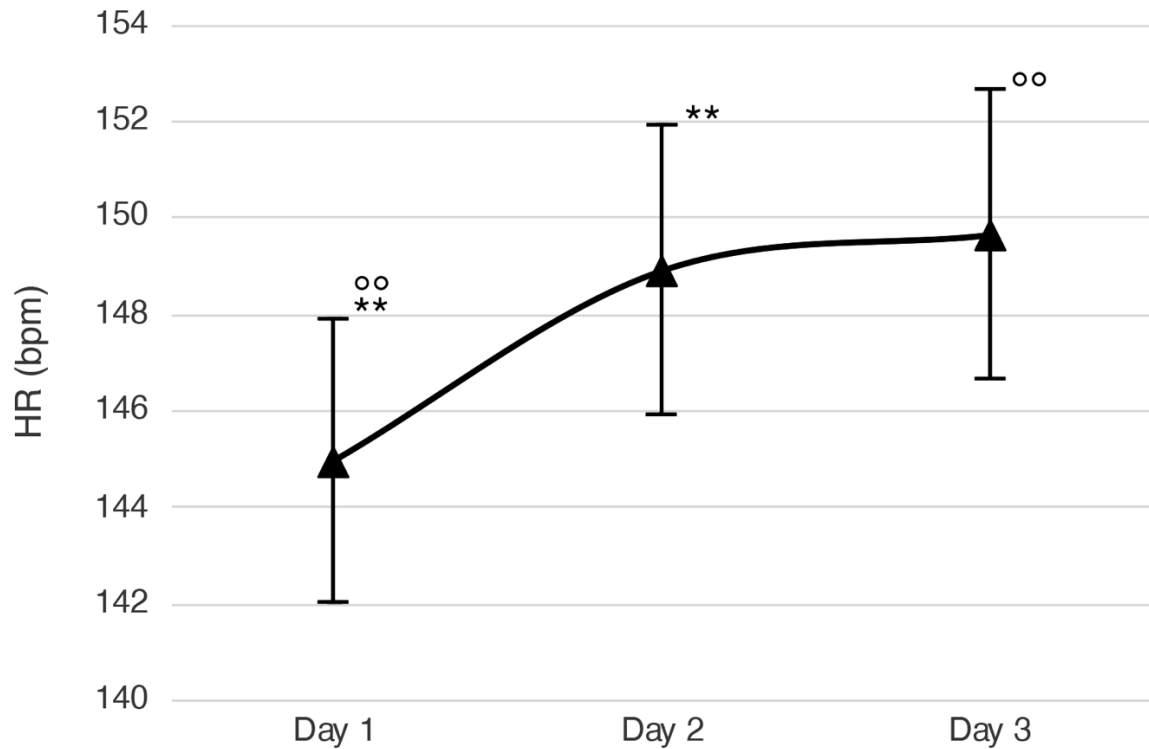
Figure 4.5. *Estimated means of heart rate (HR) during the first 3 days of life. The bars indicate the 95% confidence interval. Predictors are fixed at a gestational age of 29.6 weeks. The asterisks (**) and circles (°°) indicate contrasts significant at the 1%.*

Cardiac contractility changed significantly over the first 72 hours of life (p=0.026), outlining a progressive improvement, illustrated in Figure 4.6. In particular, ICON values on day 3 were significantly higher compared with those on day 1 (β 10.793, 95% CI 1.861-19.724, p=0.012), whereas the comparisons between day 1 and 2 and between day 2 and 3 did not reach statistical significance, despite of the increasing trends.

SVR values underwent significant changes over the first 72 hours of life (p<0.001), illustrated in Figure 4.7. In particular, SVR significantly increased on day 3 compared to day 1 (β 1.564, 95% CI 0.790-2.339, p<0.001) and 2 (β 1.115, 95% CI 0.467-1.762, p<0.001), whereas no significant difference was found within the first 48 hours after birth.
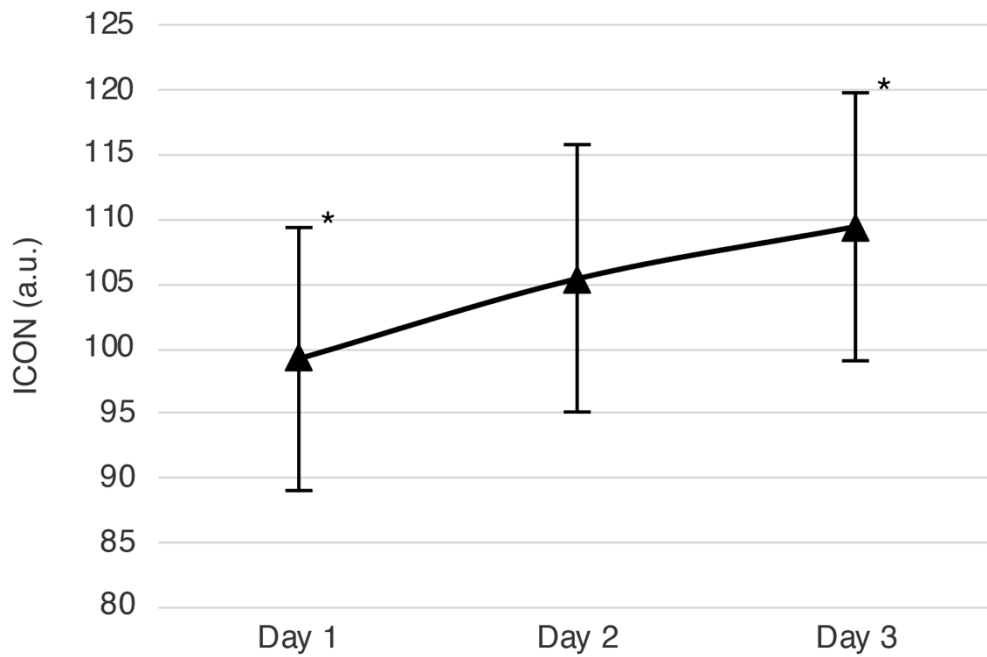
Figure 4.6. *Estimated means of cardiac contractility index (ICON) during the first 3 days of life. The bars indicate the 95% confidence interval. Predictors are fixed at a gestational age of 29.6 weeks. The asterisks indicate contrasts significant at the 5% (*).*
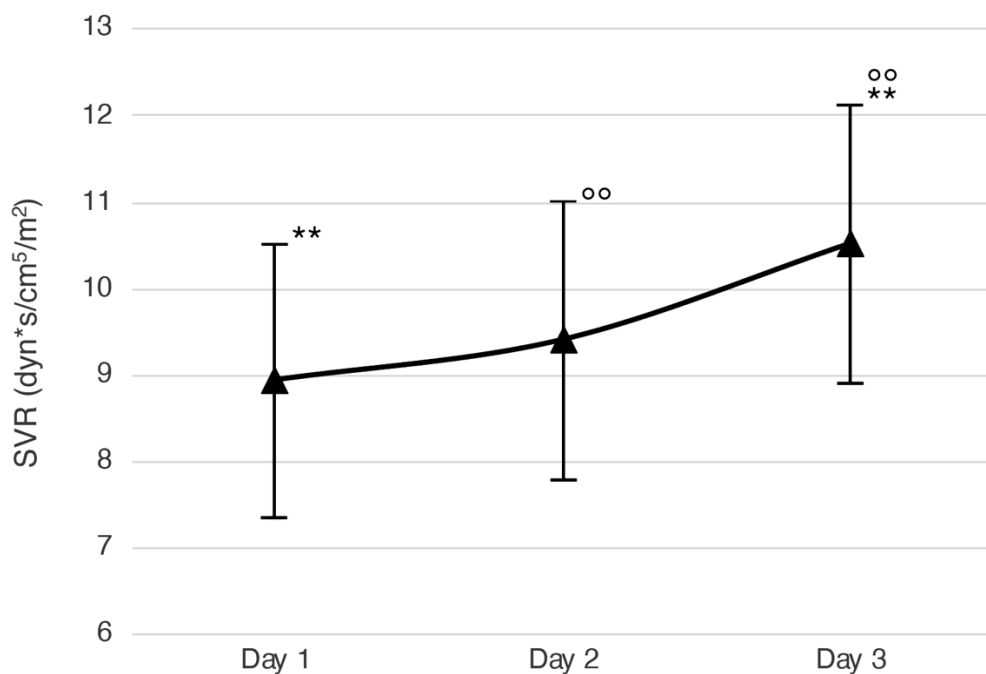
Figure 4.7. *Estimated means of systemic vascular resistance (SVR) during the first 3 days of life. The bars indicate the 95% confidence interval. Predictors are fixed at a gestational age of 29.6 weeks. The asterisks (**) and circles (°°) indicate contrasts significant at the 1%.*

Time trends of TOHRx over the first 72 hours of life are illustrated in Figure 4.8. Cerebrovascular reactivity showed a significant improvement during this period (p=001): in particular, TOHRx on day 3 were significantly decreased compared with day 1 (β -0.068, 95% CI -0.118,-0.019; p=0.003) and day 2 (β -0.057, 95% CI -0.102;-0.012, p=0.007). Although the TOHRx curve depicted a slight decrease during the first 48 hours of life, the difference between TOHRx values on day 1 and day 2 were not statistically significant.
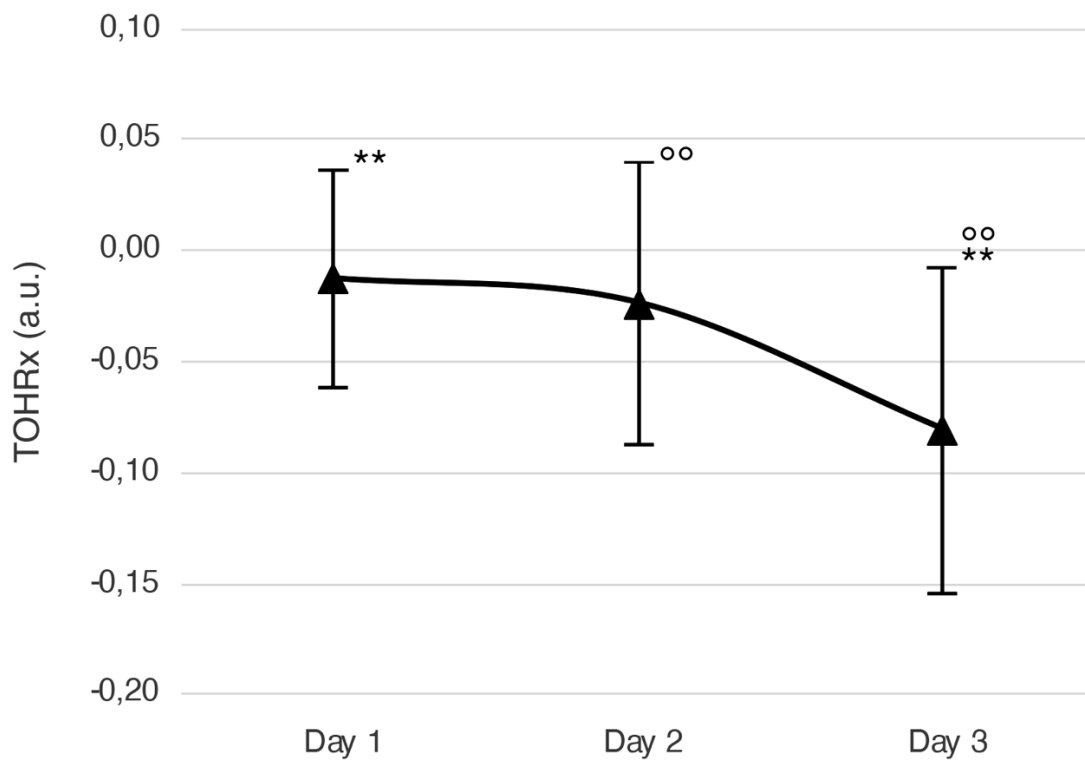
Figure 4.8. *Estimated means of the correlation coefficient between cerebral oxygenation and heart rate (TOHRx) during the first 3 days of life. The bars indicate the 95% confidence interval. Predictors are fixed at a gestational age of 29.6 weeks. The asterisks (**) and circles (°°) indicate contrasts significant at the 1%.*

Time trends of cTOI and cFTOE over the first 72 hours of life are illustrated in Figure 4.9 and Figure 4.10, respectively. These parameters remained overall stable over the first 72 hours of life and no significant differences emerged among their daily values at the GLMM models.
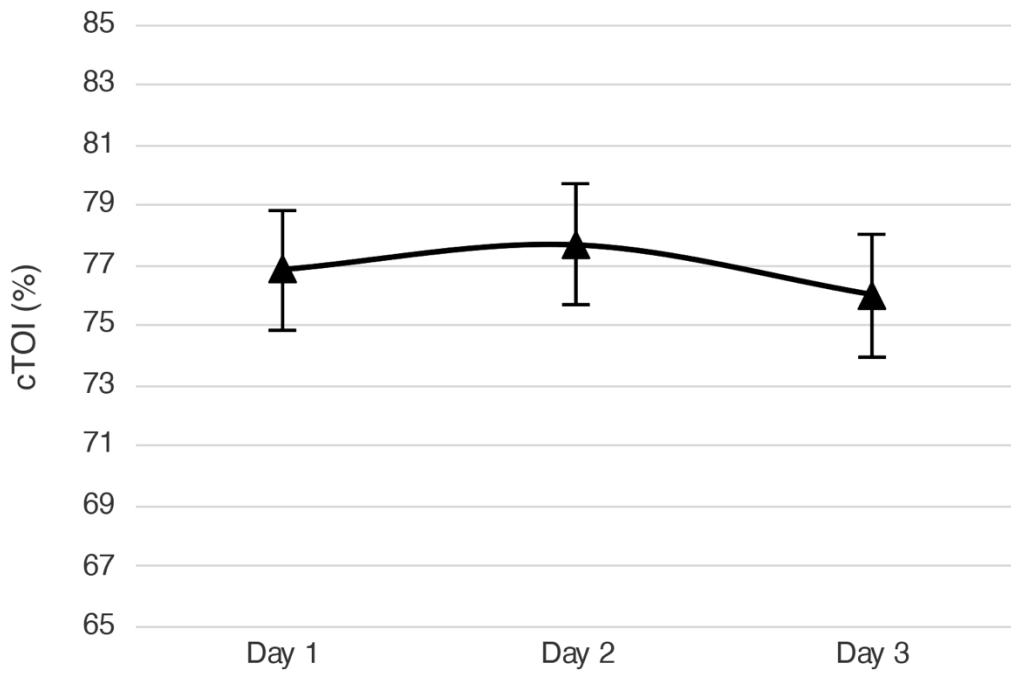
Figure 4.9. *Estimated means of cerebral tissue oxygenation index (cTOI) during the first 3 days of life. The bars indicate the 95% confidence interval. Predictors are fixed at a gestational age of 29.6 weeks.*
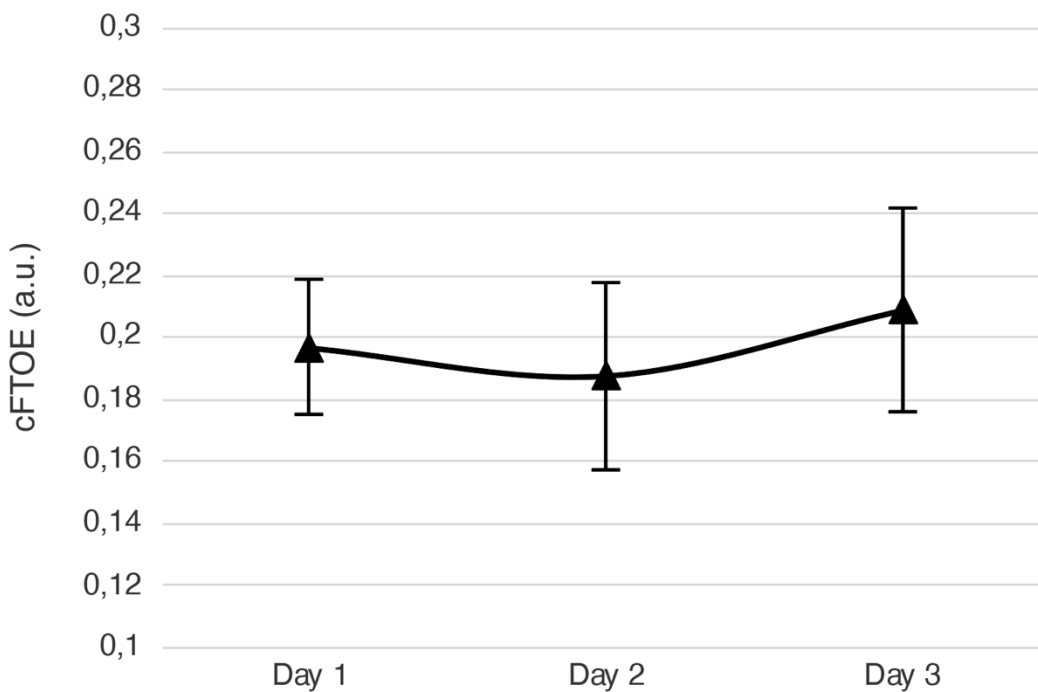

Figure 4.10. *Estimated means of cerebral fraction of tissue oxygen extraction (cFTOE) during the first 3 days of life. The bars indicate the 95% confidence interval. Predictors are fixed at a gestational age of 29.6 weeks.*

Given the known impact of PDA on transitional haemodynamic features, the time trends of the haemodynamic parameters were also stratified according to the infants' ductal status (Figure 4.11).

On day 1, the presence of a hsPDA was associated with significantly higher SV (p=0.011) and CO_{EV} values (p=0.006) compared with a closed or restrictive duct. Between 24 and 48 hours, infants with a closed or restrictive duct showed an increase in SV and CO_{EV}, and the difference with the hsPDA group, who maintained stationary SV and CO_{EV} values during the transitional period, was no longer significant.

With regard to HR, hsPDA was associated with an increase of this parameter from 24 hours onwards, which led to significantly higher mean HR values compared with those observed in infants with a restrictive or a closed duct (p <0.001 on day 2 and p=0.021 on day 3).

Although cardiac contractility improved in both groups during the transitional period, infants with a hsPDA showed higher ICON values compared to those with a restrictive or closed DA, with significant differences between the two groups on day 1 (0.009) and 3 (p=0.048).

With regard to SVR, infants with a restrictive or closed duct trended toward a gradual increase over the first 72 hours, whereas in those with a hsPDA, SVR remained stable between day 1 and day 2, before starting to increase on day 3. Although SVR levels after 24 hours of life were slightly lower in infants with a hsPDA, this difference was not significant.

Although the trend patterns in both groups showed a noticeable improvement of cerebrovascular reactivity after the first 48 hours of life, infants with a hsPDA had significantly higher values of TOHRx in on day 1 (p=0.001) and on day 2 (p=0.017) compared to those with a restrictive or a closed DA, indicating a poorer control of cerebral perfusion in relation to BP. The TOHRx reduction observed on day 3 was therefore steeper in infants with a hsPDA.
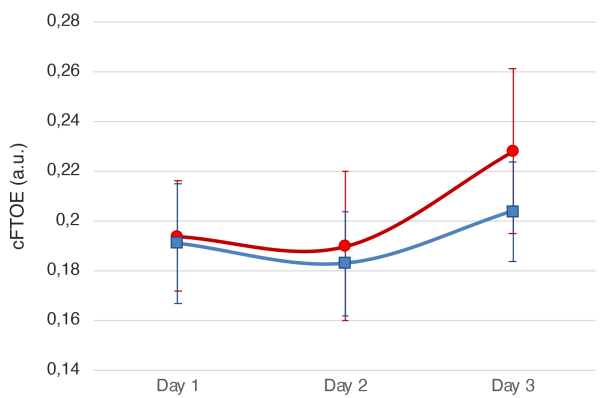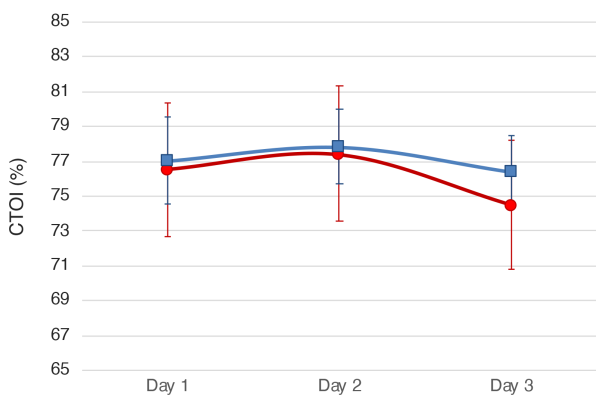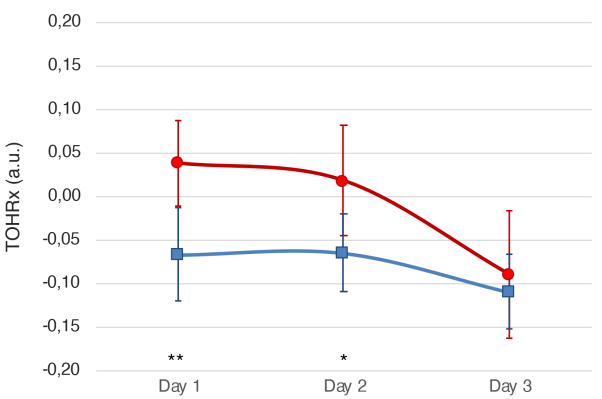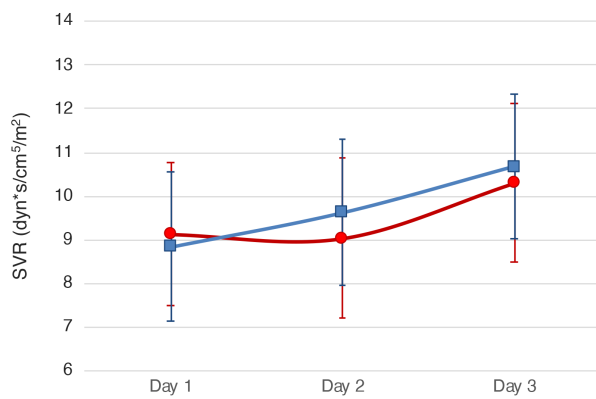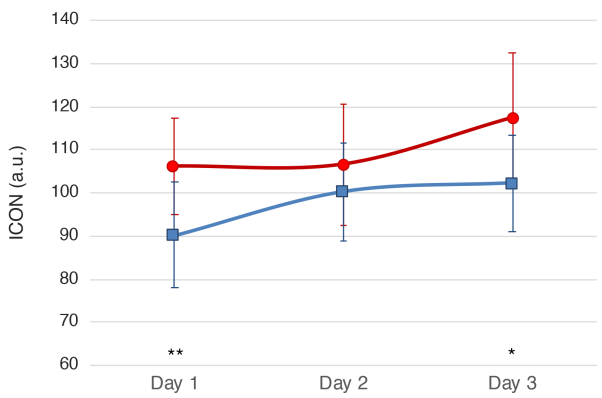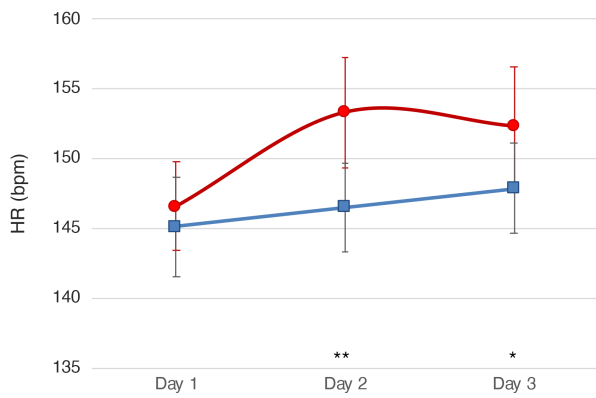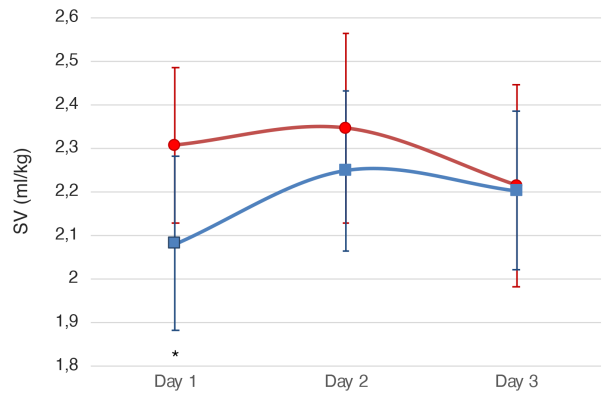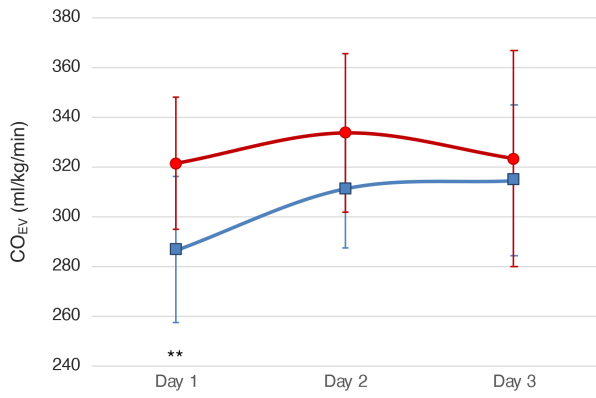
Figure 4.11. *Estimated means of cardiac output (CO$_{EV}$), stroke volume (SV), heart rate (HR), cardiac contractility (ICON), systemic vascular resistance (SVR), cerebral oxygenation (cTOI), cerebral fractional oxygen extraction (cFTOE) and of the correlation coefficient between cTOI and HR (TOHRx) during the first 3 days of life in neonates with a haemodynamically significant patent ductus arteriosus (hsPDA, red line and dots) or with a restrictive or closed duct (blue line and squares). Predictors are fixed at a gestational age of 29.6 weeks and adjusted for ongoing dopamine and dobutamine (CO$_{EV}$, SV, HR, ICON, SVR) and antenatal Doppler status (TOHRx, cTOI, cFTOE). The bars indicate the 95% confidence interval. The asterisks indicate contrasts significant at 5% (*) and 1% (**) between the two groups.*

Finally, cTOI and cFTOE trends in the two groups were evaluated. Overall time patterns of these cerebral haemodynamic parameters were stable in both groups; although infants with a hsPDA showed slightly lower cTOI and increased cFTOE values on day 3 compared to those with a restrictive or a closed duct, especially on day 3, no significant difference was observed at the between-group comparison.

Of note, due to their potential effects on the observed findings, it is important to emphasise that the present results have been corrected for GA (both cardiovascular and cerebrovascular parameters), ongoing dopamine and ongoing dobutamine treatment (cardiovascular parameters) and for antenatal Doppler status (cerebrovascular parameters). The graphs shown in Figure 4.11 are fixed at a GA of 29.6 weeks, which represents the mean value of the population included in this analysis.

Clinical determinants of cardiovascular and cerebrovascular haemodynamic parameters during the transitional period

For each of the haemodynamic parameters measured in this dissertation, a pool of antenatal, perinatal and postnatal clinical variables that make up the neonatal exposome during the transitional period was included as fixed effects in the GLMM and LMM models.

The GLMM results investigating the effects of relevant clinical characteristics on association CO_{EV} are shown in Table 4.4. CO_{EV} was significantly lower in infants with abnormal umbilical Doppler without evidence of antenatal brain sparing. Compared to those with a restrictive PDA or with a closed duct, infants with a hsPDA had a significantly higher CO_{EV}. Moreover, a significant CO_{EV} reduction was observed during dopamine administration.

The results of the GLMM evaluating the association between SV and relevant clinical characteristics are shown in Table 4.5. SV was significantly higher in infants with a hsPDA compared to those with a restrictive or closed DA, whereas a significant reduction of SV was observed during dopamine administration. Moreover, SV significantly increased with increasing GA.

The association between HR and relevant clinical characteristics is detailed in Table 4.6. A significant negative correlation between HR and GA was documented: the lower the GA, the higher the HR. Infants with echocardiographic evidence of a hsPDA had significantly higher HR compared to those with a restrictive PDA or a closed duct.

Results of the GLMM investigating the association between the cardiac contractility index and relevant clinical characteristics are shown in Table 4.7. A significant, positive correlation between ICON and GA was observed. Moreover, significantly higher ICON values were observed during dobutamine administration and in the presence of a hsPDA compared to a restrictive or a closed duct.

The association between SVR and relevant clinical characteristics is shown in Table 4.8. SVR was significantly and positively associated with mean arterial pressure. Infants with a haemodynamically significant PDA had lower SVR compared to those with a restrictive PDA or a closed duct, whereas

infants with antenatal evidence of umbilical Doppler impairment showed significantly increased SVR compared to those with normal umbilical flowmetry. A significant, negative correlation was observed between SVR and GA: the lower the GA, the higher the SVR. No significant associations were observed with the other variables included in the model.

Table 4.4. *Multivariable generalized linear mixed model evaluating the correlation between clinical variables and cardiac output (CO$_{EV}$). Abbreviations: AREDF, absent or reversed end-diastolic flow.*

Outcome: CO$_{EV}$ (l/kg/min)	Coefficient	Std. Error	95% Confidence Interval	P value
Intercept	*252.869*	*122.123*	*16.892; 498.846*	*0.036*
Gestational age	5.984	4.338	-2.570; 14.537	0.169
Apgar at 5 minutes	-14.496	9.761	-33.742; 4.751	0.139
Antenatal steroids				
Full course	1.368	22.379	-42.758; 45.495	0.951
Incomplete course or not given	*Ref.*			
Umbilical Doppler status				
AREDF, brain sparing	19.763	23.884	-27.331; 66.858	0.409
AREDF, no brain sparing	-54.637	26.591	-107.069; -2.205	**0.041**
Normal	*Ref.*			
Ductal status				
Haemodynamically significant	21.262	8.947	3.620; 38.904	**0.018**
Restrictive or closed	*Ref.*			
Dopamine administration				
Yes	-44.694	21.708	-87.498; -1.890	**0.041**
No	*Ref.*			
Dobutamine administration				
Yes	2.158	18.340	-34.004; 38.320	0.906
No	*Ref.*			
Respiratory support				
Invasive ventilation	31.994	23.074	-13.503; 77.490	0.167
Non-invasive ventilation	*Ref.*			

Table 4.5. *Multivariable generalized linear mixed model evaluating the correlation between clinical variables and stroke volume (SV). Abbreviations: AREDF, absent or reversed end-diastolic flow.*

Outcome: SV (ml/kg)	Coefficient	Std. Error	95% Confidence Interval	P value
Intercept	*0.398*	*0.851*	*-1.280; 2.076*	*0.641*
Gestational age	0.074	0.031	0.014; 0.135	**0.016**
Apgar at 5 minutes	-0.043	0.069	-0.179; 0.092	0.529
Antenatal steroids				
Full course	-0.034	0.159	-0.347; 0.278	0.830
Incomplete course or not given	*Ref.*			
Umbilical Doppler status				
AREDF, brain sparing	0.167	0.169	-0.166; 0.500	0.324
AREDF, no brain sparing	-0.321	0.182	-0.679; 0.038	0.080
Normal	*Ref.*			
Ductal status				
Haemodynamically significant	0.184	0.058	0.069; 0.298	**0.002**
Restrictive or closed	*Ref.*			
Dopamine administration				
Yes	-0.378	0.145	-0.663; -0.092	**0.010**
No	*Ref.*			
Dobutamine administration				
Yes	0.117	0.122	-0.123; 0.357	0.338
No	*Ref.*			
Respiratory support				
Invasive ventilation	0.165	0.155	-0.140; 0.470	0.287
Non-invasive ventilation	*Ref.*			

Table 4.6. *Multivariable generalized linear mixed model evaluating the correlation between clinical variables and heart rate (HR). Abbreviations: AREDF, absent or reversed end-diastolic flow.*

Outcome: HR (bpm)	Coefficient	Std. Error	95% Confidence Interval		P value
Intercept	*215.788*	*13.177*	*189.821;*	*241.755*	<0.001
Gestational age	-2.281	0.437	-3.142;	-1.420	**<0.001**
Apgar at 5 minutes	-0.322	1.018	-2.329;	1.685	0.752
Antenatal steroids					
Full course	-1.640	2.278	-6.130;	2.849	0.472
Incomplete course or not given	*Ref.*				
Umbilical Doppler status					
AREDF, brain sparing	0.405	2.609	-4.737;	5.547	0.877
AREDF, no brain sparing	-4.365	2.852	-9.985;	1.256	0.127
Normal	*Ref.*				
Ductal status					
Haemodynamically significant	2.433	1.214	0.040;	4.825	**0.046**
Restrictive or closed	*Ref.*				
Dopamine administration					
Yes	4.263	2.750	-1.155;	9.682	0.122
No	*Ref.*				
Dobutamine administration					
Yes	1.412	2.286	-3.093;	5.917	0.537
No	*Ref.*				
Respiratory support					
Invasive ventilation	-1.844	2.739	-7.242;	3.553	0.501
Non-invasive ventilation	*Ref.*				

Table 4.7. *Multivariable generalized linear mixed model evaluating the correlation between clinical variables and the cardiac contractility index (ICON). Abbreviations: AREDF, absent or reversed end-diastolic flow.*

Outcome: ICON (a.u.)	Coefficient	Std. Error	95% Confidence Interval		P value
Intercept	10.579	46.6318	-81.386;	102.543	0.821
Gestational age	3.238	1.609	0.065;	6.411	**0.046**
Apgar at 5 minutes	-2.356	3.603	-9.462;	4.749	0.514
Antenatal steroids					
Full course	5.844	8.250	-10.427;	22.114	0.480
Incomplete course or not given	*Ref.*				
Umbilical Doppler status					
AREDF, brain sparing	13.345	8.768	-3.947;	30.637	0.130
AREDF, no brain sparing	-2.874	11.150	-24.862;	19.114	0.797
Normal	*Ref.*				
Ductal status					
Haemodynamically significant	10.409	4.318	1.894;	18.924	**0.017**
Restrictive or closed	*Ref.*	.	.	.	.
Dopamine administration					
Yes	-16.908	9.292	-35.233;	1.418	0.070
No	*Ref.*				
Dobutamine administration					
Yes	16.496	7.978	0.762;	32.231	**0.040**
No	*Ref.*				
Respiratory support					
Invasive ventilation	11.326	9.749	-7.901;	30.554	0.247
Non-invasive ventilation	*Ref.*				

Table 4.8. *Multivariable generalized linear mixed model evaluating the correlation between clinical variables and systemic vascular resistance (SVR). Abbreviations: AREDF, absent or reversed end-diastolic flow.*

Outcome: SVR (dyn s/cm^5/m^2)	Coefficient	Std. Error	95% Confidence Interval	P value
Intercept	53.553	8.101	37.570; 69.356	*<0.001*
Gestational age	-1.875	0.302	-2.470; -1.280	**<0.001**
Apgar at 5 minutes	0.912	0.688	-0.445; 2.268	0.186
Antenatal steroids				
Full course	0.168	1.593	-2.975; 3.311	0.916
Incomplete course or not given	*Ref.*			
Umbilical Doppler status				
AREDF, brain sparing	5.032	1.700	1.679; 8.386	**0.003**
AREDF, no brain sparing	4.687	1.597	1.536; 7.838	**0.004**
Normal	*Ref.*			
Ductal status				
Haemodynamically significant	-1.528	0.481	-2.478; -0.579	**0.002**
Restrictive or closed	*Ref.*			
Dopamine administration				
Yes	0.237	1.139	-2.011; 2.484	0.836
No	*Ref.*			
Dobutamine administration				
Yes	0.493	1.010	-1.489; 2.476	0.624
No	*Ref.*			
Respiratory support				
Invasive ventilation	-0.020	1.234	-2.415; 2.455	0.987
Non-invasive ventilation	*Ref.*			
Mean arterial blood pressure	0.087	0.033	0.021; 0.153	**0.010**

The results of the GLMM investigating the association between cTOI and relevant clinical characteristics are shown in Table 4.9. A significant, positive correlation was observed between cTOI and GA. Cerebral oxygenation was found to be significantly associated with cardiac output: higher CO values were associated with an increased cTOI. No significant associations were observed with the other variables included in the model.

The association between cFTOE and relevant clinical characteristics are shown in Table 4.10. A significant, negative correlation was observed between cFTOE and GA; cerebral tissue oxygen extraction was increased in more preterm infants. Moreover, we observed a significant association between antenatal steroids and cFTOE, which was reduced if the infants' mothers had received a full steroid course.

The LMM results investigating the association between TOHRx and relevant clinical characteristics are shown in Table 4.11. A significant inverse correlation was found between TOHRx and MABP, indicating that the lower the blood pressure, the higher the risk of impaired cerebrovascular reactivity. Infants with antenatal evidence of abnormal umbilical Doppler and remodelling of cerebral blood flow experienced a significant impairment of cerebrovascular reactivity during the first 72 hours of life. Similarly, the presence of a hsPDA was associated with significantly higher TOHRx values, indicating altered cerebrovascular reactivity.

Table 4.9. *Multivariable generalized linear mixed model evaluating the correlation between clinical variables and cerebral oxygenation (cTOI). Abbreviations: AREDF, absent or reversed end-diastolic flow.*

Outcome: cTOI (%)	Coefficient	Std. Error	95% Confidence Interval	P value
Intercept	*48.469*	*9.381*	*29.447; 66.970*	*<0.001*
Gestational age	0.778	0.313	0.161; 1.394	**0.014**
Apgar at 5 minutes	-0.066	0.696	-1.439; 1.307	0.925
Antenatal steroids				
Full course	2.486	1.572	-0.615; 5.586	0.115
Incomplete course or not given	*Ref.*			
Umbilical Doppler status				
AREDF, brain sparing	0.209	1.682	-3.109; 3.526	0.901
AREDF, no brain sparing	0.462	2.069	-3.618; 4.542	0.824
Normal	*Ref.*			
Ductal status				
Haemodynamically significant	0.023	0.950	-1.850; 1.896	0.981
Restrictive or closed	*Ref.*			
Dopamine administration				
Yes	-1.299	1.892	-5.030; 2.431	0.493
No	*Ref.*			
Dobutamine administration				
Yes	-1.116	1.616	-4.303; 2.071	0.491
No	*Ref.*			
Respiratory support				
Invasive ventilation	-0.771	1.966	-4.649; 3.107	0.695
Non-invasive ventilation	*Ref.*	.		
Cardiac output	0.016	0.006	0.003; 0.028	**0.014**
Mean arterial blood pressure	-0.025	0.069	-0.162; 0.111	0.714

Table 4.10. *Multivariable generalized linear mixed model evaluating the correlation between clinical variables and cerebral fraction of tissue oxygen extraction (cFTOE). Abbreviations: AREDF, absent or reversed end-diastolic flow.*

Outcome: cFTOE (a.u.)	Coefficient	Std. Error	95% Confidence Interval	P value
Intercept	*0.398*	*0.079*	*0.241; 0.554*	*<0.001*
Gestational age	-0.006	0.003	-0.011; -0.001	**0.036**
Apgar at 5 minutes	0.003	0.005	-0.008; 0.013	0.621
Antenatal steroids				
Full course	-0.030	0.014	-0.058; -0.003	**0.033**
Incomplete course or not given	*Ref.*			
Umbilical Doppler status				
AREDF, brain sparing	0.005	0.015	-0.025; 0,036	0.736
AREDF, no brain sparing	-0.001	0.027	-0.054; 0.053	0.981
Normal	*Ref.*			
Ductal status				
Haemodynamically significant	-0.003	0.009	-0.020; 0.015	0.782
Restrictive or closed	*Ref.*			
Dopamine administration				
Yes	0.021	0.025	-0.029; 0.071	0.409
No	*Ref.*			
Dobutamine administration				
Yes	0.018	0.020	-0.021; 0.058	0.366
No	*Ref.*			
Respiratory support				
Invasive ventilation	-0.002	0.017	-0.036; 0.032	0.910
Non-invasive ventilation	*Ref.*			
Cardiac output	-0.185	0.070	-0.323; -0.047	**0.009**
Mean arterial blood pressure	0.001	0.001	-0.001; 0.002	0.273

Table 4.11. *Multivariable linear mixed model evaluating the correlation between clinical variables and moving correlation coefficient between heart rate and cerebral oxygenation (TOHRx). Abbreviations: AREDF, absent or reversed end-diastolic flow.*

Outcome: TOHRx (a.u.)	Coefficient	Std. Error	95% Confidence Interval	P value
Intercept	*0.108*	*0.172*	*-0.236; 0.453*	*0.532*
Gestational age	-0.003	0.006	-0.014; 0.008	0.602
Apgar at 5 minutes	-0.003	0.013	-0.028; 0.022	0.788
Antenatal steroids				
Full course	-0.008	0.029	-0.065; 0.049	0.775
Incomplete course or not given	*Ref.*			
Umbilical Doppler status				
AREDF, brain sparing	0.110	0.030	0.049; 0.171	**0.001**
AREDF, no brain sparing	0.062	0.039	-0.015; 0.141	0.102
Normal	*Ref.*			
Ductal status				
Haemodynamically significant	0.093	0.023	0.048; 0.138	**<0.001**
Restrictive or closed	*Ref.*			
Dopamine administration				
Yes	0.050	0.038	-0.027; 0.126	0.199
No	*Ref.*			
Dobutamine administration				
Yes	0.019	0.034	-0.047; 0.086	0.565
No	*Ref.*			
Respiratory support				
Invasive ventilation	0.052	0.040	-0.027; 0.132	0.196
Non-invasive ventilation	*Ref.*			
Mean arterial blood pressure	-0.004	0.002	-0.007; -0.001	**0.015**

Overall, these results allowed the identification of three main clusters of factors that exerted a significant, independent influence on both cardiovascular and cerebrovascular haemodynamics. These clusters were *antenatal Doppler status*, *gestational age at birth* and *ductal status*, that respectively contributed to the antenatal, perinatal and postnatal individual characteristics of each infant.

For this reason, a graphical representation of the cardiovascular and cerebrovascular haemodynamic profiles that emerged in relation to different features of these three clinical determinants was elaborated (Figure 4.12). For the sake of clarity, the estimated z-score means of the previously described multivariate models were included in the charts and GA was stratified according with the definitions standardly adopted in neonatal nomenclature: extremely preterm (<28 weeks), very preterm (28-31 weeks) and moderately preterm (≥32 weeks).

Figure 4.12 (page 105). *Radar charts of cardiovascular and cerebrovascular haemodynamic profiles according to the antenatal Doppler status (A), gestational age (B) and ductal status (C) of the enrolled infants. The radial axis values indicate the estimated z-score means of the parameters included in each chart.*

Abbreviations: AREDF, absent or reversed end-diastolic flow; cTOI, cerebral tissue oxygenation index; cFTOE, cerebral fraction of tissue oxygen extraction; CO, cardiac output; HR, heart rate; HS, haemodynamically significant; ICON, cardiac contractility index; SV, stroke volume; SVR, systemic vascular resistance; TOHRx, correlation coefficient between cTOI and HR.
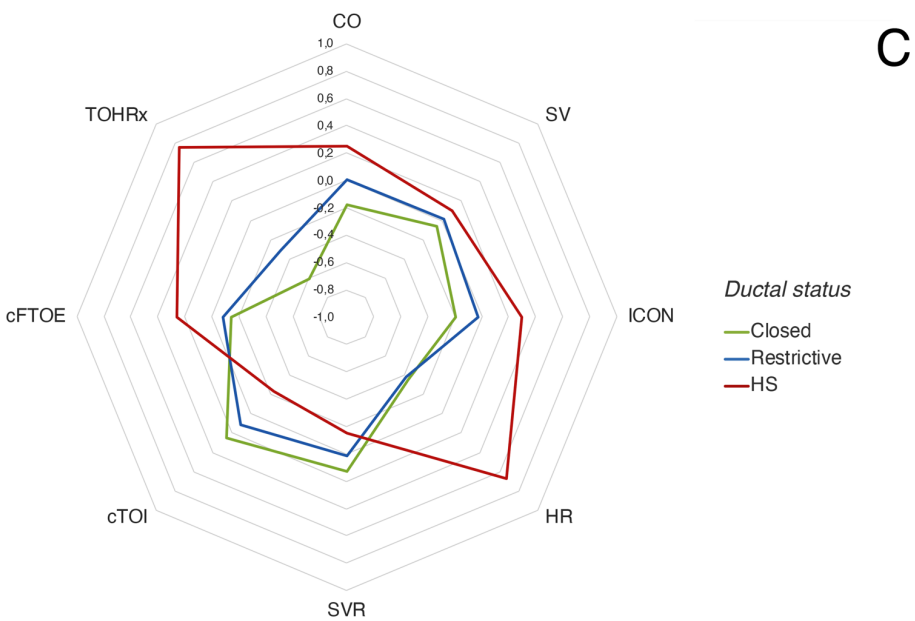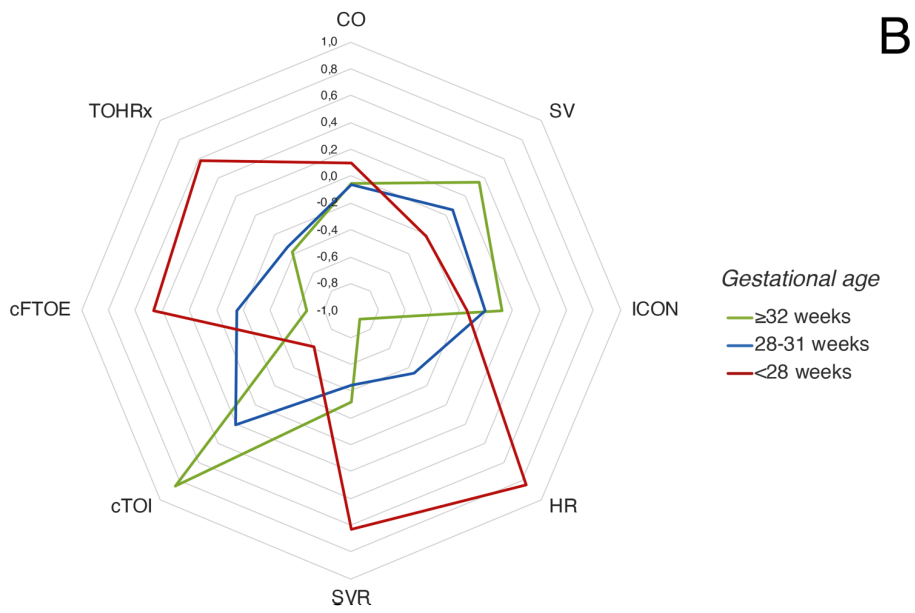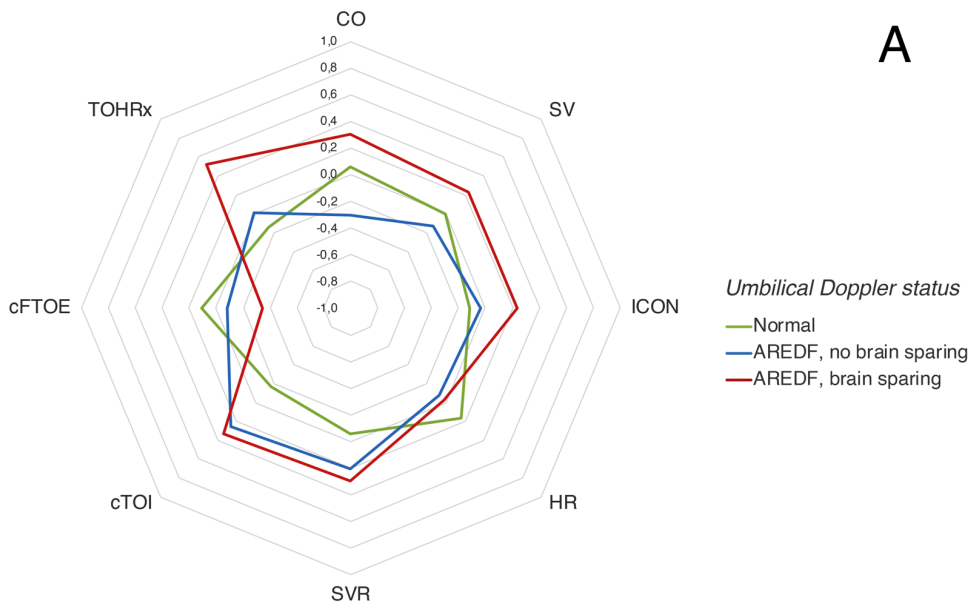
4.4. Discussion

From the results presented, cardiovascular and cerebrovascular haemodynamics during the first 72 hours of life in preterm infant undergo specific fluctuations reflecting the circulatory adaptation to postnatal life. Furthermore, the adaptive responses to this haemodynamic transition are significantly influenced by specific antenatal, perinatal and postnatal conditions that contribute to determine individual haemodynamic profiles.

Temporal patterns of cardiovascular and cerebrovascular parameters during the transitional period

The evaluation of the temporal patterns of the main cardiovascular parameters has provided a multifaceted picture of the adaptive functional changes occurring during the transitional period.

- *Temporal patters of cardiovascular parameters and influence of a haemodynamically significant patent ductus arteriosus*

Cardiac output is the result of the interaction between preload, myocardial contractility, heart rate and afterload. A significant increase in CO was observed between day 1 and day 2, whereas on day 3, a slight, non-significant decrease. Similar trend patterns have been previously reported by Noori et al. in extremely preterm infants during the transitional period [47]. The temporal patterns of the two direct determinants of CO, namely SV and HR, were then assessed. Although SV fluctuations within the first three days of life did not reach statistical significance, a trend toward an increase of SV was observed between 24 and 48 hours, followed by a slight decrease between 48 and 72 hours of life. After the first 24 hours HR showed a small but significant increase, which was maintained until 72 hours of life.

The CO trend patterns observed during the transitional period resembled the underlying changes of SV and HR. In particular, both these parameters contributed to the significant CO increase observed

between 24 and 48 hours. These findings are consistent with data obtained by Cappelleri et al. in late preterm infants during the first 48 hours of life using a non-invasive cardiac output monitoring based on thoracic bioreactance [215]; in their study, the increase of CO was predominantly driven by SV rather than HR. The inclusion of infants with lower GA, which is associated with an increased resting HR, may explain the influence of HR on CO observed in the present data.

Cardiac contractility gradually improved over the first 72 hours after preterm birth, with a statistically significant increase between day 1 and day 3. Due to the structural and functional immaturity of the preterm myocardium, the contractile function of premature neonates is often reduced; however, consistent with the present results, a significant improvement in cardiac contractility has been previously reported in very-low-birth-weight infants over the first 5 days of life [21]. These findings support the evidence of a gradual adaptation of myocardial function to the postnatal changes in systemic haemodynamics, which may be driven by a progressive increase in intracellular calcium influx during the early postnatal period [13].

SVR rose significantly after the first 48 hours of life. This increase in afterload may have played a role in determining the slight CO reduction observed between day 2 and day 3, which was mainly driven by SV. On the other hand, the improvement in cardiac contractility and increase in HR observed from 24 hours onwards may have prevented a significant reduction in CO in face of the raised afterload.

Several echocardiographic studies have investigated transitional changes in cardiovascular function. While some studies considered early transitional data as a whole [216] or focused on the first 24 hours of life [18,217,218], others performed serial evaluations over the first 48 [172,219,220] or 72 hours after birth [47]. In two echocardiographic studies performed on extremely preterm infants, a significant improvement in tissue Doppler imaging velocities of septum, left and right ventricle [219] and significantly increased CO, septal peak systolic and early diastolic strain rate have been reported between the first and the second day of life. Although no difference was observed in left ejection or

shortening fractions [220], tissue Doppler imaging and myocardial deformation measurements are able to detect subclinical myocardial dysfunctions before ventricular impairment becomes clinically apparent [221]. Sirc et al. described a progressive LVO increase in preterm infants <1250g within the first 48 hours, which resulted from improvement in the diastolic relaxation of the left ventricle [172]. This finding is in line with the increased SV and CO that we observed between day 1 and day 2. Noori et al. [47] performed a 12-hourly echocardiographic evaluation of LVO, RVO and left ventricular myocardial performance index over the first 72 hours of life in a small cohort of extremely preterm infants who developed IVH during this period compared with those who did not. The latter group underwent a trend toward a slight LVO increase on day 2, similar to that observed in the present results, whereas the myocardial performance of the left ventricle remained stable over time.

Although the dynamic changes observed in cardiovascular parameters may be multifactorial, it is not possible to disregard the role of PDA on the observed findings. For these reasons, the patterns of these parameters were also assessed in relation to the daily ductal status and compared between infants with a hsPDA and those with a restrictive or a closed duct.

The present results confirm a significant role of ductal status on cardiovascular transitional haemodynamics. In particular, the presence of a hsPDA during the first 24 hours of life was associated with significantly increased mean values of SV and CO and an enhanced cardiac contractility. Given that 80% of the infants with a hsPDA showed a predominantly or entirely left-to-right shunt across the DA following the first echocardiographic evaluation, we can postulate that the rise in venous return resulting from the transductal shunt transiently enhance the tension developed by the cardiac muscle fibres by extending the myocyte sarcomere length according to the Frank-Starling law. This assumes that SV values lie in the steeper part of the curve during this early phase.

After the second day of life, SV in the hsPDA group did not increase further, but rather showed a slight decrease on day 3. This could be ascribed to the establishment of a left-to-right shunt across the foramen ovale [222,223], which may have contributed to reduce the volume overload on the left

sections. During the same period, a significant rise in HR was observed in infants with a hsPDA compared to those with a restrictive or closed DA. Since these results were adjusted for ongoing inotropes and GA, this increase in HR likely reflects a compensatory mechanism aimed at the maintenance of stable CO levels in the presence of a persistent transductal left-to-right shunt. However, the few data currently available investigating the relationship between HR and hsPDA, evaluated during different time periods (i.e., before pharmacological or surgical DA closure) have yielded controversial results [26,224,225]. On day 2 and 3, CO was still slightly higher in hsPDA infants than in those with a non-significant or closed DA; however, the improvement in CO observed in the latter group contributed to the lack of statistical between-group difference at these time points.

In infants whose DA underwent a physiological closure or showed non-significant haemodynamic characteristics, the time patterns of CO, HR, ICON and SVR were characterized by a progressive increase throughout the transitional period, suggesting a gradual improvement of the overall cardiovascular function. A progressive improvement in calcium handling [226], which plays an important role in both cardiac contractility and vascular tone, may underlie the observed findings. Moreover, HR, cardiac contractility and SVR are largely controlled by the autonomic nervous system and catecholamines [227]. During gestation, the autonomic control of the cardiovascular system undergoes considerable development; however, the sympathetic branch develops more rapidly than the parasympathetic one, and this non-synchronous maturation underlies the predominant sympathetic effects observed in preterm infants in the early phases after birth [228]. Also catecholamines play a critical role during this phase: the increase in epinephrine and norepinephrine levels that typically follows cord clamping is heightened in preterm infants, although this rise occurs more slowly (i.e. within hours rather than minutes), probably due to their immaturity [229]. We can therefore postulate a possible modulating role for both sympathetic maturation and catecholamine rise in the observed cardiovascular patterns.

- *Temporal patters of cerebrovascular parameters and influence of a haemodynamically significant patent ductus arteriosus*

Cerebral autoregulation is aimed at maintaining stable cerebral perfusion despite fluctuating blood pressure. However, since this mechanism is not an "on-off" phenomenon, depending on the infant's level of immaturity and upon other underlying factors, it might be present, attenuated, or absent at different given times [208]. The failure of the preterm cerebral vasculature to maintain a stable CBF over a wide range of systemic BP results in the so-called pressure-passive circulation [75], whose possible role in the development of IVH has been previously described [48,89].

According to the present results, a significant improvement in cerebrovascular reactivity was observed from 48 hours of life onwards. This timing coincides with the period of highest IVH risk [230] and includes the transitional phase characterized by a high incidence of hypotension [213]. In this regard, we observed a significant independent relationship between daily-averaged MABP and cerebrovascular reactivity: the lower the blood pressure, the higher the TOHRx. A similar association had been previously reported [93,188], suggesting that in preterm infants the baseline MABP may lie closer to the lower limit of the autoregulation range.

The presence of a left-to-right transductal shunt may contribute to lower BP and to influence cerebrovascular reactivity in this delicate phase. In this regard, transitional TOHRx trends were also evaluated in relation to the DA status. During the first 48 hours after birth, infants with a hsPDA showed significantly higher values of TOHRx compared to those with a non-significant or closed duct, independently of their gestational age. This finding suggests that the haemodynamic perturbances associated with a hsPDA may challenge the physiological mechanisms of cerebral autoregulation and, together with the evidence of a hsPDA-related cerebral diastolic steal in all the 3 infants who developed severe IVH during the transitional period, provides indirect support to the available evidence on the possible predisposing role of hsPDA on IVH development [32]. However, due to the low number of infants presenting with an IVH during the transitional period in this study

(in particular of high grade), a powered statistical evaluation of the trend patterns in relation to the development of this complication was not feasible.

Although not statistically significant, the mild fluctuations of cTOI and cFTOE observed during the first 72 hours respectively resembled and mirrored the pattern previously described for CO. Similar parabolic patterns were depicted by Alderliesten et al. in their reference values curves for both cerebral oxygenation and oxygen extraction [174]. These authors also reported a non-significant trend toward a lower cerebral oxygenation and an increased cFTOE in infants with a hsPDA, especially on day 3. A similar finding was observed in the present cohort, when data were evaluated in relation to the ductal status. However, as in the study by Alderliesten et al., these differences did not reach statistical significance; this is consistent with most of the available literature investigating the relationship between cerebral oxygenation and hsPDA [229–232], which failed to prove a significant association.

- *Conclusions*

Overall, the present data suggest that cardiovascular function gradually improves over the first 72 hours of life, reflecting the underlying adaptation to postnatal circulation. This improvement was also consistent with the progressive increase in MABP observed during the transitional period. The adoption of continuous EV monitoring for this integrated haemodynamic evaluation has provided valuable information to elicit the in-vivo trajectory of PDA-related physiological changes during transition; however, echocardiographic assessment remains crucial not only to ascertain the presence of a hsPDA, but also to assess the function of left and right cardiac sections and to validate the pathophysiological observations obtained with non-invasive CO monitoring.

- *Limitations*

The increasing ranges of the 95% CIs of the daily parametric values from day 1 to 3 in infants with a hsPDA (see Figure 4.11) reflect the shift in the ductal status from haemodynamically significant to restrictive or closed observed in the enrolled infants during the transitional period, documented in

Table 4.2. Due to the progressive decrease of infants in the hsPDA group, this shift may represent a potential limitation to the assessment of cardiovascular and cerebrovascular haemodynamic fluctuations in relation to the ductal status; hence, the present results, and especially those observed on day 3, need to be further confirmed on larger samples.

Clinical determinants of cardiovascular and cerebrovascular haemodynamic parameters during the transitional period

In addition to the temporal patterns of cardiovascular and cerebrovascular haemodynamic parameters, the influence that several antenatal, perinatal and postnatal factors exert on these parameters during the transitional phase was also evaluated.

- *Haemodynamically significant patent ductus arteriosus*

The presence of a hsPDA was associated with higher values of stroke volume, heart rate, cardiac output and increased cardiac contractility. These findings, that are consistent with the temporal patterns of these parameters observed in infants with a hsPDA, reflect the volume overload associated to the left-to-right transductal shunt. Similar increases in LVO and SV, evaluated by echocardiography, have been reported in preterm infants with a hsPDA [225,231]. By stretching the myocyte sarcomere, the resulting increase in the venous return to the left atrium may enhance the force generated during the ventricle contraction, which further contributes to maintenance of the SV and CO.

Previous echocardiographic and cardiovascular MRI studies failed to demonstrate a significant association between myocardial contractility and the presence of a hsPDA [223,232,233]; however, this available literature did not investigate early postnatal transition, but later phases, when the persistence of a hsPDA may have resulted in cardiac function remodelling.

As previously discussed, the higher resting HR observed in infants with a hsPDA may reflect a compensatory mechanism aimed at supporting CO, which at a post-ductal level is decreased. Furthermore, the presence of a hsPDA was associated with globally lower values of SVR. This finding is consistent with current knowledge of decreased SVR in association with this condition [234], and it further contributes to the increased SV observed in hsPDA infants.

- *Gestational age*

Gestational age exerted a significant impact on most of the cardiovascular and cerebrovascular haemodynamic parameters examined in the present research. With regard to cardiovascular parameters, more preterm infants showed significantly higher resting HR and SVR, whereas a significant reduction in SV and cardiac contractility was observed.

In the present population, a 1-week decrease in GA led to a 2.2-point increase in resting HR; hence, the resting frequency of two neonates born at 25 and 32 weeks of gestation may differ of more than 15 bpm. These results are consistent with those by Alonzo et al. [235], who has recently proposed reference HR ranges in premature neonates based on GA and post-menstrual age, and with previous EV-based data obtained between 72 and 96 hours of life [196].

As previously mentioned, due to the asynchronous development between the sympathetic and the parasympathetic branches, the sympathetic activity predominates at lower GAs [228]. Likewise, higher levels of plasmatic catecholamines and of their urinary metabolites have been observed in preterm infants compared to term or near-term controls [236,237]. This may contribute to the significantly increased SVR and HR values observed in the more preterm infants.

A possible role of mineralocorticoids and corticosteroids on the higher SVR observed at lower GAs can also be supposed. By enhancing the cytosolic calcium availability, these hormones are actively involved in the regulation of vascular smooth muscle tone. An inverse relationship between serum cortisol levels and GA has been documented in several studies [238–240]. Another important factor to consider is that free rather than bound cortisol is the active form of the hormone, therefore reduced

levels of binding globulin and albumin, which are often observed in very preterm neonates even in the early postnatal phases, may increase cortisol activity, with possible effects on the vascular tone.

A positive relationship between GA and cardiac contractility was also observed. The immature myocardium is characterized by fewer contractile elements with an underdeveloped sarcoplasmic reticulum, thus mainly relying on L-type calcium channels, and hence on extracellular calcium concentration, to trigger contraction [13,14]. Furthermore, data from animal models have shown that in the preterm heart the expression of β1-adrenoceptors, which exert an inotropic function, is halved compared with the term heart [23]. These maturational differences of the myocardial tissue contribute to a poorer contractile function and likely underlie the reduced cardiac contractility observed with lower GAs. Similar findings were described by Saleemi et al., who documented poorer myocardial performance at 48 hours of life in extremely preterm infants compared with higher GA groups [216], and by Eriksen et al. [241], who reported a GA-dependent increase in myocardial function indices in moderately preterm neonates, evaluated on day 3.

Based on these findings, the lower SV values observed in more preterm infants likely results from the combination of a poorer myocardial function, an increased afterload and a higher resting HR. In particular, with regard to the latter factor, the SV reduction results from the shorter time of diastolic ventricular filling associated with higher HR [25].

On the cerebral side, a significant positive correlation between GA and cerebral oxygenation was observed, whereas cFTOE increased at decreasing GAs. These results confirmed the previously described relationship between GA and these parameters [174,242,243]. Although the underlying causes have not been fully clarified, it is possible that the enhanced cardio-respiratory instability that characterizes the most preterm neonates may be associated with a relatively reduced CBF and oxygen delivery to the brain parenchyma, which contributes to the increased oxygen extraction observed.

- *Cardiovascular drugs*

Dobutamine is an inotropic agent with the primary pharmacologic effect of increasing myocardial contractility that is exerted by a dose-dependent stimulation of α- and β-adrenergic receptors; hence, it represents the drug of choice in neonates with myocardial dysfunction. At moderate doses (5 µg/kg/min), dobutamine mainly results in an increased cardiac output, whereas a vasopressor effect is elicited at higher doses [138]. According to the present results, dobutamine led to a significant improvement in cardiac contractility, consistently with its mechanism of action. However, no significant difference in CO was observed between infants receiving dobutamine and those who did not. This data can be explained by the fact that, according to our NICU protocol, dobutamine was administered in the presence of hypotension with echocardiographic evidence of reduced cardiac output and impaired myocardial contractility; as the evidence of increased cardiac contractility in the treated infants suggests, dobutamine effectively corrected the myocardial dysfunction that underlaid the low cardiac output, based on which this treatment was undertaken. Hence, while the drug was ongoing, the treated infants achieved CO levels similar to those of untreated infants, whose myocardial function was physiologically preserved.

Dopamine is a vasopressor agent largely adopted for the therapeutic management of hypotensive preterm infants; its cardiovascular effects lie in a dose-dependent stimulation of α- and β-adrenergic and dopaminergic receptors [138]. The present results revealed a significant decrease in CO in association with dopamine administration. Current data on the effect of dopamine on cardiac output have led to contrasting results [244–246]. Although an increased afterload has been acknowledged as the most plausible mechanism to explain a CO reduction during dopamine administration, consistent with the poor tolerance of the preterm myocardium to afterload during early transitional phases [21,28], concomitant ductal patency may entail more complex haemodynamic interactions. In particular, in the presence of an increased pulmonary blood flow secondary to a hsPDA, dopamine may increase PVR out of proportion to SVR, reducing the extent of the left-to-right transductal shunt

and improving systemic blood flow [138]. While one may assume that the observed decrease in CO was associated with a dopamine-driven increase in afterload, surprisingly, treated infants did not show a significant SVR increase compared to the untreated group. Hence, it could be hypothesized that treated infants had a lower baseline SVR compared with untreated ones and achieved similar SVR as a result of dopamine administration. However, it is also possible that the need for dopamine treatment may have selected a subgroup with significantly compromised transitional haemodynamics, in which even subtle afterload modifications may have affected the left cardiac output.

- *Role of cardiac output and mean arterial blood pressure on cerebral haemodynamics*

According to the present results, cerebral oxygenation and cerebral fractional oxygen extraction in VLBW infants during the first 72 hours of life significantly depend upon cardiac output. Blood flow and oxygen delivery to the brain tissue results from the composite interactions of BP, SVR and cardiac function, which thus deserve to be carefully monitored during the transitional phase, when hypotension more often occur. To date, the relationship between cerebral oxygenation, cerebral fractional oxygen extraction and cardiac output has been investigated in a few studies, based on echocardiographic measurements, which have yielded controversial results [121,247–249]. A common limitation of these studies is the comparison between continuous NIRS-based values, variously averaged over different time periods, and intermittent CO values detected by echocardiography. Although this technique is widely used for the non-invasive estimation of CO, the information provided is time-limited, and may overlook potentially relevant fluctuations occurring in the period that lays between serial echocardiographic evaluations. These potential fluctuations, however, may also influence the time-averaged values of cerebral oxygenation calculated over that period, and it is possible that this methodological bias underlies the lack of correlation between cerebral oxygenation and echo-derived CO reported in previous studies [247]. Hence, the evaluation of the correlation between continuously monitored CO, cTOI and cFTOE adopted in the present research represents a novel approach compared to the available literature.

The significant association observed between cTOI and CO highlights the importance of optimizing cardiac output during the transitional period in order to maintain an adequate oxygen delivery to the brain tissue. A similar inverse relationship between CO and cFTOE during the transitional period has been previously documented [250]. Under normal circumstances, the delivery of oxygen outweighs its consumption at a tissue level. In neonates with ongoing respiratory and/or cardiovascular complications, decreased oxygen delivery is compensated by an increase in oxygen extraction in order to maintaining a stable tissue oxygenation. Hence, the increasing cFTOE associated with decreasing CO reflects an adaptive compensatory response aimed at improving tissue oxygen diffusion when oxygen delivery is reduced or compromised [249]. It is estimated that this mechanism can boost oxygen extraction up to 50–60% from baseline in case of decreased CBF; however, after a critical point characterized by the maximal oxygen extraction, a further reduction in oxygen delivery would lead to anaerobic metabolic conditions [13].

No significant relationship was found between MABP and cTOI, nor between MABP and cFTOE. This latter result is consistent with the available literature from the transitional period and afterwards [249–251]. Conversely, we observed an inverse, significant correlation between MABP and TOHRx. Since low BP may cause a drop of CPP below the lower limit of autoregulation, this finding reflects the expected physiology and is consistent with previous data by Gilmore et al. [93], based on continuous BP monitoring. Of note, since MABP tends to increase for increasing GA, it is possible that the effect of blood pressure prevailed over that of GA in the multivariate model evaluating TOHRx clinical determinants.

- *Antenatal steroids*

Infants who received a complete course of antenatal steroids showed lower cFTOE levels during transition compared with those who received an incomplete course or none. Glucocorticoid administration to women at risk of preterm delivery to accelerate fetal lung maturation has become a main standard of care [252]. Data from animal models suggest that synthetic glucocorticoids, such as

betamethasone (i.e., the steroid used for the antenatal prophylaxis in the present population), are associated with an extensive decrease in CBF, mediated by an increase in cerebral vascular resistance, that leads to a 30-40% reduction of oxygen delivery to subcortical and hindbrain structures. This finding was found to persist 48 h after treatment administration [253]. The CBF reduction was less enhanced if only a single betamethasone dose was administered [254].

In experimental settings, antenatal administration of synthetic glucocorticoids has been shown to mimic the maturational effects of advancing GA on the cardiovascular response to hypoxia by sensitizing carotid chemoreflexes and enhancing vasoconstrictor neuroendocrine responses mediated by cortisol and catecholamines [255]. Hence, it is possible that, following a full course of antenatal steroids, the occurrence of an antenatal decrease in CBF together with an enhanced maturation of cardiovascular responses to hypoxia may determine a more mature adaptation of the mechanisms involved in brain oxygen extraction, reflected by the lower cFTOE levels.

- *Placental-related intrauterine growth restriction*

Due to the fact that our hospital is a referral centre for placental-related pregnancy complications, the study population was characterized by a high IUGR prevalence with evidence of absent or reversed end-diastolic flow in the umbilical artery. This allowed us to study in detail the cardiovascular and cerebrovascular haemodynamic characteristics of this population during transition, with particular regard to the evidence, or not, of a compensatory antenatal increase of CBF. In conditions of chronic hypoxaemia such as placental insufficiency, the fetus redistributes its circulation and cardiac output to maximise oxygen and nutrient supply to the brain at the expenses of other vascular beds: this phenomenon, defined as brain-sparing [256], is characterized by a decrease in cerebral vascular resistance; the resulting cerebral vasodilatation is associated with a reduced pulsatility index in cerebral arteries. The middle cerebral artery is usually adopted as the gold-standard for this assessment, and a MCA-PI below the 5th percentile indicates the occurrence of this haemodynamic remodelling [203].

According to the present data, SVR was significantly increased in neonates with placental-related IUGR, either with or without evidence of brain sparing, implying a postnatal persistence of systemic vasoconstriction. Data from preterm infants during the first week of life have described an inverse relationship between birth weight and BP in small-for-gestational-age infants, but not in those born with an adequate weight [257]. In a similar fashion, among children born preterm, an increase in systemic arterial stiffness and mean blood pressure has been shown in those with intrauterine growth retardation [258]. Moreover, large epidemiological evidence from human studies has linked IUGR with early-onset hypertension and increased mortality from cardiovascular diseases in adult life [259–263]. Based on this evidence, it may be possible that placental-related IUGR causes specific and persistent changes in vascular structure and in the vessel dynamics, with long-term implications on cardiovascular health.

Infants with umbilical AREDF but no evidence of brain sparing showed a significant reduction of CO compared with those with normal antenatal Doppler. It is possible that this reduction was driven by a concomitant SV decrease, although the SV reduction observed in the present data did not reach statistical significance.

As previously demonstrated by fetal echocardiographic studies, the chronic exposure to increased placental vascular resistances is associated with an adaptive remodelling of the left ventricle, characterized by an impaired diastolic function [264,265]. On the other hand, the brain-sparing related cerebral vasodilation determines a decrease in left ventricular afterload, thus shifting the fetal cardiac output in favour of the left ventricle to enhance cerebral blood supply [266].

It is possible that the lower CO observed in infants with umbilical AREDF without evidence of brain sparing may result from their chronic antenatal exposure to pressure overload, with subsequent cardiac remodelling leading to a reduced left ventricular filling. Similar findings of decreased CO and increased SVR at birth were reported in an experimental lamb model of fetal growth restriction [267]. These results are in line with echocardiographic data obtained in term neonates during the early and

the late transitional period by Fouzas et al. [268], who provided evidence on the association between placental-related IUGR and described distinct changes in cardiac morphology, characterized by a subclinical myocardial dysfunction that may affect cardiovascular adaptation to extrauterine life. However, MCA Doppler data were not available in their population. Cardiac function and arterial biophysical properties have also been investigated between day 2 and 5 after birth in term infants with a birth weight <3° percentile and normal MCA Doppler, with evidence of increased SVR and impaired left myocardial function with speckle tracking analysis compared with infants with an adequate weight [269]; this study, however, was based on ponderal and growth criteria rather than on antenatal Doppler data.

The present results also demonstrated significant differences in cerebrovascular reactivity in relation to cerebral vascular redistribution, with selectively increased TOHRx values in infants with antenatal brain sparing. This finding is in accordance with previous evidence of a transitional impairment of cerebral autoregulation, measured as the correlation between MABP and cTOI, in preterm infants small for gestational age [270] or with antenatal CBF redistribution [108]. Consistent with these findings, data from human IUGR fetuses with brain sparing have documented a prenatal loss of vasoreactivity in response to maternal hyperoxygenation, which failed to elicit the expected rise in cerebral vascular resistance [271].

The altered cerebrovascular reactivity observed in association with brain sparing likely results from the structural remodelling of the cerebral vasculature observed in animal models of chronic fetal hypoxia and characterized by a reduced vascular density in the white matter, decreased perivascular astrocytes and increased permeability of the blood brain barrier, associated with a shift from calcium- and nitric oxide-mediated toward an adrenergic-mediated vasoreactivity [272,273]. Whether this altered cerebrovascular reactivity persists over time, it has not been ascertained; of note, an increased incidence of stroke has been reported in adults born small for gestational age [274].

- *Conclusions*

In summary, cardiovascular and cerebrovascular haemodynamics of preterm infants during the transitional period may be significantly influenced by specific antenatal, perinatal and postnatal factors; in particular, antenatal disturbances of fetal Doppler flowmetry, GA and the presence of a hsPDA showed the most extensive effects, which should be thus taken into account in the haemodynamic assessment and management of this population.

In particular, lower GA were associated with significantly increased SVR and HR, reduced SV and cardiac contractility, lower cerebral oxygenation and higher cerebral oxygen extraction. These findings suggest that, during transition, extremely preterm infants may benefit from a tailored cardiovascular approach, aimed at optimizing blood volume and cardiac contractility (e.g., dobutamine) rather than at supporting blood pressure by increasing SVR (e.g., dopamine). Moreover, the association between CO, cerebral oxygenation and oxygen extraction highlights the importance of this parameter for the maintenance of stable cerebral haemodynamics in this delicate population. Since the prevalence of a hsPDA increases at lower GA, however, the management of most preterm infants cannot disregard the ductal status. According to the present findings, a hsPDA significantly affects cerebral autoregulation and is associated with higher CO, SV, HR, enhanced cardiac contractility and decreased SVR. Hence, identifying infants with a hsPDA is very important; in the presence of a hsPDA, greater attention should be paid on preventing CBF fluctuations, and cardiovascular treatments should be carefully tailored on individual SVR, SV and cardiac contractility features.

Antenatal abnormal umbilical Doppler led to significantly raised SVR during the transitional period. This suggests that therapeutic cardiovascular approaches that increase SVR may be counterproductive in this population. In addition to the umbilical Doppler status, the establishment of antenatal brain sparing should also be assessed, since this condition has resulted to be associated with

a greater impairment of cerebral autoregulation and may thus identify a subgroup of infants at higher risk for neurological complications.

- *Limitations*

As seen from the clinical and neonatal characteristics of the population included in this research, a good proportion of the study infants were generally well-adapted and underwent a successful physiological transition to postnatal life. This may have contributed to the low prevalence of severe IVH observed in the present population. Since IVH is rather a consequence than a causative factor of transitional haemodynamic cardiovascular and cerebrovascular fluctuations [48,89,120], this condition was not included in the fixed effects of the GLMMs and LMM evaluating the main haemodynamic determinants during transition. However, the small number of infants who developed IVH, especially of high grade (i.e., n=3), did not allow to run a powered analysis to elicit the haemodynamic patterns associated with this complication, which thus warrants to be investigated in targeted, larger studies. On the other hand, the present population may constitute a reference cohort to evaluate the trend patterns of the main haemodynamic parameters and their association with relevant clinical factors in overall physiological conditions.

The unavailability of a simultaneous invasive BP monitoring needs to be acknowledged as a possible limitation as, if available, it would have allowed to examine the continuous trajectories of MABP over time, to compare TOHRx values against indices of cerebral autoregulation, based on continuous BP monitoring [78,93], or to investigate the dynamic correlation existing between cardiac output and afterload. However, although arterial catheterization represents the current gold-standard technique for continuous blood pressure measurement, it should be considered that a tendency towards less invasive approaches, including a decreased use of arterial lines, is being increasingly adopted in neonatal settings [275–277], and that this procedure is not exempt from adverse events.

CO_2 is a potent modulator of cerebral vasculature and, as such, may have had an influence on cerebrovascular parameters. Unfortunately, continuous monitoring of transcutaneous or end-tidal

CO_2 was not available to be included in the multiparametric monitoring system used for in present research, so it was not possible to examine CO_2 trends and their effects on the present data. However, the regular arterial blood gases that were performed during the monitoring period showed stable levels of $PaCO_2$, and the management of ventilated neonates was aimed at maintaining $PaCO_2$ and PaO_2 as stable as possible.

5. INTERPARAMETRIC CARDIAC CORRELATIONS

5.1. Introduction and aim

Cardiac output is the result of a complex interplay between different haemodynamic factors, which include preload, diastolic filling, intra-cardiac flow patterns, contractility and afterload [5,13]. Nevertheless, the two direct determinants of CO are SV and HR. It has long been assumed that, in neonates, SV is relatively fixed and HR is thus the main modulating factor of CO [13]. However, more recent studies have shown that, in preterm infants, fluctuations in cardiac output more often result from changes in the stroke volume rather than in the heart rate [25,26].

Due in part to immaturity of their autonomic and cardiovascular systems, preterm neonates have significantly higher resting heart rates when compared to term infants and older children; in addition, the chronotropic effects of the drugs that are frequently used to support their cardiovascular function may lead to further HR increases which, by shortening the time for diastolic ventricular filling, can subsequently lead to a SV decrease [20]. On the other hand, SV is directly affected by the presence of haemodynamically significant shunts, of which the most relevant is that across a large PDA.

Several other factors, including inotropes and vasopressors, may contribute to influence the contractile function of the immature myocardium, the preload and the afterload, with indirect effects on SV. Hence, it is plausible that the relationship between HR, SV and CO is not fixed and linear, but rather dynamic, and may vary at different ranges of HR, SV and upon the individual characteristics of each infant, with potentially relevant practical implications.

The research objective addressed in this section aimed at investigating the relationship between CO and its two direct determinants, monitored beat-to-beat during the first 72 hours of life, at different SV and HR ranges and according to relevant clinical and haemodynamic characteristics. For this purpose, the agreement between CO_{EV} and that measured by echocardiography was also preliminarily analysed.

5.2. Methods and Statistics

Methods

Patient recruitment, ultrasound evaluation and data collection, including the multiple parameters obtained by non-invasive multiparametric monitoring, are described in detail in Chapter 3.

Echocardiographic cardiac output values (CO_{ECHO}) were calculated as previously described in Chapter 3; the values included in the Bland-Altman analysis were obtained by averaging the VTI over 5 cycles and indexed for the infants' weight. In order to rule out a possible bias related to inter-operator variability, all the echocardiographic measurements included in the analysis were obtained by a single operator, blind to EV data at the time of the scan. For CO_{EV}, 30-sec averaged data around the time of the echocardiographic evaluation were used for Bland-Altman analysis.

Beat-to-beat data of CO_{EV}, SV and HR_{EV} obtained by EV monitoring throughout the whole transitional period were used to evaluate the parametric correlations existing among these parameters. CO_{EV} and SV were indexed using the infants' daily weight.

Statistical analysis

The agreement between daily cardiac output values obtained using echocardiography (CO_{ECHO}) and electrical velocimetry (CO_{EV}) over the first 72 hours of life was assessed and illustrated using the Bland–Altman plot. CO_{ECHO} values were used as reference. To best handle repeated measures, the analysis was performed separately on each day of life. Differences in agreement according to the presence of hsPDA were investigated using a generalized least squares (GLS) random-effects model, with the absolute delta between CO_{ECHO} and CO_{EV} as the dependent variable. The agreement between the two methods was also calculated as the percent error of CO_{EV} compared to CO_{ECHO}, which is given by the formula $|(CO_{EV} - CO_{ECHO})/CO_{ECHO}| \times 100$. The 95% confidence interval (CI) of mean error was estimated using the bias-corrected bootstrap method.

GLS random-effects models were also used to analyse the association of CO_{EV} with heart rate (HR_{EV}) and stroke volume (SV) at 1, 2 and 3 days of age. GLS estimators are useful when there is a degree of correlation between the residuals because observations are clustered into groups that have something in common (in this case, subject-specific beat-to-beat haemodynamic parameters). To investigate the presence of non-linear inter-parametric relationships, HR was collapsed into a categorical variable of seven groups using the following breakpoints: <120, 120–129, 130–139, 140–149, 150–159, 160–169 and ≥170 bpm. Similarly, SV was collapsed into a categorical variable of six groups (<1.60, 1.60–1.99, 2.00–2.19, 2.20–2.49, 2.50–2.99 and ≥3.00 ml/kg).

The clinical covariates that were mainly related to the cardiovascular status of preterm infants (GA, umbilical Doppler status, administration of dopamine and dobutamine, ductal status and type of ventilation) were included in the multivariable models to examine their impact on the association of CO with HR and SV. To improve the model sensitivity, those variables whose status changed over time (e.g., ductal status, mode of respiratory support, ongoing cardiovascular drugs) were handled as time-dependent covariates. To illustrate the moderating effect of such clinical features, we plotted the predictions from regression models corresponding to different HR and SV ranges—in case of no interaction, the trajectories are parallel. Contrast in the predicted means of CO at each level of HR and SV were examined with the Wald test. The standard errors of the regression coefficients and the predicted means of CO were estimated with the robust method. Normality of the overall error component was checked using the Q–Q plot. No collinearity issues were found.

In a secondary analysis, GLS random-effects models were used to investigate the association between SV and HR.

5.3. Results

The infants included in this sub-analysis coincide with the sample previously described in Chapter 4. The relevant neonatal and clinical characteristics of this population at baseline and over the monitoring period are available in Table 4.1 and 4.2, respectively.

Bland Altman analysis

In order to rule out a possible bias related to inter-operator variability, only the echocardiographic measurements obtained by a single operator (Dr Silvia Martini) were included in the analysis: this explains the different number of measurements over the first 3 days and the fact that the measurements were lower than the actual study sample.

The mean difference between CO_{EV} and CO_{ECHO} was 10.7 ml/kg/min (95% CI 1.3, 20.1) on day 1, 7.1 ml/kg/min (95% CI –2.1, 16.3) on day 2, and 11.0 ml/kg/min (95% CI 4.3, 17.8) in day 3 of life. The corresponding mean percentage error (MPE) of CO_{EV} was 7.6% (95% CI 4.9%, 11.3%) on day 1, 7.3% (95% CI 4.1%, 13.4%) on day 2, and 7.3% (95% CI 5.5%, 9.5%) on day 3 of life.

As shown in Figure 5.1, there was no evidence of proportional bias, i.e., the two methods agreed equally through the range of measurements. The 95% limits of agreement illustrated in the charts, which are defined as the mean difference ±1.96 times the standard deviation of the differences and indicate how far apart measurements are likely to be for most individuals, were –55.3 to 76.7 ml/kg/min on day 1, –55.8 to 70.0 ml/kg/min on day 2, and –33.4 to 55.5 ml/kg/min on day 3. In general, EV measurements were systematically higher in patients with haemodynamically significant PDA than in those with closed or restrictive PDA (mean difference in differences = 10.1 mg/kg/min; 95% CI = 0.2, 19.9; p=0.045).
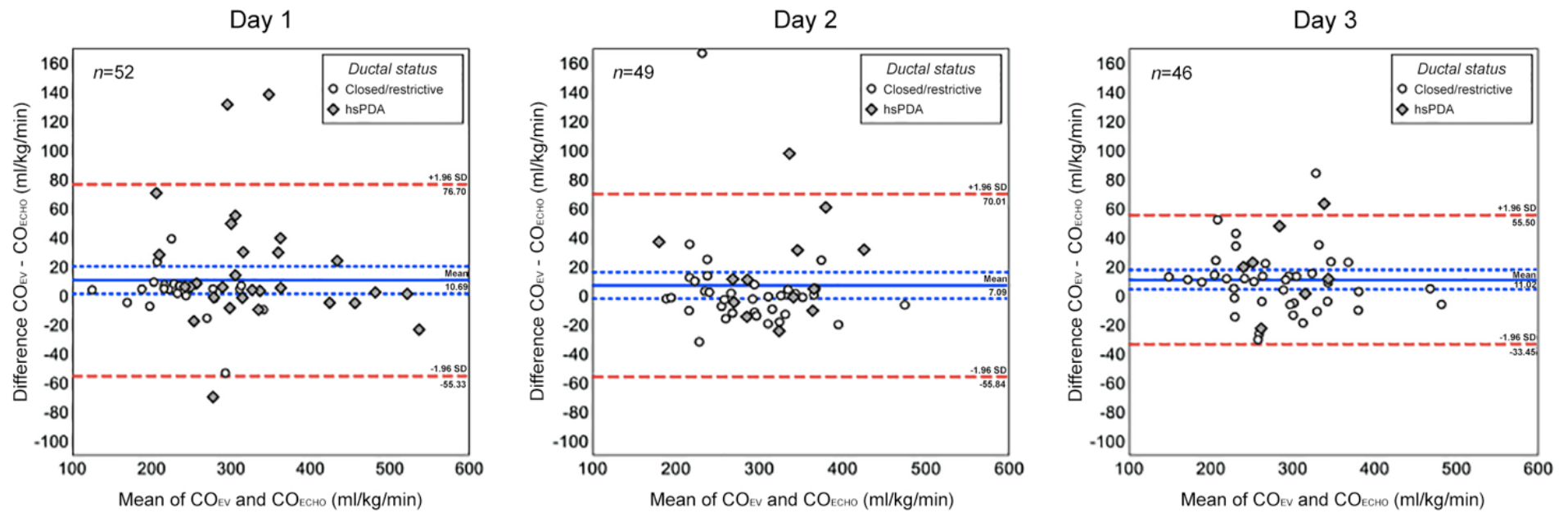
***Figure 5.1.*** *Bland–Altman plot of cardiac output measured with electrical velocimetry (CO$_{EV}$) versus echocardiography (CO$_{ECHO}$) on day 1, 2 and 3 of life. Red-dashed lines indicate the upper and lower limit of agreement. Short-dashed lines indicate the 95% confidence interval for the mean difference. Abbreviations: hsPDA, haemodynamically significant patent ductus arteriosus; SD, standard deviation.*

Interparametric cardiac correlations

Data on beat-to-beat CO, HR and SV obtained with EV at 1, 2 and 3 days of age and the number of observations for each neonate on which the related analysis was based are shown in Table 5.1.

Table 5.1. *Beat-to-beat haemodynamic parameters at 1, 2 and 3 days of age. Abbreviations: SD, standard deviation.*

Parameter	Day 1	Day 2	Day 3
Avg. n. of obs. per subject	34,133	63,499	60,217
Cardiac output, ml/kg/min			
Mean ± SD	314.9 ± 90.1	335.2 ± 104.5	323.5 ± 93.6
Median	304.0	318.7	312.3
Interquartile range	254.3–365.5	260.7–397.9	253.7–381.0
Interdecile range*	208.0–439.9	208.1–487.3	212.7–453.0
Avg. n. of obs. per subject	34,271	64,005	60,736
Heart rate, bpm			
Mean ± SD	141.2 ± 14.9	145.0 ± 17.5	145.5 ± 15.2
Median	140	143	144
Interquartile range	131–151	132–157	135–156
Interdecile range*	123–161	124–169	127–166
Avg. n. of obs. per subject	33,936	62,640	59,044
Stroke volume, ml/kg			
Mean ± SD	2.30 ± 0.64	2.37 ± 0.70	2.29 ± 0.63
Median	2.24	2.29	2.22
Interquartile range	1.86–2.69	1.87–2.82	1.83–2.68
Interdecile range*	1.52–3.16	1.51–3.36	1.54–3.14

Distance between the 1st decile (10th percentile) and the 9th decile (90th percentile).

Results of the univariate GLS random-effects model evaluating the beat-to-beat association of CO_{EV} with HR at different HR ranges are shown in Table 5.2. HR between 140 and 149 bpm were chosen as the reference interval according to currently available literature [196,235].

Table 5.2. Generalized least square random-effects model for heart rate (HR) versus cardiac output. Regression coefficients are expressed as ml/kg/min. Abbreviations: CI, confidence interval. Asterisks indicate contrasts significant at the 5% (*) and 1% (**) level.

Characteristic	Day 1		Day 2		Day 3	
	Coef.	95% CI	Coef.	95% CI	Coef.	95% CI
HR, bpm						
<120	–16.6*	–31.7, –1.5	–36.6**	–51.1, –22.1	–25.6**	–41.1, –10.1
120–129	–8.8	–21.2, 3.6	–16.5**	–24.7, –8.3	–14.5*	–26.1, –2.8
130–139	–3.8	–13.7, 6.1	–7.0*	–13.7, –0.4	–3.2	–9.4, 3.0
140–149	Ref.		Ref.		Ref.	
150–159	13.3**	7.1, 19.4	11.8**	4.9, 18.7	11.5**	5.8, 17.3
160–169	18.1**	7.5, 28.6	3.6	–8.3, 15.5	14.3*	2.8, 25.8
≥170	24.4*	0.8, 48.1	–5.2	–22.3, 11.8	5.3	–11.8, 22.5
Intercept	*315.3***	*295.4, 335.2*	*335.7***	*313.3, 358.2*	*322.1***	*303.7, 340.5*

On day 1, CO significantly increased if HR rose above the reference range, with greater increases at higher HR ranges, as suggested by the correlation coefficients shown in Table 5.2, whereas a HR drop <120 bpm led to a significant CO reduction.

On day 2, significant CO increases compared to the reference HR were achieved only within the HR range between 150 and 159. Higher HR increases did not contribute to improve CO; although the correlation between HR values ≥170 bpm and CO showed a negative coefficient, this finding was not

statistically significant. Conversely, when HR decreased <140 bpm, a progressive, significant reduction of CO was observed.

On day 3, compared to the reference interval, a significant increase of CO was obtained at HR ranges between 150 and 169 bpm, whereas an opposite effect was observed when HR dropped <130 bpm, in a linear fashion.

Estimated means of CO in relation to different HR ranges on day 1, 2, 3 and during the whole transitional period are illustrated in Figure 5.2. An overall trend towards a progressive CO increase at increasing HR values was observed for HR ranges <160. While further HR increases still contributed to increase CO on day 1, negative correlations between the two parameters were observed on day 2 and 3, flattening the overall curve for HR values ≥160 bpm.
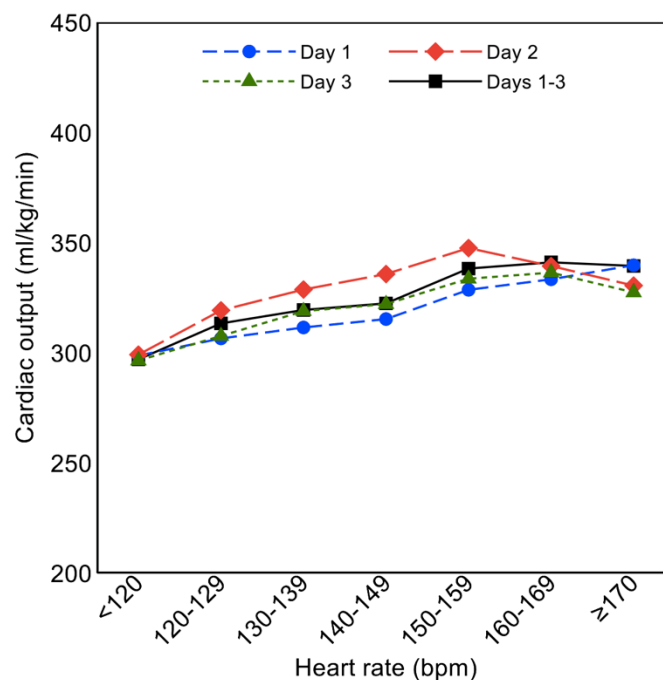
Figure 5.2. *Estimated means of cardiac output (Y-axis) at different levels of heart rate (X-axis), overall (black squares, black continuous line) and by day of age.*

Figure 5.3 illustrates the results of the multivariable GLS analysis evaluating the impact of GA, umbilical Doppler status, administration of dopamine and dobutamine, ductal status and type of ventilation on the association between different HR ranges and CO on each day of life.
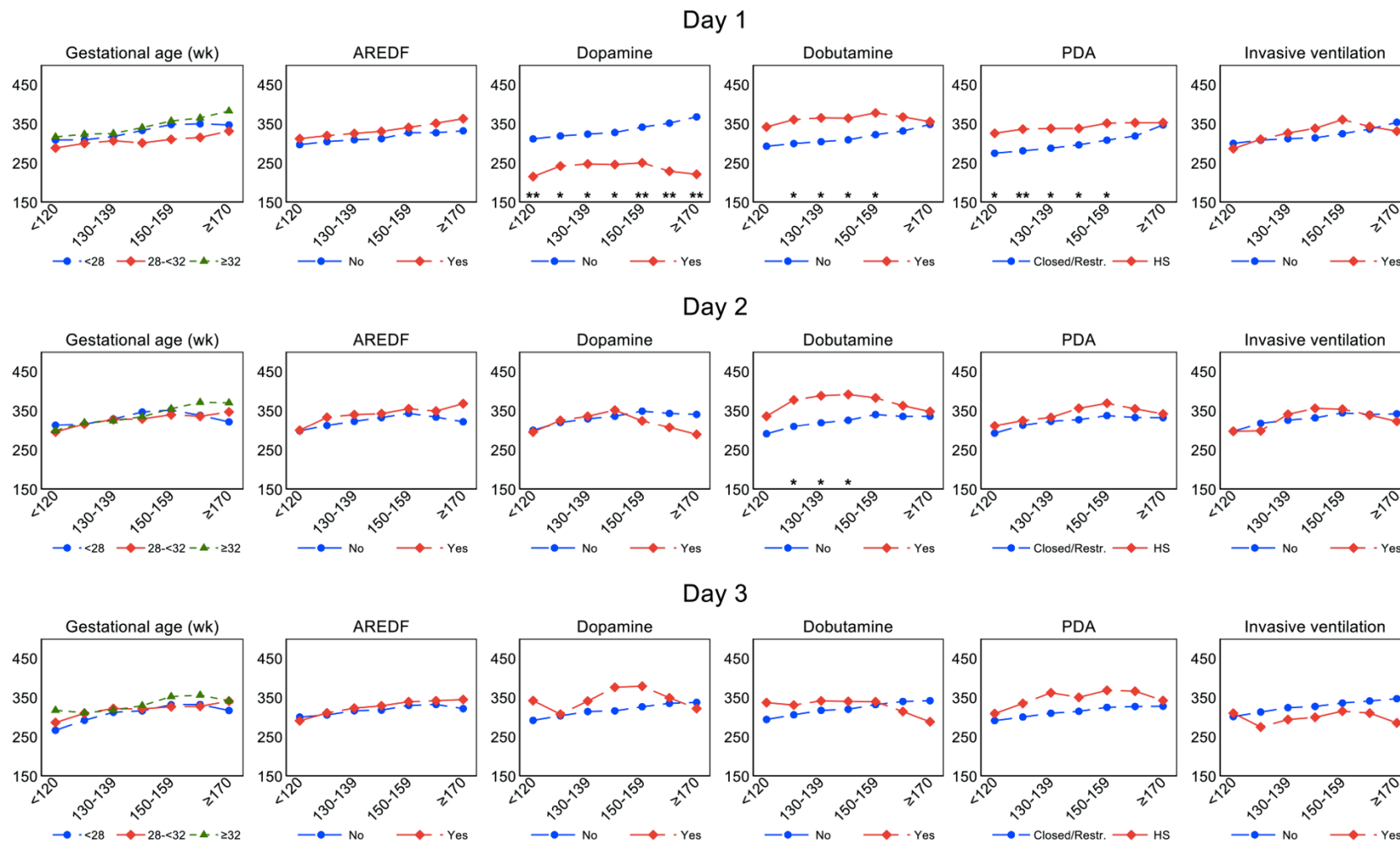
Figure 5.3. *Estimated means of CO (Y-axis, ml/kg/min) at different levels of HR (X-axis, bpm) on day 1, 2 and 3, by gestational age, antenatal Doppler status (umbilical AREDF vs. normal umbilical Doppler), dopamine/dobutamine administration, ductal status (haemodynamically significant [HS] patent ductus arteriosus [PDA] vs. restrictive or closed) and type of ventilation (invasive vs. noninvasive). Asterisks indicate contrasts significant at 5% (*) and 1% (**) level.*

No significant effects were observed for GA, antenatal Doppler status and ongoing mechanical ventilation. On the other hand, the administration of dopamine and dobutamine significantly influenced the correlation between HR and CO, with diverse effects observed at different days of life.

On day 1, the administration of dopamine was associated with an overall reduction of cardiac output in infants who received this treatment compared to those who did not, net of the other covariates included in the GLS analysis and illustrated in Figure 5.3. Moreover, if HR fell <120 bpm, dopamine administration was associated with a greater CO reduction, whereas at HR ranges ≥160 bpm, the correlation between HR and CO turned negative, showing a progressive decrease in CO for increasing HR, whereas this correlation was maintained positive in infants who did not receive dopamine. Conversely, dobutamine administration on day 1 significantly increased CO at HR ranges between 120 and 159 bpm; however, for further HR increases, this positive effect was no longer evident and the correlation between HR and CO turned negative, whereas infants who did not receive dobutamine were able to increase their CO even at HR ranges ≥160. However, dobutamine administration was not associated with an overall CO decrease at high HR ranges; in fact, the CO levels observed at HR ≥170 in treated infants were comparable to the untreated group.

With regard to the ductal status, significantly higher CO at HR ranges <160 were observed during the first 24 hours in infants with a hsPDA, whereas at further HR increases, their HR-CO curve remained flat. On the other hand, those with a restrictive or closed duct maintained a steeper curve at HR ≥160. On day 2, substantial changes were observed in the dopamine curve. Similar CO ranges were observed in the two groups; however, while the two curves were almost overlapping for HR up to 149 bpm, the relationship between HR and CO turned negative at HR values ≥150 in infants who received this vasopressor treatment. Although no significant between-group difference was observed, a progressive reduction of CO values was observed for further HR increases in association with dopamine treatment. Dobutamine maintained a significant positive effect in enhancing CO at HR ranges between 120 and 149; although further HR increases led to slight and gradual CO reductions, the CO levels achieved at HR ≥170 were comparable to those observed in the untreated group. At

this phase, the significant impact of hsPDA was no longer observed, and the HR-CO curves between the two groups were almost overlapping.

No significant differences in the HR-CO curves in relation to dopamine and dobutamine administration were observed on day 3. Of note, at this phase dobutamine administration did not lead to a substantial CO improvement compared to the untreated group at similar HR; rather a trend towards reduced CO values was observed at highest HR ranges (≥170). Conversely, dopamine showed slightly, but not significantly increased CO values compared to untreated infants when HR laid between 140 and 160.

Results of the univariate GLS random-effects model evaluating the beat-to-beat association of CO with SV at different SV volumes are shown in Table 5.3.

Table 5.3. Generalized least square random-effects model for stroke volume (SV) versus cardiac output. Regression coefficients are expressed as ml/kg/min. Abbreviations: CI, confidence interval. Asterisks indicate contrasts significant at the 5% (*) and 1% (**) level.

Characteristic	Day 1		Day 2		Day 3	
	Coef.	95% CI	Coef.	95% CI	Coef.	95% CI
SV, ml/kg						
<1.60	Ref.		Ref.		Ref.	
1.60–1.99	49.5**	44.2, 54.8	50.0**	45.4, 54.7	47.9**	41.4, 54.4
2.00–2.19	81.2**	75.0, 87.4	84.3**	78.8, 89.8	84.2**	76.7, 91.6
2.20–2.49	110.2**	103.3, 117.2	113.5**	107.0, 120.0	115.3**	107.0, 123.6
2.50–2.99	149.6**	140.5, 158.6	153.1**	144.9, 161.4	157.0**	147.5, 166.6
≥3.00	219.9**	205.9, 233.8	229.4**	217.0, 241.9	228.2**	211.3, 245.1
Intercept	*215.6***	*205.8, 225.4*	*222.7***	*213.5, 232.0*	*221.5***	*213.3, 229.7*

Estimated CO means in relation to different SV ranges on day 1, 2, 3 and during the whole transitional period are illustrated in Figure 5.4. The correlation between CO and SV was strong and followed a linear fashion: the greater the SV, the higher the CO. This trend was confirmed throughout the whole transitional period, with no substantial differences in relation to the day of life.
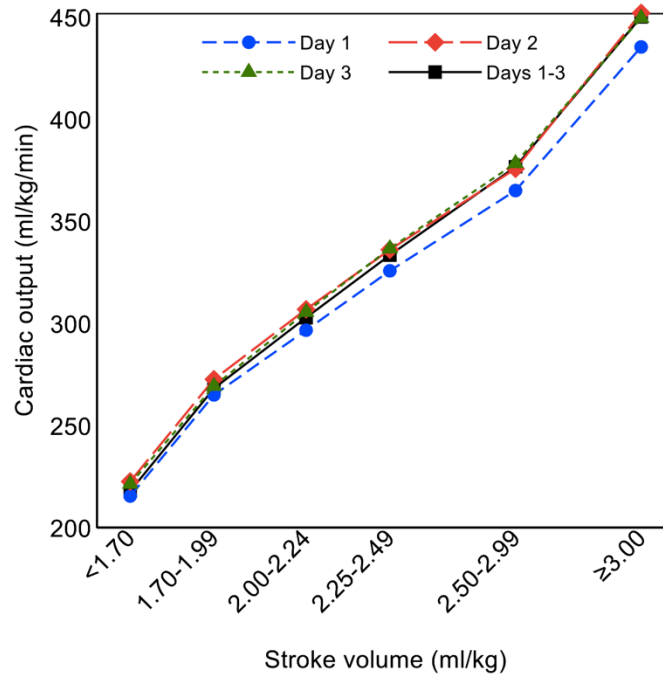

Figure 5.4. *Estimated means of cardiac output (Y-axis) at different levels of stroke volume (X-axis), overall (black squares, black continuous line) and by day of age.*

Figure 5.5 illustrates the results of the multivariable GLS analysis evaluating the impact of GA, umbilical Doppler status, administration of dopamine and dobutamine, ductal status and type of ventilation on the association between different SV ranges and CO on each day of life.

No significant effect over the first 3 days of life was observed for mechanical ventilation and antenatal Doppler status. Conversely, infants <28 weeks' gestation showed significantly higher CO values at increasing SV; in particular, a SV $\geq$ 2.5 ml/kg resulted in a significant CO improvement throughout the whole transitional period compared to those with higher GAs from day 1 to 3, whereas on day 2 significantly higher CO compared to moderately preterm infants were obtained at SV$\geq$ 2 ml/kg.
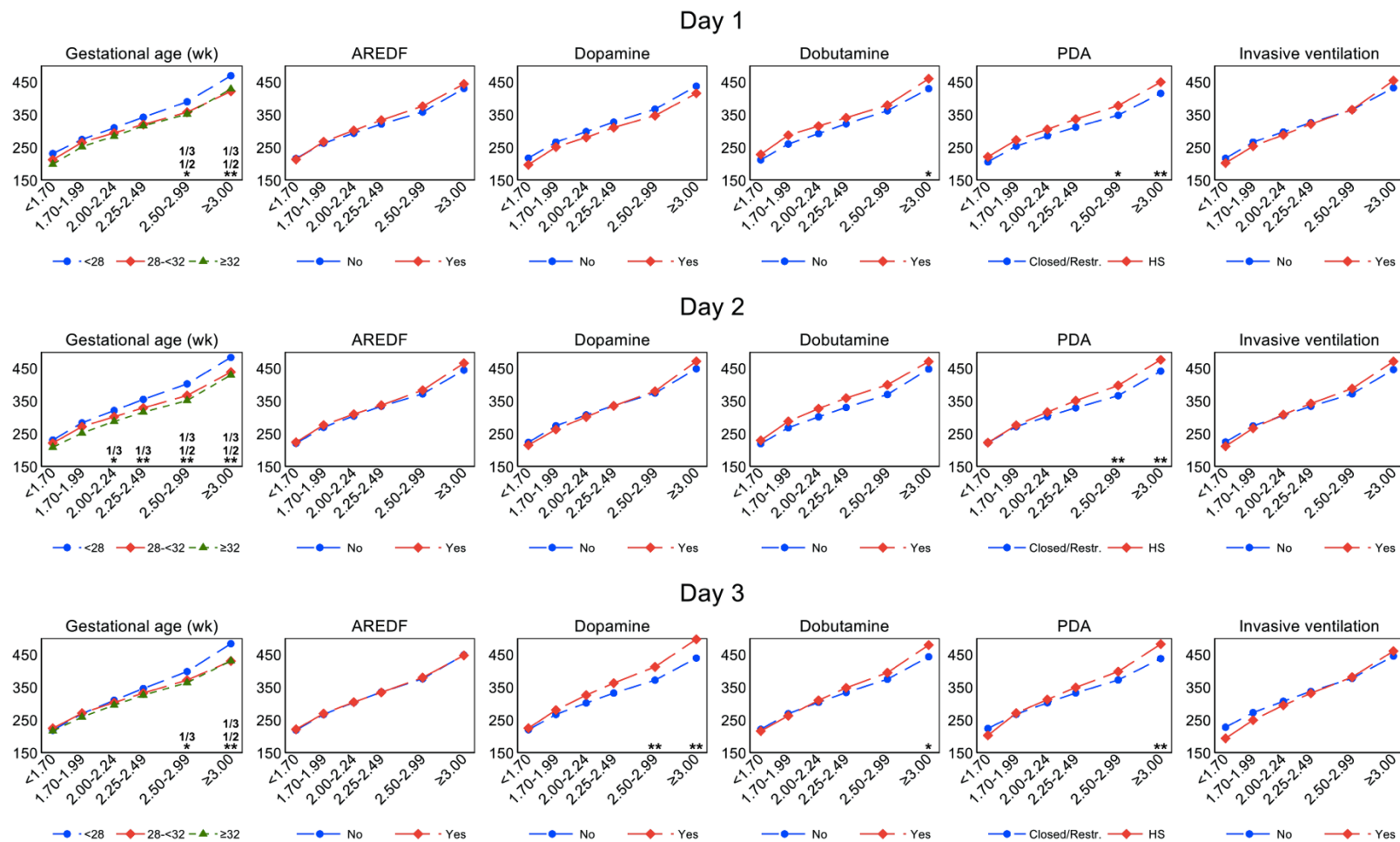
***Figure* 5.5.** *Estimated means of CO (Y-axis, ml/kg/min) at different levels of SV (X-axis, ml/kg) on day 1, 2 and 3, by gestational age, antenatal Doppler status (umbilical AREDF vs. normal umbilical Doppler), dopamine/dobutamine administration, ductal status (haemodynamically significant [HS] patent ductus arteriosus [PDA] vs. restrictive or closed) and type of ventilation (invasive vs. noninvasive). Asterisks indicate contrasts significant at 5% (*) and 1% (**) level; significant pairwise comparisons between gestational age classes <28 weeks (1), 28–<32 weeks (2) and ≥32 weeks (3) are reported as 1/2, 1/3 or 2/3.*

135

The presence of a hsPDA resulted in significant CO increases for SV≥ 2.5 ml/kg on day 1 and 2 compared to a restrictive or closed duct. Similar SV ranges were also associated with a significant CO increase in infants treated with dopamine on day 3 compared to the untreated group.

Results of GLS random-effects model evaluating the beat-to-beat association of SV_{EV} with HR at different HR ranges are shown in Table 5.4. As for the previous model, HR between 140 and 149 bpm were chosen as the reference interval according to currently available literature [196,235].
On each day of life, any HR increase above the reference interval (140-149 bpm) was associated with a concomitant SV reduction; conversely, HR reductions below the reference range led to progressive increments of SV.

Table 5.4. *Generalized least square random-effects model for heart rate (HR) versus stroke volume on day 1, 2 and 3. Regression coefficients are expressed as ml/kg. Abbreviations: CI, confidence interval. Asterisks indicate contrasts significant at the 5% (*) and 1% (**) level.*

Characteristic	Day 1		Day 2		Day 3	
	Coef.	95% CI	Coef.	95% CI	Coef.	95% CI
HR, bpm						
<120	0.38**	0.25, 0.51	0.28**	0.18, 0.38	0.32**	0.19, 0.46
120–129	0.24**	0.14, 0.34	0.19**	0.12, 0.26	0.21**	0.12, 0.31
130–139	0.12**	0.05, 0.19	0.09**	0.04, 0.15	0.12**	0.07, 0.16
140–149	Ref.		Ref.		Ref.	
150–159	–0.05*	–0.10, –0.01	–0.06*	–0.11, –0.01	–0.06**	–0.10, –0.02
160–169	–0.15**	–0.22, –0.09	–0.25**	–0.34, –0.16	–0.17**	–0.25, –0.09
≥170	–0.24**	–0.38, –0.10	–0.46**	–0.60, –0.33	–0.37**	–0.48, –0.26
Intercept	*2.24***	*2.11, 2.38*	*2.37***	*2.22, 2.53*	*2.28***	*2.16, 2.41*

Estimated means of SV in relation to different HR ranges on day 1, 2, 3 and during the whole transitional period are illustrated in Figure 5.6. The negative linear fashion that characterizes the relationship between SV and HR is clearly evident in this figure.
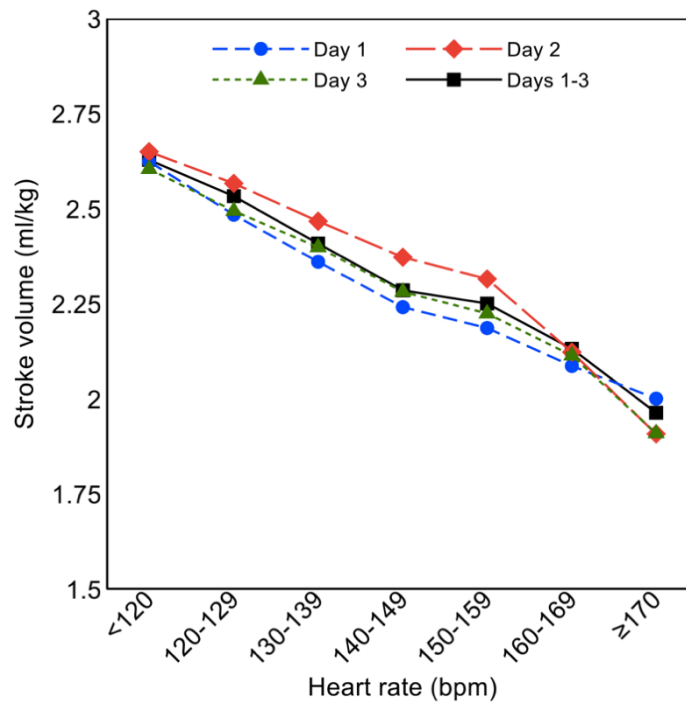
Figure 5.6. Estimated means of stroke volume (Y-axis) at different levels of heart rate (X-axis), overall (black squares, black continuous line) and by day of age.

Figure 5.7 illustrates the results of the multivariable GLS analysis evaluating the impact of GA, umbilical Doppler status, administration of dopamine and dobutamine, ductal status and type of ventilation on the association between HR at different ranges and SV on each day of life.

This finding illustrated in this figure basically resembled those observed in Figure 5.3, which depicted the correlation between HR and CO. This is due to the strong, linear relationship existing between SV and CO.
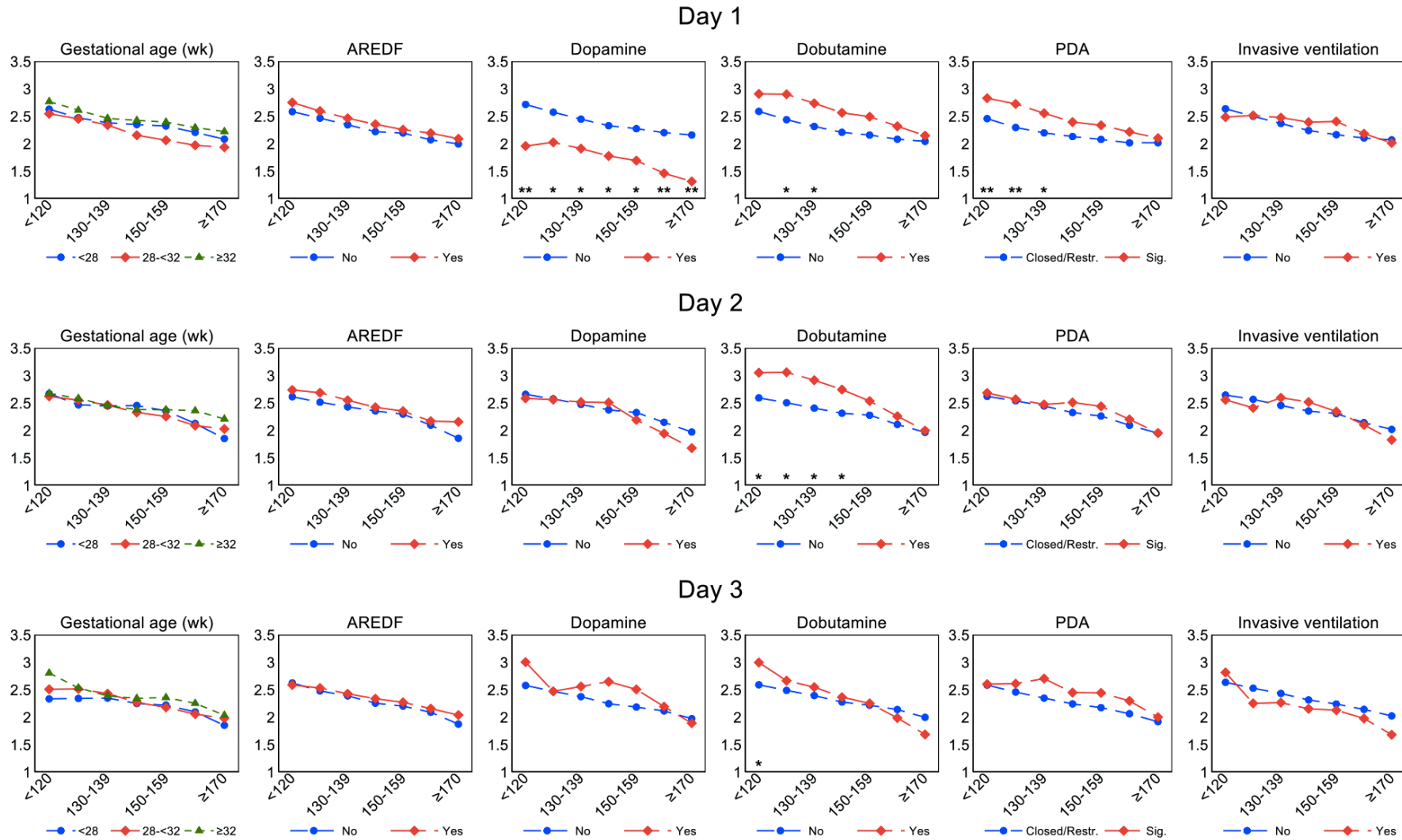
Figure 5.7. *Estimated means of SV (Y-axis, ml/kg) at different levels of HR (X-axis, bpm) on day 1, 2 and 3, by gestational age, antenatal Doppler status (umbilical*

AREDF vs. normal umbilical Doppler), dopamine/dobutamine administration, ductal status (haemodynamically significant [HS] patent ductus arteriosus [PDA]

vs. restrictive or closed) and type of ventilation (invasive vs. noninvasive). Asterisks indicate contrasts significant at the 5% (*) and 1% (**) level.

Discussion

Electrical velocimetry is a non-invasive monitoring technique that, based on the analysis of the variations in thoracic electrical bioimpedance in relation to peak aortic blood flow acceleration, allows for continuous trend monitoring of cardiac output and other haemodynamic parameters, including SV, HR, SVR and also cardiac contractility estimation [278]. In the recent years, EV has been progressively introduced in NICU settings, with increasing evidence on the feasibility of its application in preterm infants [147–149,151,194,279–281].

Bland-Altman analysis

The agreement between EV and transthoracic echocardiography in the assessment of cardiac output has proved acceptable in previous neonatal studies [148,149,151,279]. Recently, Sanders et al. have published a metanalysis aimed at assessing the accuracy and precision of this method for non-invasive CO monitoring. Eleven studies from the paediatric population were included; of these, 2 focused on the neonatal population and compared EV against echocardiography [147,280]. For paediatric studies, the pooled bias was low (−0.02 L/min); however, the pooled MPE, which reflects the accuracy of the monitoring technique, was relatively high (42%). Available literature on the neonatal population have reported %bias and MPE ranging from 1% to 9% and from 25% to 60%, respectively [149,280–282].

In the present study, the mean difference between CO_{EV} and CO_{ECHO} ranged between 7.1 and 11 ml/kg/min over the first 3 days of life, with a corresponding MPE ranging between 7.3% and 7.6%; these results indicate an overall good agreement between the two techniques and compared to the available literature, are characterized by a low MPE, which indicates satisfactory accuracy.

Echocardiography is considered by many as the current gold-standard for CO assessment in the neonatal population. Although this technique has several advantages over EV, including the capability to evaluate cardiac anatomy and to diagnose ductal patency and its haemodynamic impact,

it requires specific training and experience-dependent expertise, and is prone to both inter- and intra-operator variability. Moreover, it has been previously shown that echocardiographic CO assessment itself is burdened by a MPE of around 30% when compared to invasive gold-standard methods [141]. Hence, it cannot be considered as the absolute gold-standard to validate the reliability of EV in detecting CO. Alternative invasive techniques, such as transpulmonary dilution and arterial pulse contour analysis, guarantee more accurate CO determinations. However, these methods require arterial and central venous catheterization, which limits their applicability in the neonatal population and underlie the scarceness of data for EV comparison [278].

According to our results, the presence of a hsPDA led to a systematic CO_{EV} overestimation of additional 10 mg/kg/min compared to echocardiography. It has been previously demonstrated that the presence of physiological shunts, such as through a PFO or a patent duct, may overestimate EV-derived CO compared to echocardiographic assessments; in particular, the presence of a PDA, alone or combined with PFO, was associated with the highest relative difference compared to echocardiographic measurements [283]. Since a physiological PFO was evident in most of the monitored infants, we chose to evaluate the impact of hsPDA. A significant impact of hsPDA on CO_{EV} measurements has also been reported by Torigoe et al.; however, they reported a negative bias in association with this condition [280].

The mechanisms through which a hsPDA may influence CO_{EV} measurements, likely results from the interference of the transductal shunt on the volumetric changes and on the alignment changes of erythrocytes in the aorta during the cardiac cycle. Although an excellent correlation between EV and the invasive Fick method has been documented in children with congenital heart disease, the majority of these children had intracardiac shunts, whereas such extracardiac shunts as PDA were scarcely represented [278].

Interparametric cardiac correlations

Following the assessment of the reliability of CO_{EV} measurements, the correlation existing between CO, HR and SV, measured by EV, was evaluated.

According to the results presented, the relationship between CO and HR is not perfectly linear, but depends upon different HR ranges, whereas CO is strongly correlated with SV. Furthermore, associated factors with an active impact on cardiac function, such as administration of cardiovascular drugs or the presence of a hsPDA, significantly modulate these interparametric relationships. These findings are consistent with previous echocardiographic evidence by Winberg et al. [25], who investigated the correlation between changes in heart rate, left ventricular output, and left ventricular stroke volume in a small cohort of preterm neonates over the first 3 weeks of life, showing that the individual mean left ventricular output poorly correlated with HR, while a closer relationship was observed with SV.

An added value of the present research is that the relationship between HR and CO was evaluated at different HR ranges and during different days of life. From this evaluation we found a HR rise above determinate thresholds (i.e., 170 bpm) negatively impacts on CO; this likely results from the decrease of diastolic ventricular filling time as HR increases. The greatest impact of HR in determining CO was observed during the first day of life: CO significantly increased even at the highest HR ranges, whereas similar findings were not observed on day 2 and 3. The poorer myocardial performance that the present data (see Chapter 4) and the currently available literature have documented by echocardiography during the first 24 hours [172,219,220] may have a role in the greater CO dependence upon HR observed in on day 1. Since diastolic filling and relaxation seem to be predominantly compromised in this early phase, the ability of the myocardium to effectively increase CO by increasing SV may be transiently impaired. Once the myocardial function improves, the impact of SV on CO determination progressively increases, whereas that of HR tends to become less predominant.

According to the present data, in infants with a hsPDA, increasing SV was associated with greater increases in CO. Moreover, at lower HR ranges, these infants showed significantly higher CO compared to those with a restrictive or a closed duct, whereas at higher HR ranges, the curve flattened down. A similar relationship between LVO, SV, and HR had been previously documented in preterm infants undergoing DA ligation, suggesting that in the presence of a symptomatic PDA, changes in CO is determined more by SV than HR [26]. We have previously observed (Chapter 4) significantly higher SV in the presence of a hsPDA compared with a restrictive or closed duct. Hence, it could be hypothesized that the shortened diastolic time occurring at increased HRs may hinder ventricular filling, whereas at lower HR ranges the longer diastolic filling time allows a full SV contribution to CO determination for increased SV according to the Frank-Starling curve.

A similar mechanism could underlie the greater benefits of dobutamine administration on CO observed at HR ranges <150 bpm during the first 2 days of life: if associated with a longer diastolic filling time, the improvement in myocardial function driven by this inotrope may be more efficient in enhancing CO. Of note, as previously described in Chapter 4, in the present population dobutamine administration effectively enhanced cardiac contractility without being associated with a significant HR increase.

Conversely, dopamine administration during the first 24 hours was associated with a significantly lower CO, which further decreased at higher HR ranges. Consistent with previous evidence that the immature myocardium is particularly sensitive to afterload [21,27,28], it could be hypothesized that even a small afterload increase driven by dopamine administration further impairs myocardial function during the first 24 hours, thus leading to a reduction of SV and, subsequently, of CO. Moreover, the inverse relationship observed between HR and SV, may enhance these negative effects at higher HR ranges. Of note, the negative effect of dopamine administration on the relationship between HR and CO was no longer evident on day 2 and on day 3: it is possible that the progressive

improvement of cardiac function occurring after the first 24 hours after birth allows a progressive myocardial adaptation to increased afterload.

In extremely preterm infants, CO was found to depend more on SV than on HR. Since HR is inversely related with GA (see Chapter 4), more preterm infants have higher resting HR, which may be closer to their functional peak capacity. Hence, strategies aimed at enhancing SV (e.g., volume filling) rather than at increasing HR may effectively contribute to improve CO.

Finally, the correlation between HR and SV has demonstrated that SV changes are inversely related to the HR changes; hence, under otherwise stable conditions, the beat-to-beat fluctuations in HR are counterbalanced by changes in SV, with the ultimate goal of maintaining stable CO values.

The present evidence of a strong, positive correlation between SV and CO and of non-linear relationship between HR and SV may have important clinical implications. First, progressive increases of HR are not always beneficial for CO but may rather exert negative effects, that are further enhanced under specific haemodynamic conditions. Second, especially after the first 24 hours of life, SV represents a predominant determinant of CO and, as such, should represent a first-line target of the therapeutic approaches aimed at CO improvement. Third, the vasopressors and inotropes that are often adopted to support preterm infants' cardiovascular function may exert direct and indirect effects on the relationship between CO and its main determinants, whose knowledge would contribute to optimize the therapeutic haemodynamic management during transition in this delicate population.

The use of beat-to-beat data sampling over a 72-hour period from 64 neonates represents a point of strength of this analysis as it allowed to obtain a solid pool of data, which would have not been achieved with sole intermittent echocardiography evaluations. On the other hand, although EV achieved adequate levels of precision and accuracy when compared to echocardiographic CO assessment, the slight overestimation of CO observed at the Bland-Altman analysis in the presence of a significant transductal shunt may have partially biased the findings observed in relation to a hsPDA. Finally, since the research design was not preliminarily targeted to evaluate inter-operator

variability of echocardiographic CO assessment, only data from a single expert operator were included in the Bland-Altman analysis, and this could be not fully representative of routine clinical practice. The inter-operator agreement within CO_{ECHO} and between CO_{EV} and CO_{ECHO} deserves to be investigated in future targeted research.

6. CARDIOVASCULAR AND CEREBROVASCULAR RESPONSES TO CARDIO-RESPIRATORY EVENTS

6.1. Introduction and aim

Due to the immaturity of the physiological mechanisms involved in respiratory control and oxygenation, intermittent episodes of hypoxia and/or bradycardia are very frequent among premature infants [284]. These episodes, also defined as cardio-respiratory events (CRE), have been associated with several adverse neonatal outcomes, including higher rates of retinopathy of prematurity, bronchopulmonary dysplasia, sleep disordered breathing and poor neurodevelopment [285].

The unfavourable effects of CRE on cerebral haemodynamics in the preterm population have also been established [286,287]. A transient decrease in cerebral oxygenation has been documented during both bradycardic and hypoxic episodes, which can be deeper if the two events occur simultaneously [288,289]. Fluctuations between cerebral hypoxia and hyperoxia activate a pro-oxidant cascade that triggers an inflammatory response and alters the balance of neurotransmitters [285]. These mechanisms have been associated not only with the development of white matter injury in animal studies [290], but also with different patterns of neurocognitive impairment in preterm neonates [291–293].

The haemodynamic instability that characterizes the first 72 hours after preterm birth and the immaturity of the cardiovascular and cerebrovascular systems may worsen the impact of CRE on cerebral haemodynamics throughout this period, with possible impairment of cerebrovascular autoregulation. This is suggested by recent evidence of the association between early hypoxic burden and higher rates of IVH [176,294]. Moreover, during the transitional period, specific conditions, such as a hsPDA, influence the haemodynamic status of premature neonates and as such may also influence the haemodynamic effects of CRE [32].

Current literature on CRE and their impact on cerebral perfusion and oxygenation is mostly based on infants aged from few weeks to few months. To the best of our knowledge, the haemodynamic impact of CRE in these situations still has to be elucidated. Moreover, evidence on functional cardiac changes during CRE in the preterm population is very scarce, and only related to bradycardic episodes without desaturation [295].

The aim of this study was to investigate combined cardiovascular and cerebrovascular responses in response to different types of CRE in preterm infants during the transitional period, and to evaluate whether these responses may be influenced by antenatal, perinatal or postnatal factors.

6.2. Methods and Statistics

Methods

Patient recruitment, ultrasound evaluation and data collection, including the multiple parameters obtained by non-invasive multiparametric monitoring, are described in detail in Chapter 3. Since the occurrence of cardio-respiratory events during mechanical ventilation may underlie different pathophysiological mechanisms, for the sake of data homogeneity, invasively ventilated preterm infants were not included in the analysis related to cardio-respiratory events, which was therefore limited to the subgroup of infants assisted with non-invasive respiratory support (e.g., nasal CPAP, nasal cannulas) or self-ventilating in air. Moreover, the limited number of infants among those included in this sub-group that required inotrope medications during the monitoring period did not allow to handle this variable with a powered analysis; hence, in order to rule out possible confounding factors on haemodynamic parameters, these infants were also excluded.

Based on SpO_2/HR values, CRE were defined as follows: isolated desaturations (ID), defined as SpO_2 <85% [296,297]; isolated bradycardias (IB), defined as any HR fall <100 bpm or >30% below the baseline before the event [297–299]; combined desaturation and bradycardia (DB), if the two events occurred within a 30-sec time window [300]. Event duration was calculated as the period spent below

the SpO_2/HR thresholds used for CRE definition; due to their doubtful clinical relevance, events <10 sec were ruled out from the analysis [296]. Moreover, CRE with baseline SpO_2 <90% were ruled out from the analysis. For each parameter, the last stable values before the event onset (baseline) and their zenit/nadir, concomitant to the lowest SpO_2 and/or HR (event), were tracked down (Figure 6.1); percentage changes (%Δ) between baseline and event values were then calculated and used for statistical analysis.

Statistical analysis

The analytical strategy used for this analysis is based on generalized estimating equations (GEEs), introduced by Zeger and Liang [301]. This method is appropriate for the analysis of correlated data that arise from longitudinal studies, in which measurements/data from different subjects are collected at different time points; the interpretation of regression coefficients is the same as in regression models. A pool of >1000 events nested within 40 infants was adequately powered to test the relationship between cerebrovascular and cardiovascular responses and the independent variables included in the GEE models.

In particular, GEEs with a normal distribution and autoregressive correlation structure were used to analyse the effects of different CRE types on the %Δ of cerebrovascular (cTOI and cFTOE) and cardiovascular parameters (HR, SV, CO_{EV}, ICON, SVR), to compare %Δ between bradycardic events with HR nadir < or ≥ 80bpm and to compare SpO_2 during and after desaturations in relation to oxygen adjustments. GEEs with normal distribution and exchangeable correlation structure were used to assess the impact of clinical variables (gestational age, antenatal Doppler status, antenatal steroids administration, ductal status and ongoing respiratory support) and of different CRE types on %ΔcTOI, %ΔcFTOE and %ΔCO. In these models, the PDA status and the mode of ventilatory support were used as time-dependent covariates, and all the events were nested within individuals. Standard errors were adjusted for the number of non-redundant parameters.
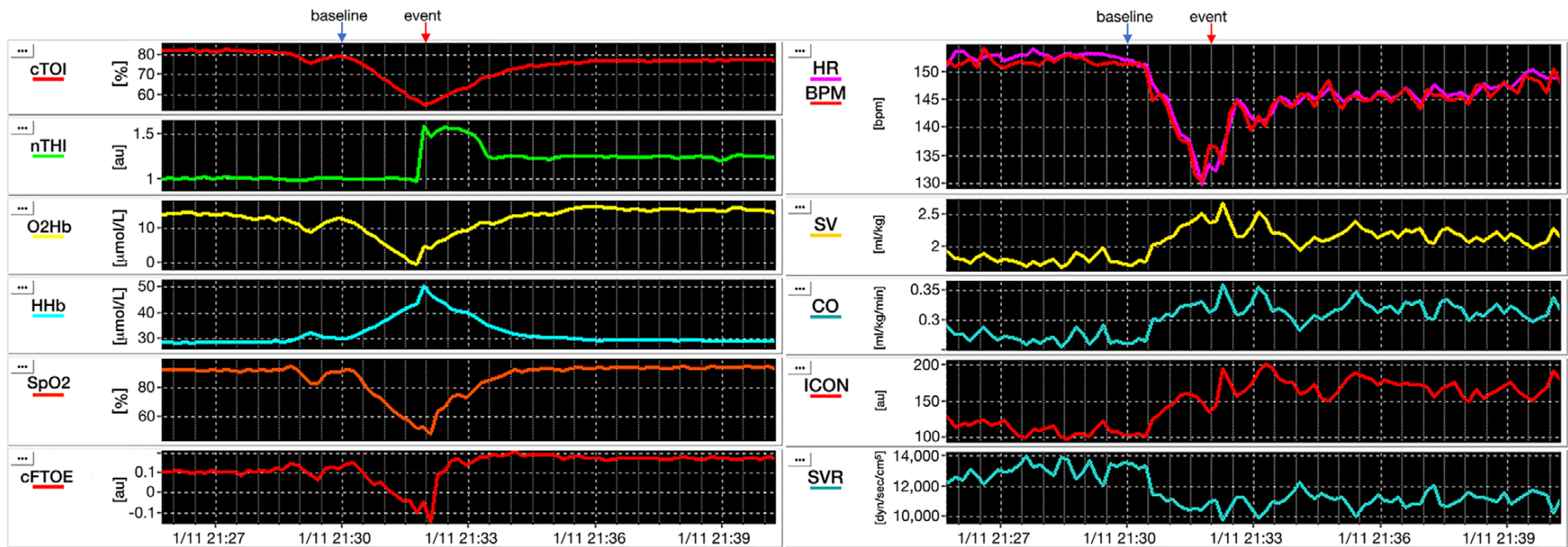
Figure 6.1. Example of an isolated desaturation using ICM+ screenshot of simultaneous changes occurring in the study parameters during a cardio-respiratory event characterized by desaturation and bradycardia. The arrows indicate the time points used for baseline and event values. Adapted from Martini et al. J Physiol (2020) [302].

6.3. Results

This analysis was performed in December 2019 on the 40 neonates non-invasively ventilated or self-ventilating in air enrolled between March 2018 and December 2019. The results were published in September 2020 [302]. In the present dissertation the antenatal Doppler data of the included infants have been stratified according to the presence/absence of the brain sparing phenomenon, and the PDA status has been handled as a binomial variable (hsPDA vs. restrictive or closed DA) for the sake of data homogeneity in respect to the analyses described in the other chapters.

The neonatal characteristics of the subgroup of infants included in this analysis are shown in Table 6.1, whereas their daily clinical and haemodynamic features are detailed in Table 6.2. All the infants received caffeine prophylaxis for apnoea of prematurity.

A total of 1426 events were recorded from the study cohort over the first 72 hours of life; of these, 903 were ID (63.3%), 224 IB (15.7%) and 299 DB (21%). Baseline and event values of each study parameter for each event type are provided in Table 6.3.

Of the 1202 events characterized by a SpO_2 drop, 795 events (66.1%), of which 638 ID and 157 DB, resolved spontaneously or with physical stimulation, whereas the remaining 407 (33.9%), of which 265 ID and 142 DB, required an increase in the fraction of inspired oxygen (FiO_2). This latter group was characterized by significantly deeper nadir values of SpO_2 (70 [interquartile range, IQR, 63.3-74.2] %) and HR (127 [IQR 103-143] bpm) compared to those events which did not require FiO_2 adjustments (SpO_2 81 [IQR 78.8-82.7] %, $p<0.001$; HR 142 [IQR 121-156] bpm, $p<0.001$). The zenit SpO_2 in the recovery phase was significantly higher after those desaturation events requiring a FiO_2 adjustment compared to those who resolved without FiO_2 changes (SpO_2 97 [IQR 95.7-98.2] % vs. 95.5 [IQR 93-97.6] %, $p=0.002$).

***Table 6.1.** Clinical characteristics of the sub-group of infants included in CRE analysis.*

Neonatal characteristics	(n=40)
Gestational age (weeks), mean (standard deviation, SD)	30.5 (2.2)
Birth weight (g), mean (SD)	1279 (326)
Length at birth (cm), mean (SD)	38.5 (2.9)
Head circumference at birth (cm), mean (SD)	28 (2.1)
Antenatal corticosteroids, n (%)	
Complete course	30 (75)
Incomplete course or not given	10 (25)
Intrauterine growth restriction, n (%)	17 (42.5)
Umbilical artery Doppler status, n (%)	15 (37.5)
AREDF w/ brain sparing	10 (25)
AREDF w/o brain sparing	5 (12.5)
Small for gestational age, n (%)	13 (32.5)
Caesarean section, n (%)	37 (92.5)
Male gender, n (%)	20 (50)
Twinhood, n (%)	11 (27.5)
Apgar score at 1 min, median (interquartile range [IQR])	7 (6-8)
Apgar at 5 min, median (IQR)	9 (9-9)

Table 6.2. Clinical and haemodynamic characteristics of the subgroup of infants included in CRE analysis) on day 1, 2 and 3 after birth.

Clinical and haemodynamic characteristics	Day 1	Day 2	Day 3
Weight (g), mean ± standard deviation (SD)	1266 ± 330	1219 ± 328	1161 ± 316
Status of ductus arteriosus, n (%)			
Haemodynamically significant	13 (32.5)	8 (20)	3 (7.5)
Restrictive	18 (45)	14 (35)	7 (17.5)
Closed	9 (22.5)	18 (45)	30 (75)
Ventilatory support, n (%)			
Continuous Positive Airway Pressure	34 (85)	31 (77.5)	27 (57.5)
Nasal cannulas or self-ventilating in air	6 (15)	9 (22.5)	17 (42.5)
Intraventricular haemorrhage, n (%)			
Grade I	4 (10)	4 (10)	6 (15)
Grade II to IV	0 (0)	0 (0)	0 (0)
Baseline values, mean ± SD			
Peripheral arterial oxygen saturation (%)	96.5 ± 2.8	96 ± 3.2	95.8 ± 2.7
Cerebral tissue oxygenation index (%)	74.3 ± 8.2	75.9 ± 8.0	75.2 ± 7.7
Cerebral fraction of oxygen extraction	0.23 ± 0.09	0.21 ± 0.08	0.22 ± 0.08
Heart rate (bpm)	150.5 ± 16.7	147.1 ± 17.8	152.3 ± 18.2
Stroke volume (ml/kg)	2.23 ± 0.65	2.49 ± 0.7	2.38 ± 0.61
Cardiac output (ml/kg/min)	331.3 ± 94.7	356.6 ± 91.5	357.3 ± 99.1
Index of cardiac contractility	104.6 ± 45.3	120.2 ± 44.7	115.7 ± 40.9
Systemic vascular resistance (dyn s/cm^5/m^2)	9704 ± 3936	8729 ± 3421	9904 ± 3373

Table 6.3. *Baseline and event values of the haemodynamic parameters for isolated desaturations, combined desaturations and bradycardias, isolated bradycardias.*

Events/parameters	Baseline (mean ± SD)	Event (mean ± SD)
Isolated desaturations (n=903)		
Peripheral arterial oxygen saturation (%)	95.6 ± 3.1	76.9 ± 8.3
Cerebral tissue oxygenation index (%)	75.2 ± 7.9	67.3 ± 8.5
Cerebral fraction of oxygen extraction	0.21 ± 0.08	0.14 ± 0.11
Heart rate (bpm)	152.1 ± 15.6	144.7 ± 18
Stroke volume (ml/kg)	2.44 ± 0.65	2.52 ± 0.68
Cardiac output (ml/kg/min)	362.3 ± 95.5	360.1 ± 103.8
Index of cardiac contractility	117.6 ± 46.3	115.9 ± 48.7
Systemic vascular resistances (dyn s/cm^5/m^2)	9211 ± 4623	9206 ± 4690
Combined desaturations and bradycardias (n=299)		
Peripheral arterial oxygen saturation (%)	96.3 ± 2.7	73.6 ± 9.3
Cerebral tissue oxygenation index (%)	76.4 ± 7.7	63.6 ± 8.9
Cerebral fraction of oxygen extraction	0.20 ± 0.08	0.16 ± 0.11
Heart rate (bpm)	156.8 ± 17.6	86.5 ± 13.4
Stroke volume (ml/kg)	2.22 ± 0.6	2.60 ± 0.67
Cardiac output (ml/kg/min)	340.1 ± 93.8	239.8 ± 70.9
Index of cardiac contractility	107.7 ± 36.1	97.2 ± 34.3
Systemic vascular resistances (dyn s/cm^5/m^2)	11558 ± 5190	16220 ± 10439
Isolated bradycardias (n=224)		
Peripheral arterial oxygen saturation (%)	96.4 ± 2.2	94.5 ± 4.6
Cerebral tissue oxygenation index (%)	75.1 ± 7.9	72.6 ± 7.1
Cerebral fraction of oxygen extraction	0.22 ± 0.08	0.23 ± 0.07
Heart rate (bpm)	137.7 ± 19.1	89.8 ± 9.8
Stroke volume (ml/kg)	2.54 ± 0.67	2.77 ± 0.57
Cardiac output (ml/kg/min)	335.8 ± 87.1	263.4 ± 58.6
Index of cardiac contractility	109.3 ± 34.8	107.4 ± 28.2
Systemic vascular resistances (dyn s/cm^5/m^2)	11378 ± 5027	13805 ± 6710

Percentage changes of cerebrovascular parameters in response to different CRE types are shown in Figure 6.2; %ΔcTOI significantly differed among CRE types, with the deepest reductions observed during DB compared to ID (p<0.001) and IB (p<0.001), whereas IB had the mildest impact. Both ID (p<0.001) and DB (p<0.001) led to a significant reduction of %ΔcFTOE compared to IB, which showed minimal effects on this parameter. A significant difference in %ΔcFTOE was also observed between ID and DB (p=0.019).
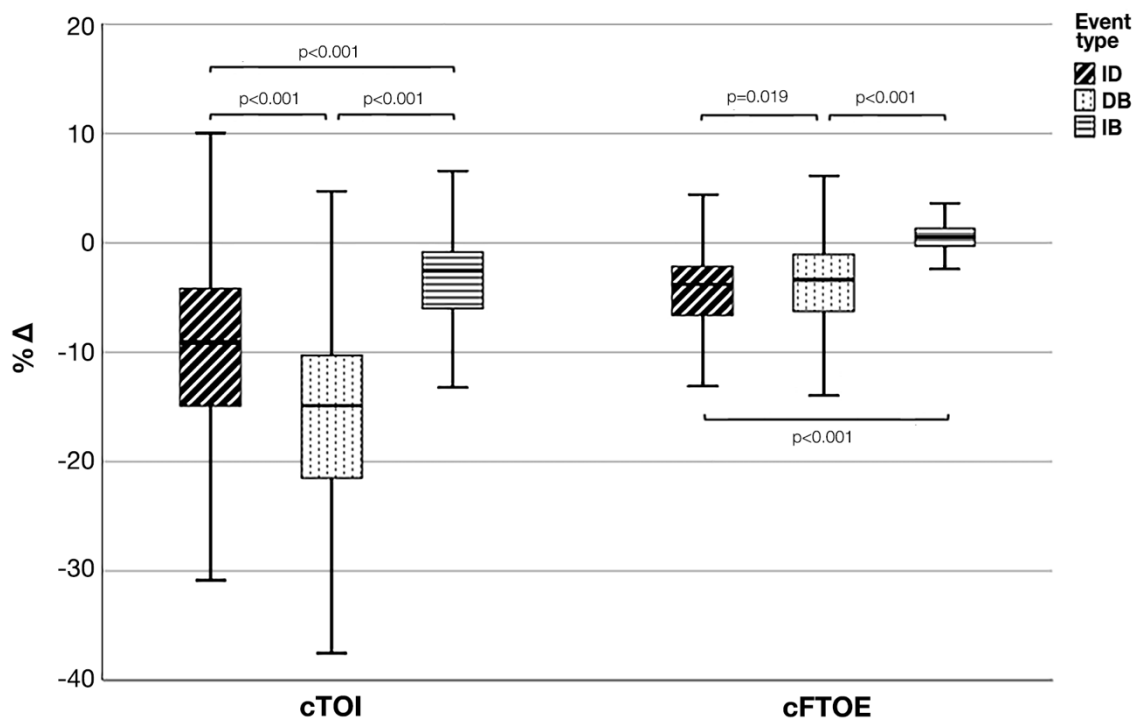

Figure 6.2. Percentage change (%Δ) of cerebral tissue oxygenation index (cTOI) and cerebral fraction of tissue oxygen extraction (cFTOE) during isolated desaturation (ID), isolated bradycardia (IB) and combination desaturation and bradycardia (DB). The central line in the boxplot is the median, the margins of the box are the 25th and the 75th percentiles and the whiskers represent 1.5 times the interquartile range (1.5*IQR). P-values for significant comparisons (generalized estimating equations) are provided.

Figure 6.3 illustrates percentage variations of cardiovascular parameters in response to different CRE types. Consistent with the definition of DB and IB, a significant HR drop was observed during these events compared to ID (p<0.001 for both comparisons); however, the HR decrease was significantly deeper if bradycardia was accompanied by a concomitant desaturation (p=0.020). Despite the %ΔSV increase, there was significant overall reduction of %ΔCO during bradycardic episodes, either when alone or associated with desaturation, compared to ID (p<0.001 for both comparisons). Conversely, when compared to ID, %ΔSVR significantly increased during DB (p<0.001) and IB (p<0.001). The combination of desaturation and bradycardia also resulted in significant reduction of %ΔICON compared to desaturations alone (p=0.043).
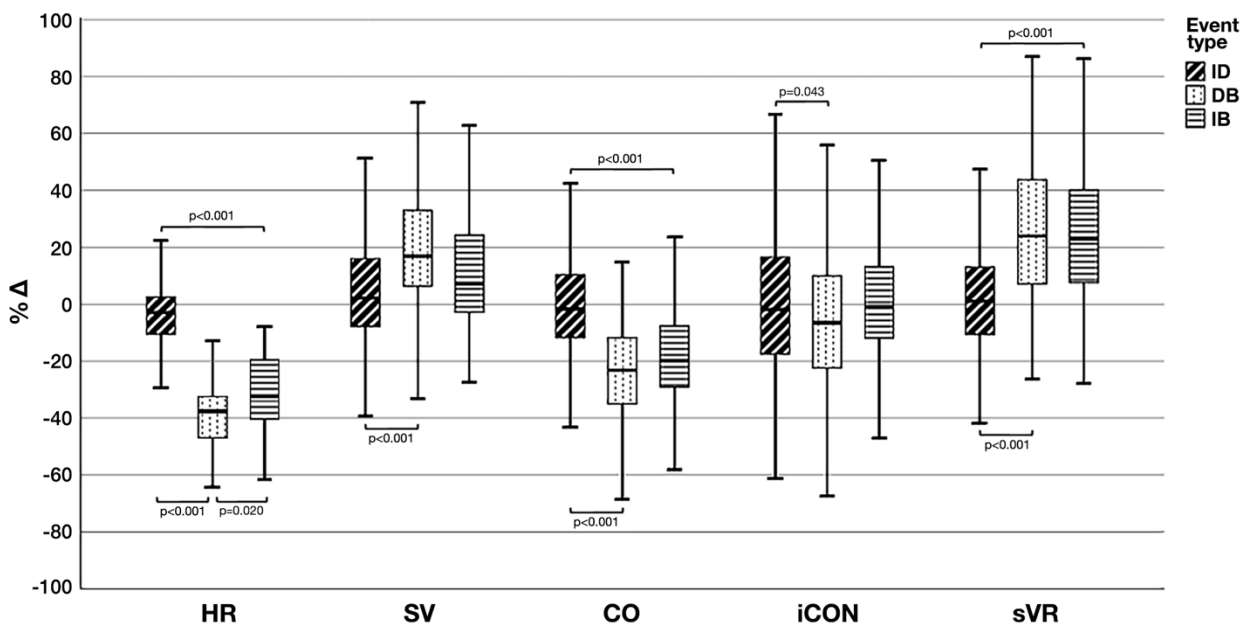
Figure 6.3. *Percentage change (%Δ) of heart rate (HR), stroke volume (SV), cardiac output (CO), index of cardiac contractility (ICON) and systemic vascular resistance (SVR) during isolated desaturation (ID), isolated bradycardia (IB) and combination desaturation and bradycardia (DB). The central line in the boxplot is the median, the margins of the box are the 25th and the 75th percentiles and the whiskers represent 1.5 times the interquartile range (1.5*IQR). P-values for significant comparisons (generalized estimating equations) are provided.*

For bradycardic events (DB and IB), %Δ of cardiovascular and cerebrovascular parameters were compared between CRE with a nadir HR ≥ (n=419) or <80 bpm (n=104). As shown in Figure 6.4, a nadir HR <80 bpm was associated with significantly deeper %ΔcTOI (p=0.015), %ΔCO (p<0.001) and more positive %ΔsVR (p<0.001) compared to nadir HR values ≥ 80 bpm, while no significant effect was observed for %ΔcFTOE, %ΔSV and %ΔICON.

The results of GEE models, detailed in Table 6.4, confirmed the impact of different CRE types on %ΔcTOI, %ΔcFTOE and %ΔCO and showed that different neonatal characteristics exert a significant influence on these parameters. In particular, the presence of an hsPDA was independently associated with greater cTOI reductions (p=0.007) and higher cFTOE values (p=0.029) in response to CRE, whereas intrauterine-growth restricted neonates with antenatal evidence of cerebral blood flow redistribution showed more negative variations of %ΔcFTOE (p=0.042). A significant positive correlation was observed between %ΔCO and GA (p=0.036), and significantly higher %ΔCO were also found in neonates with abnormal antenatal Doppler, with or without brain sparing evidence (p=0.039 and p=0.036, respectively).

Table 6.4. Results of three generalized estimating equation models predicting percentage changes of cerebral tissue oxygenation index (%ΔcTOI), cerebral fraction of oxygen extraction (%ΔcFTOE) and cardiac output (%ΔCO), respectively. β are regression coefficients that can be interpreted as in a linear regression model. The confidence interval reflects the error of the estimate of the regression coefficient; when the confidence interval includes zero, the association between the dependent and the independent variable is not significant. When the independent variable is categorical, one group is used as the reference category (ref). Abbreviations: CI, confidence interval; GA, gestational age; AREDF, umbilical absent or reversed end-diastolic flow; CPAP, continuous positive airway pressure; SVIA, self-ventilating in air; ID, isolated desaturation; DB, desaturation with bradycardia; IB, isolated bradycardia

Variable	%ΔcTOI (n=1426)		%ΔcFTOE (n=1426)		%ΔCO (n=1426)	
	β (95%CI)	P-value	β (95%CI)	P-value	β (95%CI)	P-value
GA, weeks	-0.415 (-0.990, 0.160)	0.157	0.423 (-0.297, 1.143)	0.250	0.900 (0.061, 1.739)	**0.036**
Antenatal Doppler status						
AREDF, brain sparing	-0.459 (-3.257, 2.338)	0.748	-3.669 (-7.201, -0.137)	**0.042**	4.017 (0.269, 7.765)	**0.039**
AREDF, no brain sparing	1.373 (-2.660, 5.406)	0.505	-1.060 (-6.617, 4.497)	0.709	6.493 (0.244, 12.743)	**0.036**
Normal	Ref.		Ref.		Ref.	
Antenatal steroids,						
Complete course	-0.449 (-3.366, 2.467)	0.763	-0.057 (-3.514, 3.400)	0.974	0.665 (-3.750, 5.079)	0.768
Incomplete/not given	Ref.		Ref.		Ref.	
Ductal status,						
Haemodynamically sign.	-2.842 (-4.915, -0.770)	**0.007**	5.559 (0.574, 10.544)	**0.029**	1.652 (-4.334, 7.627)	0.588
Restrictive or closed	Ref.		Ref.		Ref.	
Respiratory support,						
CPAP	-0.166 (-2.048, 1.717)	0.863	-0.940 (-4.846, 2.967)	0.637	-2.148 (-6.002, 1.706)	0.275
Nasal cannulas/SVIA	Ref.		Ref.		Ref.	
Event type,						
IB	6.503 (4.665, 8.340)	**<0.001**	Ref.		-20.869 (-26.457, -15.281)	**<0.001**
DB	-6.280 (-7.655, -4.904)	**<0.001**	-4.858 (-9.972, 0.257)	0.063	-20.360 (-25.067, -15.652)	**<0.001**
ID	Ref.		-7.184 (-11.635, -2.733)	**0.002**	Ref.	

§Reference category
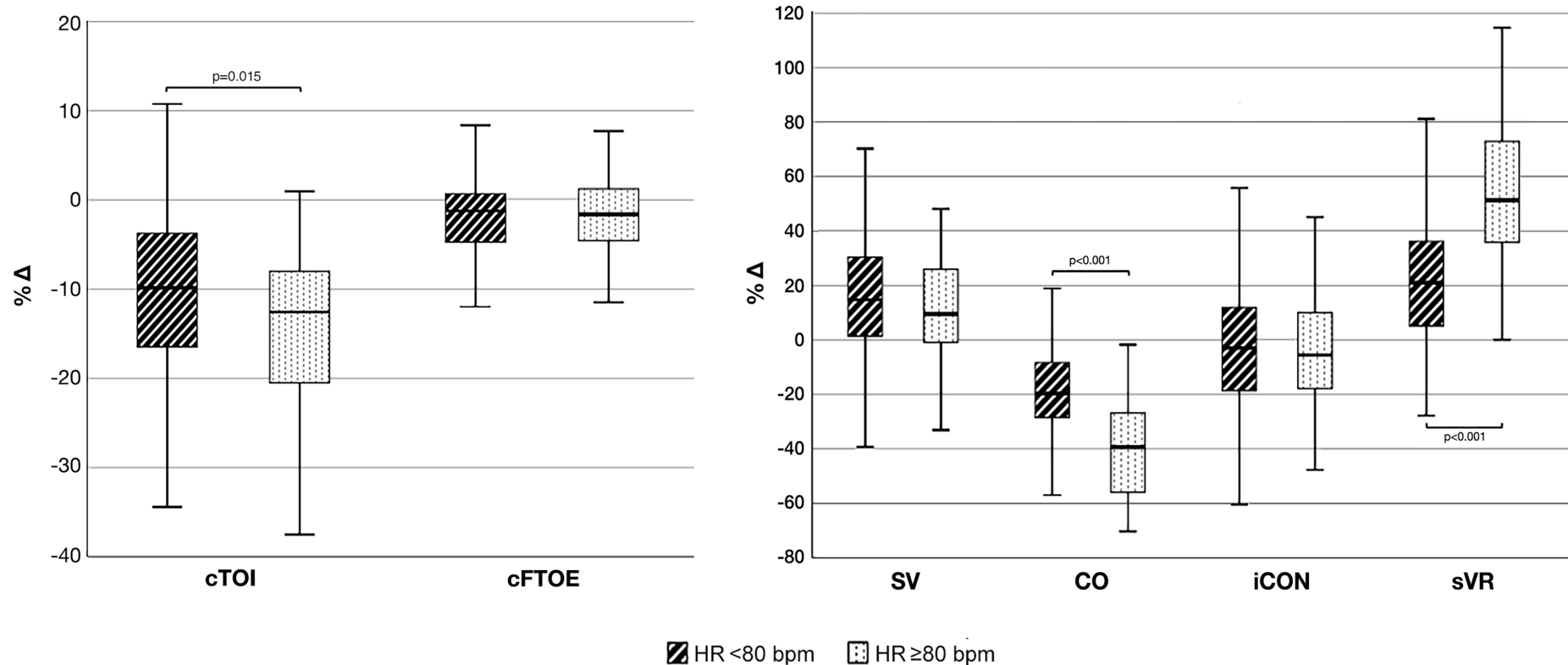
Figure 6.4. *Percentage change (%Δ) of cerebral tissue oxygenation index (cTOI), cerebral fraction of tissue oxygen extraction (cFTOE), stroke volume (SV), cardiac output (CO), index of cardiac contractility (ICON) and systemic vascular resistance (SVR) during bradycardic events characterized by a HR nadir < or ≥80 bpm. The central line in the boxplot is the median, the margins of the box are the 25th and the 75th percentiles and the whiskers represent 1.5 times the interquartile range (1.5*IQR). P-values for significant comparisons are provided.*

6.4. Discussion

To the best of our knowledge, this is the first data providing a combined non-invasive investigation of cardiac and cerebral haemodynamics in response to CRE in preterm infants during the transitional period. Our findings indicate that different types of CRE elicit variable cardiovascular and cerebrovascular fluctuations. These in turn, are significantly influenced not only by the event type, but also by specific neonatal characteristics, such as abnormal umbilical Doppler or the presence of a hsPDA.

CRE characterized by a combined drop in SpO_2 and HR had the highest impact on cerebral oxygenation; this is consistent with previous findings describing a significant reduction of this parameter during DB when compared to isolated events [288,289].

In 1985, Perlman and Volpe [303] carried out a Doppler evaluation of blood flow velocity fluctuations in the anterior cerebral arteries during apnoeic episodes accompanied by bradycardia in preterm infants aged 2 to 45 days. During a bradycardia, especially if the HR fell below 80 bpm, they observed a significant decrease in cerebral blood flow velocity and associated reduction in BP. A causal relationship between the two findings was postulated, raising important questions on the efficacy of the physiological mechanisms of cerebral autoregulation during these events, characterized by a sudden onset and a relatively short duration.

Later on, Pichler et al. [304] performed a combined evaluation of cerebral oxygenation and cerebral blood volume during a small number of apnoeic episodes, characterized by desaturation with or without bradycardia (HR <80 bpm). In the presence of bradycardia, a greater reduction of cerebral oxygenation and of cerebral blood volume occurred compared to desaturation alone. The authors hypothesized that a decrease in cerebral blood flow occurs during bradycardic episodes, highlighting the importance of associated cardio-vascular changes on cerebral haemodynamics.

This research provides simultaneous evaluation of cerebral and cardiovascular haemodynamic changes in response to CRE in preterm infants during the transitional period. We observed a

significant reduction in CO during bradycardic episodes, with lower values if the bradycardia was accompanied by desaturation. CO is the product of HR and SV. With a fall in HR, there was a compensatory increase in SV. The inverse correlation between HR and the left-ventricular ejection time, which is a main determinant for SV [305], can explain this finding. While HR decreased, SV significantly increased during IB and DB, compared to ID. However, according to our results, the effect of HR drop predominated over the increase in SV resulting in a net decrease in CO during bradycardic events. Moreover, the occurrence of bradycardia and desaturation together was associated with a significant reduction of cardiac contractility, which could play a role in the deeper reduction of CO observed during DB.

The effect of bradycardia on myocardial function has been previously evaluated by de Waal et al. on a small number of episodes by means of functional echocardiography [295]. In line with the present findings, the authors reported an increased SV but a lower total CO during bradycardic events; they also observed a deficit in left atrial contractility. Bradycardic episodes, with or without desaturation, were also associated also with a significant increase in sVR. This might represent a physiological attempt to compensate the reduction in CO occurring with the bradycardia by increasing the systemic vascular tone. However, as there was no continuous invasive BP monitoring when collecting this data, this finding should be interpreted with caution.

In the present cohort, the presence of a hsPDA led to a greater fall in cTOI and increase in cFTOE during CRE, independently of their type. A significantly lower cerebral oxygenation has been previously reported by several NIRS studies in preterm infants with a hsPDA compared to those with a non-significant PDA or with a closed duct [306–309], reflecting reduced cerebral blood flow due to the significant left-to-right transductal shunting [310]. These findings suggest that, in infants with a hsPDA, CRE are more likely to result in a greater degree of cerebral hypoxia, which has been recently proposed as a possible risk factor for IVH development over the first days of life [176,294]. Moreover, both hsPDA [311] and intermittent hypoxia [290,312] have been associated with a higher

risk of periventricular leukomalacia. We speculate that particular attention should be made in infants with a hsPDA experiencing repeated CRE. However, the evaluation of a possible association with IVH/PVL was not feasible in the present study, as only few infants had low-grade IVH during the study period and none went on to develop PVL.

Antenatal Doppler impairment was associated with different haemodynamic responses to CRE, with particular reference to cFTOE and CO. Infants with antenatal evidence of brain sparing showed a lower increase of cFTOE in response to CRE, irrespective of the type of event, whereas a smaller CO reduction during CRE was observed in the presence of antenatal AREDF, with or without blood flow redistribution. Identifying fetuses with placental-related intrauterine growth restriction, characterized by the antenatal Doppler evidence of AREDF in the umbilical artery and/or in the ductus venosus, is very important. This condition is associated with chronic fetal hypoxia, which ultimately leads to a circulatory redistribution aimed at favouring brain perfusion [313]. Our findings suggest that the physiological adaptations occurring antenatally in response to the persistently reduced blood and oxygen delivery through the placenta, and to the subsequent compensatory cardiovascular remodelling [314], aimed at guaranteeing an adequate blood perfusion and oxygenation of the brain, may persist over the 3 days after birth [270]. The high prevalence of AREDF in the study cohort, which is due to the characteristics of the local preterm population as our hospital is a tertiary referral centre for placental-related pregnancy complications, including placental-related IUGR, allowed to evaluate the effects of this condition also in relation to the antenatal patterns of blood flow redistribution.

According to the present results, lower GAs resulted in a greater drop in CO during CRE associated with bradycardia. It has been shown that preterm infants have an immature myocardial tissue, with fewer contractile elements, higher water content, greater surface-to-volume ratio, and a reliance on L-type calcium channels that utilize extracellular calcium as a source of the second messenger driving cardiomyocyte contraction [208]. A GA-dependent impairment of myocardial function has been

demonstrated by functional echocardiographic studies [216,315], and a positive correlation between GA and baseline CO has also been documented using electrical cardiometry in healthy and stable preterm neonates [150,196]. Hence, the immature cardiac function associated with lower GAs may explain the greater impact of CO that we observed in more premature infants during CRE.

To date, increasing evidence correlates vital parameters during the first golden minutes after birth with postnatal adaptation [316]. As illustrated in Table 6.1, most of the study infants showed an adequate early postnatal adaptation, and 1 in 3 did not require positive pressure ventilation in the delivery room. Consistent with the mentioned evidence, these infants maintained an overall stable condition during the transitional period and a low number of complications possibly triggered by poor neonatal adaption were observed.

An important limitation of the present study is the lack of invasive continuous BP monitoring (i.e., through an indwelling arterial catheter). However, this was an observational study based on relatively stable preterm infants, and in our routine practice arterial lines are not placed in infants without a significant haemodynamic instability (e.g., hypotension requiring inotropes).

Furthermore, the small number of infants with extremely low gestational ages (e.g., <28 weeks' gestation) or with adverse postnatal adaptation also needs to be acknowledged among the study limitations. This is mainly due to the exclusion of invasively ventilated neonates, in order to rule out several factors related to mechanical ventilation (e.g., ventilation settings, respiratory rate, endotracheal suctioning, tube obstruction or dislodgement) which may have influenced not only CRE features but also cardiovascular and cerebrovascular parameters. As a consequence, however, the infants included were generally well-adapted and developed very few complications during transition. Although this cohort may constitute a reference range for cerebral and cardiovascular haemodynamic parameters, larger studies including ventilated and haemodynamically unstable neonates, may elucidate the role of BP and the integrity of the physiological mechanisms of cerebral autoregulation during intermittent hypoxia and bradycardia in sicker preterm infants.

7. CONCLUSIONS AND FUTURE WORK

The transition from intrauterine to extrauterine life is a critical phase of physiological adaptation in preterm infants. Due to their functional and anatomical immaturity, this population is prone to enhanced haemodynamic instability during the transitional period, which put them at risk of developing significant clinical complications. The validation of comprehensive haemodynamic monitoring, aimed at the assessment of cardiovascular function and end-organ perfusion throughout this challenging phase, would not only improve knowledge of transitional physiology and pathophysiology following preterm birth, but would also support the development of a tailored therapeutic management.

In the present research, integrated, continuous and non-invasive monitoring of cardiovascular and cerebrovascular haemodynamics throughout the first 72 hours of life was performed on 64 preterm infants. The obtained results support the technical feasibility of this monitoring approach even at extremely low gestational ages (e.g., 24 weeks). Together with NIRS and pulse oximetry, the comprehensive monitoring adopted in this research project also included electrical velocimetry. This technique, which has been introduced in neonatal settings only in recent years, demonstrated a good agreement for cardiac output estimation when compared with functional echocardiography, which is the most widely used technique for non-invasive cardiac output assessment in the preterm population; however, a slight overestimation was observed in infants with a haemodynamically significant PDA, consistent with the currently available literature.

A non-invasive marker for cerebrovascular reactivity, based on the correlation between cerebral oxygenation and heart rate, was also evaluated in this dissertation, providing encouraging results in support of its inclusion in the haemodynamic monitoring during postnatal transition.

In Chapter 4, the time trends of cardiovascular and cerebrovascular haemodynamics during the transitional period have been evaluated, demonstrating the occurrence of a progressive improvement in the overall cardiovascular function, especially within the first 48 hours of life, and in

cerebrovascular reactivity. Moreover, the influence of a haemodynamically significant PDA on the observed trends has been demonstrated, supporting the pathophysiological relevance of this condition. The association between cardiovascular and cerebrovascular parameters and a pool of antenatal, perinatal and postnatal factors that overall contribute to characterize the early exposome of preterm infants has also been investigated. This analysis revealed specific interactions between these factors and the haemodynamic parameters and allowed to outline characteristic haemodynamic profiles in association with the following neonatal features: gestational age, antenatal Doppler status (with particular reference to the presence or absence of the brain sparing phenomenon), and ductal status. These results underpin how multifaceted the transitional haemodynamic status is in such a heterogenic population as preterm infants and provide valuable hints in support of the development of an individualized haemodynamic management of preterm infants during this delicate phase.

In chapter 5, the relationship existing between CO and its two main determinants, namely HR and SV, was evaluated, revealing that the correlation between CO and HR is not linear and is significantly influenced by HR ranges themselves, the ductal status and ongoing cardiovascular drugs; hence, knowledge of where a neonate lies within this curve, may be useful for CO optimization. Moreover, a strong relationship between SV and CO has been demonstrated, especially after the first 24 hours of life, thus supporting evidence according to which SV is a predominant CO determinant even in preterm infants and, as such, should be primarily taken into account in the haemodynamic management of this population.

In chapter 6, the cardiovascular and cerebrovascular responses to brief and acute cardio-respiratory events, which are particularly common in preterm infants during the transitional period, were examined. According to the obtained results, the haemodynamic impact of these events on both cardiovascular and cerebral sides is modulated not only by the event characteristics themselves, but also by individual neonatal features that coincided within the three characteristics underlying the

haemodynamic profiles described in Chapter 4: gestational age, antenatal Doppler status and ductal status.

The present research indicates that cardiovascular and cerebrovascular haemodynamics undergo significant changes over the first 72 hours of life and are significantly influenced by specific antenatal, perinatal or postnatal factors – inclusive of cardiovascular treatments – that contribute to outline characteristic haemodynamic profiles, whose knowledge may support the development of individualized strategies for the haemodynamic management of high-risk preterm neonates.

In particular, the following key findings have emerged from the present research:

1) *The haemodynamic status of preterm infants varies upon several underlying or ongoing conditions: in particular, GA, antenatal Doppler characteristics and the state of the PDA impart significant differences in cardiovascular and cerebrovascular physiology during the transitional phase. Hence, these factors and their possible dynamic interactions should be taken into account in the clinical and therapeutic management of the preterm population, which cannot therefore be considered as a haemodynamically homogenous group. Moreover, the emerged haemodynamic profiles should also be considered as a way of stratifying preterm neonates when designing future studies or developing therapeutic protocols.*

2) *The contribution of SV and HR in determining CO vary over the first 3 days of life and in relation to specific clinical and therapeutic factors. The importance of SV on CO determination, the enhanced susceptibility of the preterm myocardium to afterload observed in the first 24 hours and the impact of different HR ranges should not be underestimated, but rather taken carefully into account to build tailored pharmacological approaches for CO optimization.*

3) Although cardio-respiratory events are very frequent among preterm infants, their cardiovascular and cerebrovascular impact should not be ignored. Since some events are less benign than others, it is important to classify them correctly. Moreover, knowledge of the clinical factors associated with deeper haemodynamic fluctuations in response to these events (e.g., low GA, hsPDA) it is important to identify infants that may be more susceptible to the effects of repeated hypoxia-ischemia-reperfusion cycles.

While the increased representation of intrauterine growth-restricted infants with fully available data on antenatal Doppler represents a point of strength of the present study, the unavailability of a simultaneous invasive blood pressure monitoring needs to be acknowledged as a research limitation. In fact, if available, it would have allowed not only to examine the continuous trajectories of MABP over time, but also to compare the observed TOHRx values against alternative indices of cerebral autoregulation loss, derived from methods of autoregulation assessment based on continuous blood pressure monitoring.

The small number of preterm infants who developed IVH, especially of high grades, within the first 72 hours, represents an additional limitation to the present research, as it did not allow to perform a targeted analysis of cardiovascular and cerebrovascular transitional features in relation to the development of this complication, which thus represents a key target for future research.

Based on the present data, additional research objectives that deserve to be addressed in targeted investigations have been identified. The first is whether early cardiovascular and cerebrovascular patterns may effectively predict spontaneous ductal closure, or the responsiveness to pharmacological treatment. The second would aim to investigate whether (and when) the particular haemodynamic patterns observed in infants with antenatal impairment of umbilical Doppler resolve, or persist over time. Third, in settings where continuous BP data are available, the investigation of MABP changes

during to CRE may add valuable information to contextualize the cardiovascular and cerebrovascular responses to these events described in Chapter 6.

Finally, targeted research aimed at evaluating the relationship between cardiovascular and cerebrovascular parameters, lung pressures and volumes in invasively ventilated preterm infants has been developed in the context of this research project, and is currently ongoing, with the aim to assess more in deep the haemodynamic effects of mechanical ventilation in sick preterm infants.

The body of work presented in this thesis demonstrates the feasibility and validity of multiparameter monitoring in neonatal clinical settings to provide useful information on the cardiovascular and cerebrovascular circulation of very preterm infants during the transitional phase. Continuous monitoring of transitional circulation combining EV and NIRS enables real-time assessment of the response to therapies, CRE and other interventions both at a cardiovascular and cerebral level. From a haemodynamic perspective, the present data indicate the importance of stratifying this population particularly based on their antenatal physiology, GA and postnatal ductal status in both clinical practice and future research.

8. REFERENCES

[1]   Kiserud T. Physiology of the fetal circulation. Semin Fetal Neonatal Med 2005;10:493–503. doi:10.1016/j.siny.2005.08.007.

[2]   Linask KK, Han M, Bravo-Valenzuela NJM. Changes in vitelline and utero-placental hemodynamics: implications for cardiovascular development. Front Physiol 2014;5:390. doi:10.3389/fphys.2014.00390.

[3]   Knöfler M. Critical growth factors and signalling pathways controlling human trophoblast invasion. Int J Dev Biol 2010;54:269–80. doi:10.1387/ijdb.082769mk.

[4]   Figueroa-Diesel H, Hernandez-Andrade E, Acosta-Rojas R, Cabero L, Gratacos E. Doppler changes in the main fetal brain arteries at different stages of hemodynamic adaptation in severe intrauterine growth restriction. Ultrasound Obstet Gynecol 2007;30:297–302. doi:10.1002/uog.4084.

[5]   Finnemore A, Groves A. Physiology of the fetal and transitional circulation. Semin Fetal Neonatal Med 2015;20:210–6. doi:10.1016/j.siny.2015.04.003.

[6]   Kamoji VM, Dorling JS, Manktelow B, Draper ES, Field DJ. Antenatal umbilical Doppler abnormalities: An independent risk factor for early onset neonatal necrotizing enterocolitis in premature infants. Acta Paediatr Int J Paediatr 2008;97:327–31. doi:10.1111/j.1651-2227.2008.00671.x.

[7]   Hines MH. Neonatal cardiovascular physiology. Semin Pediatr Surg 2013;22:174–8. doi:10.1053/j.sempedsurg.2013.10.004.

[8]   Crossley KJ, Allison BJ, Polglase GR, Morley CJ, Davis PG, Hooper SB. Dynamic changes in the direction of blood flow through the ductus arteriosus at birth. J Physiol 2009;587:4695–704. doi:10.1113/jphysiol.2009.174870.

[9]   Kamlin COF, O'Donnell CPF, Davis PG, Morley CJ. Oxygen saturation in healthy infants immediately after birth. J Pediatr 2006;148:585–9. doi:10.1016/j.jpeds.2005.12.050.

[10]   Kondo M, Itoh S, Kunikata T, Kusaka T, Ozaki T, Isobe K, et al. Time of closure of ductus venosus in term and preterm neonates. Arch Dis Child 2001;85. doi:10.1136/fn.85.1.f57.

[11]   Walther FJ, Benders MJ, Leighton JO. Early changes in the neonatal circulatory transition. J Pediatr 1993;123:625–32. doi:10.1016/S0022-3476(05)80966-7.

[12]   Dees E, Baldwin HS. Developmental Biology of the Heart. Avery's Dis. Newborn Tenth Ed., Elsevier Inc.; 2018, p. 724-740.e3. doi:10.1016/B978-0-323-40139-5.00050-4.

[13]   Vrancken SL, van Heijst AF, de Boode WP. Neonatal Hemodynamics: From developmental physiology to comprehensive monitoring. Front Pediatr 2018;6:1–15. doi:10.3389/fped.2018.00087.

[14]   Anderson PAW. The heart and development. Semin Perinatol 1996;20:482–509. doi:10.1016/S0146-0005(96)80064-4.

[15]   Opitz CA, Leake MC, Makarenko I, Benes V, Linke WA. Developmentally Regulated Switching of Titin Size Alters Myofibrillar Stiffness in the Perinatal Heart. Circ Res 2004;94:967–75. doi:10.1161/01.RES.0000124301.48193.E1.

[16]   Lahmers S, Wu Y, Call DR, Labeit S, Granzier H. Developmental Control of Titin Isoform Expression and Passive Stiffness in Fetal and Neonatal Myocardium. Circ Res 2004;94:505–13. doi:10.1161/01.RES.0000115522.52554.86.

[17]   Groves AM, Durighel G, Finnemore A, Tusor N, Merchant N, Razavi R, et al. Disruption of intracardiac flow patterns in the newborn infant. Pediatr Res 2012;71:380–5. doi:10.1038/pr.2011.77.

[18]   Mori K, Nakagawa R, Nii M, Edagawa T, Takehara Y, Inoue M, et al. Pulsed wave Doppler tissue echocardiography assessment of the long axis function of the right and left ventricles

during the early neonatal period. Heart 2004;90:175–80. doi:10.1136/hrt.2002.008110.

[19]   Bers   DM.   Cardiac   excitation-contraction   coupling.   Nature   2002;415:198–205.
        doi:10.1038/415198a.

[20]   Cox DJ, Groves AM. Inotropes in preterm infants - Evidence for and against. Acta Paediatr Int
        J Paediatr 2012;101:17–23. doi:10.1111/j.1651-2227.2011.02545.x.

[21]   Takahashi Y, Harada K, Kishkurno S, Arai H, Ishida A, Takada G. Postnatal left ventricular
        contractility   in   very   low   birth   weight   infants.   Pediatr   Cardiol   1997;18:112–7.
        doi:10.1007/s002469900127.

[22]   Wiegerinck RF, Cojoc A, Zeidenweber CM, Ding G, Shen M, Joyner RW, et al. Force
        frequency relationship of the human ventricle increases during early postnatal development.
        Pediatr Res 2009;65:414–9. doi:10.1203/PDR.0b013e318199093c.

[23]   Kim MY, Finch AM, Lumbers ER, Boyce AC, Gibson KJ, Eiby YA, et al. Expression of
        adrenoceptor subtypes in preterm piglet heart is different to term heart. PLoS One 2014;9.
        doi:10.1371/journal.pone.0092167.

[24]   Schiffmann H, Flesch M, Häuseler C, Pfahlberg A, Böhm M, Hellige G. Effects of different
        inotropic interventions on myocardial function in the developing rabbit heart. Basic Res
        Cardiol 2002;97:76–87. doi:10.1007/s395-002-8390-1.

[25]   Winberg P, Ergander U. Relationship between heart rate, left ventricular output, and stroke
        volume in preterm infants during fluctuations in heart rate. Pediatr Res 1992;31:117–20.
        doi:10.1203/00006450-199202000-00005.

[26]   Lindner W, Seidel M, Versmold HT, Döhlemann C, Riegel KP. Stroke volume and left
        ventricular output in preterm infants with patent ductus arteriosus. Pediatr Res 1990;27:278–
        81. doi:10.1203/00006450-199003000-00015.

[27]   Rowland DG, Gutgesell HP. Noninvasive assessment of myocardial contractility, preload, and

afterload in healthy newborn infants. Am J Cardiol 1995;75:818–21. doi:10.1016/S0002-9149(99)80419-6.

[28]   Igarashi H, Shiraishi H, Endoh H, Yanagisawa M. Left ventricular contractile state in preterm infants: Relation between wall stress and velocity of circumferential fiber shortening. Am Heart J 1994;127:1336–40. doi:10.1016/0002-8703(94)90053-1.

[29]   Saini SS, Kumar P, Kumar RM. Hemodynamic changes in preterm neonates with septic shock: A prospective observational study. Pediatr Crit Care Med 2014;15:443–50. doi:10.1097/PCC.0000000000000115.

[30]   Barrington KJ. Common hemodynamic problems in the neonate. Neonatology 2013;103:335–40. doi:10.1159/000349933.

[31]   Noori S, Stavroudis TA, Seri I. Principles of developmental cardiovascular physiology and pathophysiology. In: Elsevier Sauders, editor. Neonatol. Quest. Controv. hemodynamics Cardiol. 2nd ed., Philadelphia, USA: 2012, p. 3–22.

[32]   Deshpande P, Baczynski M, McNamara PJ, Jain A. Patent ductus arteriosus: The physiology of transition. Semin Fetal Neonatal Med 2018;23:225–31. doi:10.1016/j.siny.2018.05.001.

[33]   Polglase GR, Miller SL, Barton SK, Kluckow M, Gill AW, Hooper SB, et al. Respiratory support for premature neonates in the delivery room: Effects on cardiovascular function and the development of brain injury. Pediatr Res 2014;75:682–8. doi:10.1038/pr.2014.40.

[34]   Hamrick SEG, Hansmann G. Patent ductus arteriosus of the preterm infant. Pediatrics 2010;125:1020–30. doi:10.1542/peds.2009-3506.

[35]   Gonzalez A, Sosenko IRS, Chandar J, Hummler H, Claure N, Bancalari E. Influence of infection on patent ductus arteriosus and chronic lung disease in premature infants weighing 1000 grams or less. J Pediatr 1996;128:470–8. doi:10.1016/S0022-3476(96)70356-6.

[36]   Alyamac Dizdar E, Ozdemir R, Nur Sari F, Yurttutan S, Gokmen T, Erdeve O, et al. Low

platelet count is associated with ductus arteriosus patency in preterm newborns. Early Hum Dev 2012;88:813–6. doi:10.1016/j.earlhumdev.2012.05.007.

[37]   Sallmon H, Weber SC, Hüning B, Stein A, Horn PA, Metze BC, et al. Thrombocytopenia in the first 24 hours after birth and incidence of patent ductus arteriosus. Pediatrics 2012;130. doi:10.1542/peds.2012-0499.

[38]   Semberova J, Sirc J, Miletin J, Kucera J, Berka I, Sebkova S, et al. Spontaneous Closure of Patent Ductus Arteriosus in Infants ≤1500 g. Pediatrics 2017;140. doi:10.1542/peds.2016-4258.

[39]   Singh Y, Tissot C. Echocardiographic evaluation of transitional circulation for the neonatologists. Front Pediatr 2018;6. doi:10.3389/fped.2018.00140.

[40]   Sellmer A, Bjerre JV, Schmidt MR, McNamara PJ, Hjortdal VE, Høst B, et al. Morbidity and mortality in preterm neonates with patent ductus arteriosus on day 3. Arch Dis Child Fetal Neonatal Ed 2013;98. doi:10.1136/archdischild-2013-303816.

[41]   Noori S, McCoy M, Friedlich P, Bright B, Gottipati V, Seri I, et al. Failure of ductus arteriosus closure is associated with increased mortality in preterm infants. Pediatrics 2009;123. doi:10.1542/peds.2008-2418.

[42]   Schena F, Francescato G, Cappelleri A, Picciolli I, Mayer A, Mosca F, et al. Association between Hemodynamically Significant Patent Ductus Arteriosus and Bronchopulmonary Dysplasia. J Pediatr 2015;166:1488–92. doi:10.1016/j.jpeds.2015.03.012.

[43]   Kluckow M, Evans N. Ductal shunting, high pulmonary blood flow, and pulmonary hemorrhage. J Pediatr 2000;137:68–72. doi:10.1067/mpd.2000.106569.

[44]   Evans N, Kluckow M. Early ductal shunting and intraventricular haemorrhage in ventilated preterm infants. Arch Dis Child Fetal Neonatal Ed 1996;75:F183-6.

[45]   Osborn DA, Evans N, Kluckow M. Hemodynamic and antecedent risk factors of early and late

periventricular/intraventricular hemorrhage in premature infants. Pediatrics 2003;112:33–9. doi:10.1542/peds.112.1.33.

[46] Kluckow M, Evans N. Low superior vena cava flow and intraventricular haemorrhage in preterm infants. Arch Dis Child Fetal Neonatal Ed 2000;82. doi:10.1136/fn.82.3.f188.

[47] Noori S, McCoy M, Anderson MP, Ramji F, Seri I. Changes in cardiac function and cerebral blood flow in relation to peri/intraventricular hemorrhage in extremely preterm infants. J Pediatr 2014;164:264-70.e1-3. doi:10.1016/j.jpeds.2013.09.045.

[48] O'Leary H, Gregas MC, Limperopoulos C, Zaretskaya I, Bassan H, Soul JS, et al. Elevated cerebral pressure passivity is associated with prematurity-related intracranial hemorrhage. Pediatrics 2009;124:302–9. doi:10.1542/peds.2008-2004.

[49] de Boode WP. Individualized Hemodynamic Management in Newborns. Front Pediatr 2020;8. doi:10.3389/fped.2020.580470.

[50] Willie CK, Tzeng YC, Fisher JA, Ainslie PN. Integrative regulation of human brain blood flow. J Physiol 2014;592:841–59. doi:10.1113/jphysiol.2013.268953.

[51] Vutskits L. Cerebral blood flow in the neonate. Paediatr Anaesth 2014;24:22–9. doi:10.1111/pan.12307.

[52] Leahy FAN, Cates D, MacCallum M, Rigatto H. Effect of CO2 and 100% O2 on cerebral blood flow in preterm infants. J Appl Physiol Respir Environ Exerc Physiol 1980;48:468–72. doi:10.1152/jappl.1980.48.3.468.

[53] Levene MI, Shortland D, Gibson N, Evans DH. Carbon dioxide reactivity of the cerebral circulation in extremely premature infants: effects of postnatal age and indomethacin. Pediatr Res 1988;24:175–9. doi:10.1203/00006450-198808000-00007.

[54] Pryds O, Greisen G, Lou H, Frils-Hansen B, Friis-Hansen B. Heterogeneity of cerebral vasoreactivity in preterm infants supported by mechanical ventilation. J Pediatr

1989;115:638–45. doi:10.1016/s0022-3476(89)80301-4.

[55]   Greisen G. Autoregulation of cerebral blood flow in newborn babies. Early Hum Dev 2005;81:423–8. doi:10.1016/j.earlhumdev.2005.03.005.

[56]   Perlman JM, Volpe JJ. Seizures in the preterm infant: Effects on cerebral blood flow velocity, intracranial pressure, and arterial blood pressure. J Pediatr 1983;102:288–93. doi:10.1016/S0022-3476(83)80545-9.

[57]   Hendrikx D, Smits A, Lavanga M, De Wel O, Thewissen L, Jansen K, et al. Measurement of neurovascular coupling in neonates. Front Physiol 2019;10. doi:10.3389/fphys.2019.00065.

[58]   Phillips AA, Chan FH, Zheng MMZ, Krassioukov A V., Ainslie PN. Neurovascular coupling in humans: Physiology, methodological advances and clinical implications. J Cereb Blood Flow Metab 2015;36:647–64. doi:10.1177/0271678X15617954.

[59]   Martini S, Paoletti V, Faldella G, Corvaglia L. Cerebral Oxygenation Patterns during Electroclinical Neonatal Seizures. Neuropediatrics 2019;50:408–9. doi:10.1055/s-0039-1693058.

[60]   Boylan GB, Young K, Panerai RB, Rennie JM, Evans DH. Dynamic cerebral autoregulation in sick newborn infants. Pediatr Res 2000;48:12–7. doi:10.1203/00006450-200007000-00005.

[61]   Hendrikx D, Thewissen L, Smits A, Naulaers G, Allegaert K, Van Huffel S, et al. Nonlinear transfer entropy to assess the neurovascular coupling in premature neonates. Adv. Exp. Med. Biol., vol. 1232, Springer; 2020, p. 11–7. doi:10.1007/978-3-030-34461-0_2.

[62]   Pryds O, Andersen GE, Friis-Hansen B. Cerebral blood flow reactivity in spontaneously breathing, preterm infants shortly after birth. Acta Paediatr Scand 1990;79:391–6. doi:10.1111/j.1651-2227.1990.tb11482.x.

[63]   Skov L, Pryds O. Capillary recruitment for preservation of cerebral glucose influx in hypoglycemic, preterm newborns: Evidence for a glucose sensor? Pediatrics 1992;90:193–5.

[64] Hollinger BR, Bryan RM. β-Receptor-mediated increase in cerebral blood flow during hypoglycemia. Am J Physiol - Hear Circ Physiol 1987;253. doi:10.1152/ajpheart.1987.253.4.h949.

[65] Busija DW, Leffler CW. Dilator effects of amino acid neurotransmitters on piglet pial arterioles. Am J Physiol - Hear Circ Physiol 1989;257. doi:10.1152/ajpheart.1989.257.4.h1200.

[66] Goadsby PJ. Autonomic nervous system control of the cerebral circulation. Handb. Clin. Neurol., vol. 117, Elsevier B.V.; 2013, p. 193–201. doi:10.1016/B978-0-444-53491-0.00016-X.

[67] Radaelli A, Castiglioni P, Centola M, Cesana F, Balestri G, Ferrari AU, et al. Adrenergic origin of very low-frequency blood pressure oscillations in the unanesthetized rat. Am J Physiol - Hear Circ Physiol 2006;290. doi:10.1152/ajpheart.00773.2005.

[68] Pryds O. Control of cerebral circulation in the high-risk neonate. Ann Neurol 1991;30:321–9. doi:10.1002/ana.410300302.

[69] Monin P, Feillet F, Hascoet JM, Vert P. Effect of sympathetic nervous system on cerebral blood flow in the newborn piglet. Biol Neonate 1990;58:192–9. doi:10.1159/000243268.

[70] Wagerle LC, Kurth CD, Roth RA. Sympathetic reactivity of cerebral arteries in developing fetal lamb and adult sheep. Am J Physiol 1990;258:H1432-8. doi:10.1152/ajpheart.1990.258.5.H1432.

[71] Greisen G. Effect of cerebral blood flow and cerebrovascular autoregulation on the distribution, type and extent of cerebral injury. Brain Pathol 1992;2:223–8. doi:10.1111/j.1750-3639.1992.tb00695.x.

[72] Frösen J, Joutel A. Smooth muscle cells of intracranial vessels: From development to disease. Cardiovasc Res 2018;114:501–12. doi:10.1093/cvr/cvy002.

[73]   Mandalà M, Pedatella AL, Morales Palomares S, Cipolla MJ, Osol G. Maturation is associated with changes in rat cerebral artery structure, biomechanical properties and tone. Acta Physiol 2012;205:363–71. doi:10.1111/j.1748-1716.2011.02406.x.

[74]   Kooi EMW, Richter AE. Cerebral Autoregulation in Sick Infants: Current Insights. Clin Perinatol 2020;47:449–67. doi:10.1016/j.clp.2020.05.003.

[75]   Vesoulis ZA, Mathur AM. Cerebral Autoregulation, Brain Injury, and the Transitioning Premature Infant. Front Pediatr 2017;5:64. doi:10.3389/fped.2017.00064.

[76]   Langager AM, Hammerberg BE, Rotella DL, Stauss HM. Very low-frequency blood pressure variability depends on voltage-gated L-type $Ca2+$ channels in conscious rats. Am J Physiol - Hear Circ Physiol 2007;292. doi:10.1152/ajpheart.00874.2006.

[77]   Iwasaki KI, Ogawa Y, Shibata S, Aoki K. Acute exposure to normobaric mild hypoxia alters dynamic relationships between blood pressure and cerebral blood flow at very low frequency. J Cereb Blood Flow Metab 2007;27:776–84. doi:10.1038/sj.jcbfm.9600384.

[78]   Thewissen L, Caicedo A, Lemmers P, Van Bel F V., Van Huffel S V., Naulaers G. Measuring Near-Infrared Spectroscopy Derived Cerebral Autoregulation in Neonates: From Research Tool Toward Bedside Multimodal Monitoring. Front Pediatr 2018;6:117. doi:10.3389/fped.2018.00117.

[79]   Stauss HM. Identification of blood pressure control mechanisms by power spectral analysis. Clin Exp Pharmacol Physiol 2007;34:362–8. doi:10.1111/j.1440-1681.2007.04588.x.

[80]   Fantini S, Sassaroli A, Tgavalekos KT, Kornbluth J. Cerebral blood flow and autoregulation: current measurement techniques and prospects for noninvasive optical methods. Neurophotonics 2016;3:031411. doi:10.1117/1.nph.3.3.031411.

[81]   Bellapart J, Fraser JF. Transcranial Doppler Assessment of Cerebral Autoregulation. Ultrasound Med Biol 2009;35:883–93. doi:10.1016/j.ultrasmedbio.2009.01.005.

[82]   Barnett SB. Intracranial temperature elevation from diagnostic ultrasound. Ultrasound Med.

          Biol., vol. 27, Ultrasound Med Biol; 2001, p. 883–8. doi:10.1016/S0301-5629(01)00367-2.

[83]   Boylan GB, Panerai RB, Rennie JM, Evans DH, Rabe-Hesketh S, Binnie CD. Cerebral blood

          flow velocity during neonatal seizures. Arch Dis Child Fetal Neonatal Ed 1999;80.

          doi:10.1136/fn.80.2.F105.

[84]   Panerai RB, Kelsall AW, Rennie JM, Evans DH. Cerebral autoregulation dynamics in

          premature newborns. Stroke 1995;26:74–80.

[85]   Caicedo A, De Smet D, Naulaers G, Ameye L, Vanderhaegen J, Lemmers P, et al. Cerebral

          tissue oxygenation and regional oxygen saturation can be used to study cerebral autoregulation

          in   prematurely   born   infants.   Pediatr   Res   2011;69:548–53.

          doi:10.1203/PDR.0b013e3182176d85.

[86]   Verhagen EA, Hummel L a, Bos AF, Kooi EMW. Near-infrared spectroscopy to detect absence

          of cerebrovascular autoregulation in preterm infants. Clin Neurophysiol 2014;125:47–52.

          doi:10.1016/j.clinph.2013.07.001.

[87]   De Smet D, Vanderhaegen J, Naulaers G, Van Huffel S. New measurements for assessment of

          impaired cerebral autoregulation using near-infrared spectroscopy. Adv Exp Med Biol

          2009;645:273–8. doi:10.1007/978-0-387-85998-9_41.

[88]   Chock VY, Ramamoorthy C, Van Meurs KP. Cerebral autoregulation in neonates with a

          hemodynamically significant patent ductus arteriosus. J Pediatr 2012;160:936–42.

          doi:10.1016/j.jpeds.2011.11.054.

[89]   Alderliesten T, Lemmers PMA, Smarius JJM, van de Vosse RE, Baerts W, van Bel F. Cerebral

          oxygenation, extraction, and autoregulation in very preterm infants who develop peri-

          intraventricular hemorrhage. J Pediatr 2013;162:698-704.e2. doi:10.1016/j.jpeds.2012.09.038.

[90]   Lee JK, Kibler KK, Benni PB, Easley RB, Czosnyka M, Smielewski P, et al. Cerebrovascular

reactivity measured by near-infrared spectroscopy. Stroke 2009;40:1820–6. doi:10.1161/STROKEAHA.108.536094.

[91]   Eriksen VR, Hahn GH, Greisen G. Dopamine therapy is associated with impaired cerebral autoregulation in preterm infants. Acta Paediatr Int J Paediatr 2014;103:1221–6. doi:10.1111/apa.12817.

[92]   Lee JK, Poretti A, Perin J, Huisman TAGM, Parkinson C, Chavez-Valdez R, et al. Optimizing Cerebral Autoregulation May Decrease Neonatal Regional Hypoxic-Ischemic Brain Injury. Dev. Neurosci., vol. 39, S. Karger AG; 2017, p. 248–56. doi:10.1159/000452833.

[93]   Gilmore MM, Stone BS, Shepard JA, Czosnyka M, Easley RB, Brady KM. Relationship between cerebrovascular dysautoregulation and arterial blood pressure in the premature infant. J Perinatol 2011;31:722–9. doi:10.1038/jp.2011.17.

[94]   Tyszczuk L, Meek J, Elwell C, Wyatt JS. Cerebral blood flow is independent of mean arterial blood pressure in preterm infants undergoing intensive care. Pediatrics 1998;102:337–41.

[95]   Munro MJ, Walker AM, Barfield CP. Hypotensive extremely low birth weight infants have reduced cerebral blood flow. Pediatrics 2004;114:1591–6. doi:10.1542/peds.2004-1073.

[96]   Caicedo A, Naulaers G, Lemmers P, van Bel F, Wolf M, Van Huffel S. Detection of cerebral autoregulation by near-infrared spectroscopy in neonates: performance analysis of measurement methods. J Biomed Opt 2012;17:117003. doi:10.1117/1.JBO.17.11.117003.

[97]   Christensen KB, Hahn GH, Christensen KB, Leung TS, Greisen G. Precision of coherence analysis to detect cerebral autoregulation by near-infrared spectroscopy in preterm infants. J Biomed Opt 2010;15:37002. doi:10.1117/1.3426323.

[98]   Rhee CJ, da Costa CS, Austin T, Brady KM, Czosnyka M, Lee JK. Neonatal cerebrovascular autoregulation. Pediatr Res 2018;84:602–10. doi:10.1038/s41390-018-0141-6.

[99]   Zhang Y, Chan GSHH, Tracy MB, Lee QY, Hinder M, Savkin A V., et al. Spectral analysis of

systemic and cerebral cardiovascular variabilities in preterm infants: relationship with clinical risk index for babies (CRIB). Physiol Meas 2011;32:1913–28. doi:10.1088/0967-3334/32/12/003.

[100] Hermansen MC, Hermansen GM. Intravascular catheter complications in the neonatal intensive care unit. Clin Perinatol 2005;32:141–56. doi:10.1016/j.clp.2004.11.005.

[101] Mitra S, Czosnyka M, Smielewski P, O'Reilly H, Brady K, Austin T. Heart rate passivity of cerebral tissue oxygenation is associated with predictors of poor outcome in preterm infants. Acta Paediatr 2014;103:e374-82. doi:10.1111/apa.12696.

[102] da Costa CS, Czosnyka M, Smielewski P, Mitra S, Stevenson GN, Austin T. Monitoring of Cerebrovascular Reactivity for Determination of Optimal Blood Pressure in Preterm Infants. J Pediatr 2015;167:86–91. doi:10.1016/j.jpeds.2015.03.041.

[103] Pearce WJ. Fetal Cerebrovascular Maturation: Effects of Hypoxia. Semin Pediatr Neurol 2018;28:17–28. doi:10.1016/j.spen.2018.05.003.

[104] Wong FY, Leung TS, Austin T, Wilkinson M, Meek JH, Wyatt JS, et al. Impaired autoregulation in preterm infants identified by using spatially resolved spectroscopy. Pediatrics 2008;121:e604-11. doi:10.1542/peds.2007-1487.

[105] Verma PK, Panerai RB, Rennie JM, Evans DH. Grading of cerebral autoregulation in preterm and term neonates. Pediatr Neurol 2000;23:236–42. doi:10.1016/s0887-8994(00)00184-3.

[106] Rhee CJ, Fraser CD, Kibler K, Easley RB, Andropoulos DB, Czosnyka M, et al. The ontogeny of cerebrovascular pressure autoregulation in premature infants. J Perinatol 2014;34:926–31. doi:10.1038/jp.2014.122.

[107] Vesoulis ZA, Liao SM, Mathur AM. Gestational age-dependent relationship between cerebral oxygen extraction and blood pressure. Pediatr Res 2017;82:934–9. doi:10.1038/pr.2017.196.

[108] Polavarapu SR, Fitzgerald GD, Contag S, Hoffman SB. Utility of prenatal Doppler ultrasound

to predict neonatal impaired cerebral autoregulation. J Perinatol 2018;38:474–81. doi:10.1038/s41372-018-0050-x.

[109] Cohen E, Baerts W, Caicedo Dorado A, Naulaers G, van Bel F, Lemmers PMA. Cerebrovascular autoregulation in preterm fetal growth restricted neonates. Arch Dis Child Fetal Neonatal Ed 2019;104:F467–72. doi:10.1136/archdischild-2017-313712.

[110] Bozzetti V, Paterlini G, Bel F van, Visser GHA, Tosetti L, Gazzolo D, et al. Cerebral and somatic NIRS-determined oxygenation in IUGR preterm infants during transition. J Matern Fetal Neonatal Med 2015:1–4. doi:10.3109/14767058.2014.1003539.

[111] Solanki NS, Hoffman SB. Association between dopamine and cerebral autoregulation in preterm neonates. Pediatr Res 2020. doi:10.1038/s41390-020-0790-0.

[112] Eriksen VR, Rasmussen MB, Hahn GH, Greisen G. Dopamine therapy does not affect cerebral autoregulation during hypotension in newborn piglets. PLoS One 2017;12. doi:10.1371/journal.pone.0170738.

[113] Rasmussen MB, Gramsbergen JB, Eriksen VR, Greisen G. Dopamine plasma clearance is increased in piglets compared to neonates during continuous dopamine infusion. Acta Paediatr Int J Paediatr 2018;107:249–54. doi:10.1111/apa.14018.

[114] Lemmers PMAA, Toet M, van Schelven LJ, van Bel F. Cerebral oxygenation and cerebral oxygen extraction in the preterm infant: the impact of respiratory distress syndrome. Exp Brain Res 2006;173:458–67. doi:10.1007/s00221-006-0388-8.

[115] Li X-F, Cheng T-T, Guan R-L, Liang H, Lu W-N, Zhang J-H, et al. Effects of different surfactant administrations on cerebral autoregulation in preterm infants with respiratory distress syndrome. J Huazhong Univ Sci Technol Med Sci = Hua Zhong Ke Ji Da Xue Xue Bao Yi Xue Ying Wen Ban = Huazhong Keji Daxue Xuebao Yixue Yingdewen Ban 2016;36:801–5. doi:10.1007/s11596-016-1665-9.

[116] Thewissen L, Caicedo A, Dereymaeker A, Van Huffel S, Naulaers G, Allegaert K, et al. Cerebral autoregulation and activity after propofol for endotracheal intubation in preterm neonates. Pediatr Res 2018;84:719–25. doi:10.1038/s41390-018-0160-3.

[117] Kaiser JR, Gauss CH, Williams DK. Surfactant administration acutely affects cerebral and systemic hemodynamics and gas exchange in very-low-birth-weight infants. J Pediatr 2004;144:809–14. doi:10.1016/j.jpeds.2004.03.022.

[118] Volpe JJ. Intraventricular hemorrhage in the premature infant—current concepts. Part II. Ann Neurol 1989;25:109–16. doi:10.1002/ana.410250202.

[119] Ballabh P. Intraventricular hemorrhage in premature infants: Mechanism of disease. Pediatr Res 2010;67:1–8. doi:10.1203/PDR.0b013e3181c1b176.

[120] Cimatti AG, Martini S, Galletti S, Vitali F, Aceti A, Frabboni G, et al. Cerebral Oxygenation and Autoregulation in Very Preterm Infants Developing IVH During the Transitional Period: A Pilot Study. Front Pediatr 2020;8. doi:10.3389/fped.2020.00381.

[121] Sortica da Costa C, Cardim D, Molnar Z, Kelsall W, Ng I, Czosnyka M, et al. Changes in hemodynamics, cerebral oxygenation and cerebrovascular reactivity during the early transitional circulation in preterm infants. Pediatr Res 2019;86:247–53. doi:10.1038/s41390-019-0410-z.

[122] Hoffman SB, Cheng YJ, Magder LS, Shet N, Viscardi RM. Cerebral autoregulation in premature infants during the first 96 hours of life and relationship to adverse outcomes. Arch Dis Child Fetal Neonatal Ed 2019;104:F473–9. doi:10.1136/archdischild-2018-315725.

[123] Beausoleil TP, Janaillac M, Barrington KJ, Lapointe A, Dehaes M. Cerebral oxygen saturation and peripheral perfusion in the extremely premature infant with intraventricular and/or pulmonary haemorrhage early in life. Sci Rep 2018;8. doi:10.1038/s41598-018-24836-8.

[124] Papile LA, Burstein J, Burstein R, Koffler H. Incidence and evolution of subependymal and

intraventricular hemorrhage: A study of infants with birth weights less than 1,500 gm. J Pediatr 1978;92:529–34. doi:10.1016/S0022-3476(78)80282-0.

[125] Volpe JJ. Brain injury in premature infants: a complex amalgam of destructive and developmental disturbances. Lancet Neurol 2009;8:110–24. doi:10.1016/S1474-4422(08)70294-1.

[126] Khwaja O, Volpe JJ. Pathogenesis of cerebral white matter injury of prematurity. Arch Dis Child Fetal Neonatal Ed 2008;93:F153-61. doi:10.1136/adc.2006.108837.

[127] Chalak LF, Tarumi T, Zhang R. The "neurovascular unit approach" to evaluate mechanisms of dysfunctional autoregulation in asphyxiated newborns in the era of hypothermia therapy. Early Hum Dev 2014;90:687–94. doi:10.1016/j.earlhumdev.2014.06.013.

[128] Levene MI, Fenton AC, Evans DH, Archer LNJ, Shortland DB, Gibson NA. Severe birth asphyxia and abnormal cerebral blood-flow velocity. Dev Med Child Neurol 1989;31:427–34. doi:10.1111/j.1469-8749.1989.tb04020.x.

[129] Pryds O, Greisen G, Lou H, Friis-Hansen B. Vasoparalysis associated with brain damage in asphyxiated term infants. J Pediatr 1990;117:119–25. doi:10.1016/S0022-3476(05)72459-8.

[130] Proisy M, Corouge I, Leghouy A, Nicolas A, Charon V, Mazille N, et al. Changes in brain perfusion in successive arterial spin labeling MRI scans in neonates with hypoxic-ischemic encephalopathy. NeuroImage Clin 2019;24. doi:10.1016/j.nicl.2019.101939.

[131] Wintermark P, Hansen A, Gregas MC, Soul J, Labrecque M, Robertson RL, et al. Brain perfusion in asphyxiated newborns treated with therapeutic hypothermia. Am J Neuroradiol 2011;32:2023–9. doi:10.3174/ajnr.A2708.

[132] Massaro AN, Govindan RB, Vezina G, Chang T, Andescavage NN, Wang Y, et al. Impaired cerebral autoregulation and brain injury in newborns with hypoxic-ischemic encephalopathy treated with hypothermia. J Neurophysiol 2015;114:818–24. doi:10.1152/jn.00353.2015.

[133] Ancora G, Maranella E, Grandi S, Sbravati F, Coccolini E, Savini S, et al. Early predictors of short term neurodevelopmental outcome in asphyxiated cooled infants. A combined brain amplitude integrated electroencephalography and near infrared spectroscopy study. Brain Dev 2013;35:26–31. doi:10.1016/j.braindev.2011.09.008.

[134] Greisen G. Cerebral blood flow and oxygenation in infants after birth asphyxia. Clinically useful information? Early Hum Dev 2014;90:703–5. doi:10.1016/j.earlhumdev.2014.06.007.

[135] Ancel P-Y, Goffinet F, Kuhn P, Langer B, Matis J, Hernandorena X, et al. Survival and Morbidity of Preterm Children Born at 22 Through 34 Weeks' Gestation in France in 2011. JAMA Pediatr 2015;169:230. doi:10.1001/jamapediatrics.2014.3351.

[136] de Boode WP. Clinical monitoring of systemic hemodynamics in critically ill newborns. Early Hum Dev 2010;86:137–41. doi:10.1016/j.earlhumdev.2010.01.031.

[137] Tibby SM, Hatherill M, Marsh MJ, Murdoch IA. Clinicians' abilities to estimate cardiac index in ventilated children and infants. Arch Dis Child 1997;77:516–8. doi:10.1136/adc.77.6.516.

[138] Noori S, Seri I. Neonatal Blood Pressure Support: The Use of Inotropes, Lusitropes, and Other Vasopressor Agents. Clin Perinatol 2012;39:221–38. doi:10.1016/j.clp.2011.12.010.

[139] de Boode WP. Advanced Hemodynamic Monitoring in the Neonatal Intensive Care Unit. Clin Perinatol 2020;47:423–34. doi:10.1016/j.clp.2020.05.001.

[140] Groves AM, Singh Y, Dempsey E, Molnar Z, Austin T, El-Khuffash A, et al. Introduction to neonatologist-performed echocardiography. Pediatr Res 2018;84. doi:10.1038/s41390-018-0076-y.

[141] Chew M, Poelaert J. Accuracy and repeatability of pediatric cardiac output measurement using Doppler: 20-year review of the literature . Intensive Care Med 2003;29:1889–94. doi:10.1007/s00134-003-1967-9.

[142] El-Khuffash AF, McNamara PJ. Neonatologist-performed functional echocardiography in the

neonatal intensive care unit. Semin Fetal Neonatal Med 2011;16:50–60. doi:10.1016/j.siny.2010.05.001.

[143] Kedrov AA, Liberman TU. Rheocardiography. Klin Med 1949;27:40–6.

[144] Kubicek WG, Karnegis JN, Patterson RP, Witsoe DA, Mattson RH. Development and evaluation of an impedance cardiac output system. Aerosp Med 1966;37:1208–12.

[145] Bernstein DP, Osypka MJ. Apparatus and method for determining an approximation of the stroke volume and the cardiac output of the heart. US Pat 2003;6:438.

[146] Narula J, Chauhan S, Ramakrishnan S, Gupta SK. Electrical Cardiometry: A Reliable Solution to Cardiac Output Estimation in Children With Structural Heart Disease. J Cardiothorac Vasc Anesth 2017;31:912–7. doi:10.1053/j.jvca.2016.12.009.

[147] Noori S, Drabu B, Soleymani S, Seri I. Continuous non-invasive cardiac output measurements in the neonate by electrical velocimetry: a comparison with echocardiography. Arch Dis Child - Fetal Neonatal Ed 2012;97:F340–3. doi:10.1136/fetalneonatal-2011-301090.

[148] Grollmuss O, Demontoux S, Capderou A, Serraf A, Belli E. Electrical velocimetry as a tool for measuring cardiac output in small infants after heart surgery. Intensive Care Med 2012;38:1032–9. doi:10.1007/s00134-012-2530-3.

[149] Grollmuss O, Gonzalez P. Non-invasive cardiac output measurement in low and very low birth weight infants: a method comparison. Front Pediatr 2014;2:16. doi:10.3389/fped.2014.00016.

[150] Boet A, Jourdain G, Demontoux S, De Luca D. Stroke volume and cardiac output evaluation by electrical cardiometry: Accuracy and reference nomograms in hemodynamically stable preterm neonates. J Perinatol 2016;36:748–52. doi:10.1038/jp.2016.65.

[151] Hsu KH, Wu TW, Wu IH, Lai MY, Hsu SY, Huang HW, et al. Electrical Cardiometry to Monitor Cardiac Output in Preterm Infants with Patent Ductus Arteriosus: A Comparison with Echocardiography. Neonatology 2017;112:231–7. doi:10.1159/000475774.

[152] van Laere D, van Overmeire B, Gupta S, El Khuffash A, Savoia M, McNamara PJ, et al. Application of NPE in the assessment of a patent ductus arteriosus. Pediatr Res 2018;84:46–56. doi:10.1038/s41390-018-0077-x.

[153] Scheeren TWL, Schober P, Schwarte LA. Monitoring tissue oxygenation by near infrared spectroscopy (NIRS): background and current applications. J Clin Monit Comput 2012;26:279–87. doi:10.1007/s10877-012-9348-y.

[154] Masters B, So P. Handbook of Biomedical Nonlinear Optical Microscopy. New York: Oxford University Press; 2008.

[155] Jöbsis FF. Noninvasive, infrared monitoring of cerebral and myocardial oxygen sufficiency and circulatory parameters. Science 1977;198:1264–7.

[156] Delpy DT, Cope M, van der Zee P, Arridge S, Wray S, Wyatt J. Estimation of optical pathlength through tissue from direct time of flight measurement. Phys Med Biol 1988;33:1433–42.

[157] Matcher SJ, Cope M, Delpy DT. Use of the water absorption spectrum to quantify tissue chromophore concentration changes in near-infrared spectroscopy. Phys Med Biol 1994;39:177–96.

[158] Jacques SL. Optical properties of biological tissues: a review. Phys Med Biol 2013;58:R37–61. doi:10.1088/0031-9155/58/11/R37.

[159] Owen-Reece H, Smith M, Elwell CE, Goldstone JC. Near infrared spectroscopy. Br J Anaesth 1999;82:418–26. doi:10.1093/bja/82.3.418.

[160] Watzman HM, Kurth CD, Montenegro LM, Rome J, Steven JM, Nicolson SC. Arterial and venous contributions to near-infrared cerebral oximetry. Anesthesiology 2000;93:947–53.

[161] Martini S, Corvaglia L. Splanchnic NIRS monitoring in neonatal care: rationale, current applications and future perspectives. J Perinatol 2018;38:431–43. doi:10.1038/s41372-018-

0075-1.

[162] Austin T. Optical imaging of the neonatal brain. Arch Dis Child Fetal Neonatal Ed 2007;92. doi:10.1136/adc.2006.103846.

[163] Gibson AP, Austin T, Everdell NL, Schweiger M, Arridge SR, Meek JH, et al. Three-dimensional whole-head optical tomography of passive motor evoked responses in the neonate. Neuroimage 2006;30:521–8. doi:10.1016/j.neuroimage.2005.08.059.

[164] Austin T, Gibson AP, Branco G, Yusof RM, Arridge SR, Meek JH, et al. Three dimensional optical imaging of blood volume and oxygenation in the neonatal brain. Neuroimage 2006;31:1426–33. doi:10.1016/j.neuroimage.2006.02.038.

[165] Matcher SJ, Kirkpatrick PJ, Nahid K, Cope M, Delpy DT. Absolute quantification methods in tissue near-infrared spectroscopy. In: Chance B, Alfano RR, editors., International Society for Optics and Photonics; 1995, p. 486–95. doi:10.1117/12.209997.

[166] Ferrari M, Mottola L, Quaresima V. Principles, techniques, and limitations of near infrared spectroscopy. Can J Appl Physiol 2004;29:463–87.

[167] Naulaers G, Meyns B, Miserez M, Leunens V, Van Huffel S, Casaer P, et al. Use of tissue oxygenation index and fractional tissue oxygen extraction as non-invasive parameters for cerebral oxygenation. A validation study in piglets. Neonatology 2007;92:120–6. doi:10.1159/000101063.

[168] Brazy JE, Lewis D V., Mitnick MH, Jöbsis-Vander Vliet FF. Monitoring of cerebral oxygenation in the intensive care nursery. Adv Exp Med Biol 1985;191:843–8. doi:10.1007/978-1-4684-3291-6_84.

[169] Kurth CD, Steven JL, Montenegro LM, Watzman HM, Gaynor JW, Spray TL, et al. Cerebral oxygen saturation before congenital heart surgery. Ann Thorac Surg 2001;72:187–92.

[170] Spaeder MC, Klugman D, Skurow-Todd K, Glass P, Jonas RA, Donofrio MT. Perioperative

Near-Infrared Spectroscopy Monitoring in Neonates With Congenital Heart Disease. Pediatr Crit Care Med 2017;18:213–8. doi:10.1097/PCC.0000000000001056.

[171] Dehaes M, Aggarwal A, Lin P-Y, Rosa Fortuno C, Fenoglio A, Roche-Labarbe N, et al. Cerebral Oxygen Metabolism in Neonatal Hypoxic Ischemic Encephalopathy during and after Therapeutic Hypothermia. J Cereb Blood Flow Metab 2014;34:87–94. doi:10.1038/jcbfm.2013.165.

[172] Sirc J, Dempsey EMM, Miletin J. Cerebral tissue oxygenation index, cardiac output and superior vena cava flow in infants with birth weight less than 1250 grams in the first 48 hours of life. Early Hum Dev 2013;89:449–52. doi:10.1016/j.earlhumdev.2013.04.004.

[173] Fujioka T, Takami T, Ishii H, Kondo A, Sunohara D, Kawashima H. Difference in Cerebral and Peripheral Hemodynamics among Term and Preterm Infants during the First Three Days of Life. Neonatology 2014;106:181–7. doi:10.1159/000362152.

[174] Alderliesten T, Dix L, Baerts W, Caicedo A, van Huffel S, Naulaers G, et al. Reference values of regional cerebral oxygen saturation during the first 3 days of life in preterm neonates. Pediatr Res 2016;79:55–64. doi:10.1038/pr.2015.186.

[175] Noori S, Seri I. Hemodynamic antecedents of peri/intraventricular hemorrhage in very preterm neonates. Semin Fetal Neonatal Med 2015;20:232–7. doi:10.1016/j.siny.2015.02.004.

[176] Ng IHX, da Costa CS, Zeiler FA, Wong FY, Smielewski P, Czosnyka M, et al. Burden of hypoxia and intraventricular haemorrhage in extremely preterm infants. Arch Dis Child - Fetal Neonatal Ed 2019:fetalneonatal-2019-316883. doi:10.1136/archdischild-2019-316883.

[177] Plomgaard AM, Alderliesten T, Austin T, Van Bel F, Benders M, Claris O, et al. Early biomarkers of brain injury and cerebral hypo- and hyperoxia in the SafeBoosC II trial. PLoS One 2017;12. doi:10.1371/journal.pone.0173440.

[178] Sood ED, Benzaquen JS, Davies RR, Woodford E, Pizarro C. Predictive value of perioperative

near-infrared spectroscopy for neurodevelopmental outcomes after cardiac surgery in infancy. J Thorac Cardiovasc Surg 2013;145:438-445.e1. doi:10.1016/j.jtcvs.2012.10.033.

[179] Verhagen EA, Van Braeckel KNJA, van der Veere CN, Groen H, Dijk PH, Hulzebos C V, et al. Cerebral oxygenation is associated with neurodevelopmental outcome of preterm children at age 2 to 3 years. Dev Med Child Neurol 2015;57:449–55. doi:10.1111/dmcn.12622.

[180] Cerbo R, Orcesi S, Scudeller L, Borellini M, Croci C, Ravelli C, et al. Near-Infrared Spectroscopy Monitoring, Superior Vena Cava Flow, and Neurodevelopmental Outcome at 2 years in a Cohort of Very Low-Birth-Weight Infants. Am J Perinatol 2016;33:1093–8. doi:10.1055/s-0036-1586103.

[181] Alderliesten T, van Bel F, van der Aa NE, Steendijk P, van Haastert IC, de Vries LS, et al. Low Cerebral Oxygenation in Preterm Infants Is Associated with Adverse Neurodevelopmental Outcome. J Pediatr 2019;207:109-116.e2. doi:10.1016/j.jpeds.2018.11.038.

[182] Pellicer A, Bravo M del C. Near-infrared spectroscopy: A methodology-focused review. Semin Fetal Neonatal Med 2011;16:42–9. doi:10.1016/j.siny.2010.05.003.

[183] Sorensen LC, Greisen G. Precision of measurement of cerebral tissue oxygenation index using near-infrared spectroscopy in preterm neonates. J Biomed Opt 2006;11:054005. doi:10.1117/1.2357730.

[184] Mintzer JP, Parvez B, Chelala M, Alpan G, LaGamma EF. Quiescent variability of cerebral, renal, and splanchnic regional tissue oxygenation in very low birth weight neonates. J Neonatal Perinatal Med 2014;7:199–206. doi:10.3233/NPM-14814035.

[185] Pocivalnik M, Pichler G, Zotter H, Tax N, Müller W, Urlesberger B. Regional tissue oxygen saturation: comparability and reproducibility of different devices. J Biomed Opt 2011;16:057004. doi:10.1117/1.3575647.

[186] Schneider A, Minnich B, Hofstätter E, Weisser C, Hattinger-Jürgenssen E, Wald M. Comparison of four near-infrared spectroscopy devices shows that they are only suitable for monitoring cerebral oxygenation trends in preterm infants. Acta Paediatr 2014;103:934–8. doi:10.1111/apa.12698.

[187] Dix LML, van Bel F, Baerts W, Lemmers PMA. Comparing near-infrared spectroscopy devices and their sensors for monitoring regional cerebral oxygen saturation in the neonate. Pediatr Res 2013;74:557–63. doi:10.1038/pr.2013.133.

[188] da Costa CS, Greisen G, Austin T. Is near-infrared spectroscopy clinically useful in the preterm infant? Arch Dis Child - Fetal Neonatal Ed 2015;100:F558–61. doi:10.1136/archdischild-2014-307919.

[189] Pellicer A, Greisen G, Benders M, Claris O, Dempsey E, Fumagalli M, et al. The SafeBoosC phase II randomised clinical trial: A treatment guideline for targeted near-infrared-derived cerebral tissue oxygenation versus standard treatment in extremely preterm infants. Neonatology 2013;104:171–8. doi:10.1159/000351346.

[190] Hyttel-Sorensen S, Pellicer A, Alderliesten T, Austin T, Van Bel F, Benders M, et al. Cerebral near infrared spectroscopy oximetry in extremely preterm infants: Phase II randomised clinical trial. BMJ 2015;350. doi:10.1136/bmj.g7635.

[191] Hansen ML, Pellicer A, Gluud C, Dempsey E, Mintzer J, Hyttel-Sørensen S, et al. Cerebral near-infrared spectroscopy monitoring versus treatment as usual for extremely preterm infants: A protocol for the SafeBoosC randomised clinical phase III trial. Trials 2019;20. doi:10.1186/s13063-019-3955-6.

[192] El-Khuffash A, McNamara PJ. Hemodynamic Assessment and Monitoring of Premature Infants. Clin Perinatol 2017;44:377–93. doi:10.1016/j.clp.2017.02.001.

[193] Paviotti G, Todero S, Demarini S. Cardiac output decreases and systemic vascular resistance

increases in newborns placed in the left-lateral position. J Perinatol 2017;37:563–5. doi:10.1038/jp.2016.251.

[194] Ma M, Noori S, Maarek JM, Holschneider DP, Rubinstein EH, Seri I. Prone positioning decreases cardiac output and increases systemic vascular resistance in neonates. J Perinatol 2015;35:424–7. doi:10.1038/jp.2014.230.

[195] Lien R, Hsu KH, Chu JJ, Chang YS. Hemodynamic alterations recorded by electrical cardiometry during ligation of ductus arteriosus in preterm infants. Eur J Pediatr 2015;174:543–50. doi:10.1007/s00431-014-2437-9.

[196] Hsu KH, Wu TW, Wang YC, Lim WH, Lee CC, Lien R. Hemodynamic reference for neonates of different age and weight: A pilot study with electrical cardiometry. J Perinatol 2016;36:481–5. doi:10.1038/jp.2016.2.

[197] Rodriguez Sanchez de la Blanca A, Sanchez Luna M, Gonzalez Pacheco N, Arriaga Redondo M, Navarro Patiño N. Electrical velocimetry for non-invasive monitoring of the closure of the ductus arteriosus in preterm infants. Eur J Pediatr 2018;177:299–235. doi:10.1007/s00431-017-3063-0.

[198] Elsayed YN, Amer R, Seshia MM. The impact of integrated evaluation of hemodynamics using targeted neonatal echocardiography with indices of tissue oxygenation: a new approach. J Perinatol 2017;37:527–35. doi:10.1038/jp.2016.257.

[199] Elsayed YN, Louis D, Ali YH, Amer R, Seshia MM, McNamara PJ. Integrated evaluation of hemodynamics: a novel approach for the assessment and management of preterm infants with compromised systemic circulation. J Perinatol 2018;38:1337–43. doi:10.1038/s41372-018-0188-6.

[200] Pinsky MR, Payen D. Functional hemodynamic monitoring. Crit Care 2005;9:566–72.

[201] Whitehead H V., Vesoulis ZA, Maheshwari A, Rao R, Mathur AM. Anemia of prematurity

and cerebral near-infrared spectroscopy: should transfusion thresholds in preterm infants be revised? J Perinatol 2018;38:1022–9. doi:10.1038/s41372-018-0120-0.

[202] Gagnon MH, Wintermark P. Effect of persistent pulmonary hypertension on brain oxygenation in asphyxiated term newborns treated with hypothermia. J Matern Neonatal Med 2016;29:2049–55. doi:10.3109/14767058.2015.1077221.

[203] Miller SL, Huppi PS, Mallard C. The consequences of fetal growth restriction on brain structure and neurodevelopmental outcome. J Physiol 2016;594:807–23. doi:10.1113/JP271402.

[204] Jain A, Shah PS. Diagnosis, evaluation, and management of patent ductus arteriosus in preterm neonates. JAMA Pediatr 2015;169:863–72. doi:10.1001/jamapediatrics.2015.0987.

[205] de Boode WP, Kluckow M, McNamara PJ, Gupta S. Role of neonatologist-performed echocardiography in the assessment and management of patent ductus arteriosus physiology in the newborn. Semin Fetal Neonatal Med 2018;23:292–7. doi:10.1016/j.siny.2018.03.007.

[206] Smielewski P, Czosnyka M, Steiner L, Belestri M, Piechnik S, Pickard JD. ICM+: Software for on-line analysis of bedside monitoring data after severe head trauma. Acta Neurochir. Suppl., Springer Wien; 2005, p. 43–9. doi:10.1007/3-211-32318-X_10.

[207] da Costa CS, Czosnyka M, Smielewski P, Austin T. Optimal Mean Arterial Blood Pressure in Extremely Preterm Infants within the First 24 Hours of Life. J Pediatr 2018;203:242–8. doi:10.1016/j.jpeds.2018.07.096.

[208] Wu T-WW, Azhibekov T, Seri I. Transitional hemodynamics in preterm neonates: Clinical relevance. Pediatr Neonatol 2016;57:7–18. doi:10.1016/j.pedneo.2015.07.002.

[209] Noori S, Stavroudis TA, Seri I. Systemic and Cerebral Hemodynamics During the Transitional Period After Premature Birth. Clin Perinatol 2009;36:723–36. doi:10.1016/j.clp.2009.07.015.

[210] O'Leary H, Gregas MC, Limperopoulos C, Zaretskaya I, Bassan H, Soul JS, et al. Elevated

Cerebral Pressure Passivity Is Associated With Prematurity-Related Intracranial Hemorrhage. Pediatrics 2009;124:302–9. doi:10.1542/peds.2008-2004.

[211] Soul JS, Hammer PE, Tsuji M, Saul JP, Bassan H, Limperopoulos C, et al. Fluctuating pressure-passivity is common in the cerebral circulation of sick premature infants. Pediatr Res 2007;61:467–73. doi:10.1203/pdr.0b013e31803237f6.

[212] Da Costa CS, Czosnyka M, Smielewski P, Mitra S, Stevenson GN, Austin T. Monitoring of cerebrovascular reactivity for determination of optimal blood pressure in preterm infants. J Pediatr 2015;167:86–91. doi:10.1016/j.jpeds.2015.03.041.

[213] Dasgupta SJ, Gill AB. Hypotension in the very low birthweight infant: The old, the new, and the uncertain. Arch Dis Child Fetal Neonatal Ed 2003;88. doi:10.1136/fn.88.6.f450.

[214] Nuntnarumit P, Yang W, Bada-Ellzey HS. Blood pressure measurements in the newborn. Clin Perinatol 1999;26:981–96. doi:10.1016/s0095-5108(18)30030-7.

[215] Cappelleri A, Bussmann N, Harvey S, Levy PT, Franklin O, El-Khuffash A. Myocardial function in late preterm infants during the transitional period: Comprehensive appraisal with deformation mechanics and non-invasive cardiac output monitoring. Cardiol Young 2020;30:249–55. doi:10.1017/S1047951119003020.

[216] Saleemi MSH, El-Khuffash A, Franklin O, Corcoran JD. Serial changes in myocardial function in preterm infants over a four week period: the effect of gestational age at birth. Early Hum Dev 2014;90:349–52. doi:10.1016/j.earlhumdev.2014.04.012.

[217] Lee A, Nestaas E, Liestøl K, Brunvand L, Lindemann R, Fugelseth D. Tissue Doppler imaging in very preterm infants during the first 24 h of life: An observational study. Arch Dis Child Fetal Neonatal Ed 2014;99. doi:10.1136/archdischild-2013-304197.

[218] Negrine RJS, Chikermane A, Wright JGC, Ewer AK. Assessment of myocardial function in neonates using tissue Doppler imaging. Arch Dis Child Fetal Neonatal Ed 2012;97.

doi:10.1136/adc.2009.175109.

[219] Breatnach CR, EL-Khuffash A, James A, McCallion N, Franklin O. Serial measures of cardiac performance using tissue Doppler imaging velocity in preterm infants < 29 weeks gestations. Early Hum Dev 2017;108:33–9. doi:10.1016/j.earlhumdev.2017.03.012.

[220] James AT, Corcoran JD, Jain A, McNamara PJ, Mertens L, Franklin O, et al. Assessment of myocardial performance in preterm infants less than 29 weeks gestation during the transitional period. Early Hum Dev 2014;90:829–35. doi:10.1016/j.earlhumdev.2014.09.004.

[221] El-Khuffash AF, Jain A, Dragulescu A, Mcnamara PJ, Mertens L. Acute changes in myocardial systolic function in preterm infants undergoing patent ductus arteriosus ligation: A tissue doppler and myocardial deformation study. J Am Soc Echocardiogr 2012;25:1058–67. doi:10.1016/j.echo.2012.07.016.

[222] Evans N, Iyer P. Assessment of ductus arteriosus shunt in preterm infants supported by mechanical ventilation: Effect of interatrial shunting☆☆☆★. J Pediatr 1994;125:778–85. doi:10.1016/s0022-3476(94)70078-8.

[223] James AT, Corcoran JD, Breatnach CR, Franklin O, Mertens L, El-Khuffash A. Longitudinal Assessment of Left and Right Myocardial Function in Preterm Infants Using Strain and Strain Rate Imaging. Neonatology 2015;109:69–75. doi:10.1159/000440940.

[224] Alagarsamy S, Chhabra M, Gudavalli M, Nadroo AM, Sutija VG, Yugrakh D. Comparison of clinical criteria with echocardiographic findings in diagnosing PDA in preterm infants. J Perinat Med 2005;33:161–4. doi:10.1515/JPM.2005.030.

[225] Shimada S, Kasai T, Hoshi A, Murata A, Chida S. Cardiocirculatory effects of patent ductus arteriosus in extremely low-birth-weight infants with respiratory distress syndrome. Pediatr Int 2003;45:255–62. doi:10.1046/j.1442-200X.2003.01713.x.

[226] Mahony L. Regulation of intracellular calcium concentration in the developing heart.

Cardiovasc Res 1996;31:E61-7.

[227] Fyfe KL, Yiallourou SR, Wong FY, Horne RSC. The development of cardiovascular and cerebral vascular control in preterm infants. Sleep Med Rev 2014;18:299–310. doi:10.1016/j.smrv.2013.06.002.

[228] Mulkey SB, Plessis A dú. The Critical Role of the Central Autonomic Nervous System in Fetal-Neonatal Transition. Semin Pediatr Neurol 2018;28:29–37. doi:10.1016/j.spen.2018.05.004.

[229] Hillman NH, Kallapur SG, Jobe AH. Physiology of transition from intrauterine to extrauterine life. Clin Perinatol 2012;39:769–83. doi:10.1016/j.clp.2012.09.009.

[230] Levene MI, Fawer CL, Lamont RF. Risk factors in the development of intraventricular haemorrhage in the preterm neonate. Arch Dis Child 1982;57:410–7. doi:10.1136/adc.57.6.410.

[231] Shimada S, Kasai T, Konishi M, Fujiwara T. Effects of patent ductus arteriosus on left ventricular output and organ blood flows in preterm infants with respiratory distress syndrome treated with surfactant. J Pediatr 1994;125:270–7. doi:10.1016/S0022-3476(94)70210-1.

[232] Barlow AJ, Ward C, Webber S, Sinclair BG, Potts JE, Sandor GGS. Myocardial Contractility in Premature Neonates with and Without Patent Ductus Arteriosus. Pediatr Cardiol 2004;25:102–7. doi:10.1007/s00246-003-0452-0.

[233] Broadhouse KM, Finnemore AE, Price AN, Durighel G, Cox DJ, Edwards AD, et al. Cardiovascular magnetic resonance of cardiac function and myocardial mass in preterm infants: A preliminary study of the impact of patent ductus arteriosus. J Cardiovasc Magn Reson 2014;16. doi:10.1186/s12968-014-0054-4.

[234] El-Khuffash A, McNamara PJ, Noori S. Diagnosis, Evaluation, and Monitoring of Patent Ductus Arteriosus in the Very Preterm Infant. In: Elsevier Saunders, editor. Neonatol. Quest.

Controv. hemodynamics Cardiol. 3rd ed., Philadelphia, USA: 2019.

[235] Alonzo CJ, Nagraj VP, Zschaebitz J V., Lake DE, Moorman JR, Spaeder MC. Heart rate ranges in premature neonates using high resolution physiologic data. J Perinatol 2018;38:1242–5. doi:10.1038/s41372-018-0156-1.

[236] Mehandru PL, Assel BG, Nuamah IF, Fanaroff AA, Kalhan SC. Catecholamine response at birth in preterm newborns. Neonatology 1993;64:82–8. doi:10.1159/000243975.

[237] Dalmaz Y, Peyrin L, Dutruge J, Sann L. Neonatal pattern of adrenergic metabolites in urine of small for gestational age and preterm infants. J Neural Transm 1980;49:151–65. doi:10.1007/BF01245221.

[238] Scott SM, Watterberg KL. Effect of gestational age, postnatal age, and illness on plasma cortisol concentrations in premature infants. Pediatr Res 1995;37:112–6. doi:10.1203/00006450-199501000-00021.

[239] Rokicki W, Forest MG, Loras B, Bonnet H, Bertrand J. Free cortisol of human plasma in the first three months of life. Biol Neonate 1990;57:21–9. doi:10.1159/000243148.

[240] Ng SM, Ogundiya A, DIdi M, Turner MA. Adrenal function of extremely premature infants in the first 5 days after birth. J Pediatr Endocrinol Metab 2019;32:363–7. doi:10.1515/jpem-2018-0417.

[241] Eriksen BH, Nestaas E, Hole T, Liestøl K, Støylen A, Fugelseth D. Myocardial function in term and preterm infants. Influence of heart size, gestational age and postnatal maturation. Early Hum Dev 2014;90:359–64. doi:10.1016/j.earlhumdev.2014.04.010.

[242] El-Dib M, Aly S, Govindan R, Mohamed M, Du Plessis A, Aly H. Brain Maturity and Variation of Oxygen Extraction in Premature Infants. Am J Perinatol 2016;33:814–20. doi:10.1055/s-0036-1572542.

[243] Mohamed MA, Frasketi MJ, Aly S, El-Dib M, Hoffman HJ, Aly H. Changes in cerebral tissue

oxygenation and fractional oxygen extraction with gestational age and postnatal maturation in preterm infants. J Perinatol 2020. doi:10.1038/s41372-020-00794-w.

[244] Roze JC, Tohier C, Maingueneau C, Lefevre M, Mouzard A. Response to dobutamine and dopamine in the hypotensive very preterm infant. Arch Dis Child 1993;69:59–63. doi:10.1136/adc.69.1_spec_no.59.

[245] Zhang J, Penny DJ, Kim NS, Yu VYH, Smolich JJ. Mechanisms of blood pressure increase induced by dopamine in hypotensive preterm neonates. Arch Dis Child Fetal Neonatal Ed 1999;81. doi:10.1136/fn.81.2.F99.

[246] Lundstrøm K, Pryds O, Greisen G. The haemodynamic effects of dopamine and volume expansion in sick preterm infants. Early Hum Dev 2000;57:157–63. doi:10.1016/S0378-3782(00)00048-7.

[247] Janaillac M, Beausoleil T, Karam O, Raboisson M-J, Barrington KJ, Dehaes M, et al. Relationships Between Near-Infrared Spectroscopy, Preductal Perfusion Index and Cardiac Outputs in Extremely Preterm Infants in the First 72 Hours of Life. Paediatr Child Health 2018;23:e23–4. doi:10.1093/pch/pxy054.059.

[248] van der Laan ME, Roofthooft MTR, Fries MWA, Schat TE, Bos AF, Berger RMF, et al. Multisite Tissue Oxygenation Monitoring Indicates Organ-Specific Flow Distribution and Oxygen Delivery Related to Low Cardiac Output in Preterm Infants With Clinical Sepsis. Pediatr Crit Care Med 2016;17:764–71. doi:10.1097/PCC.0000000000000833.

[249] Victor S, Appleton RE, Beirne M, Marson AG, Weindling AM. The relationship between cardiac output, cerebral electrical activity, cerebral fractional oxygen extraction and peripheral blood flow in premature newborn infants. Pediatr Res 2006;60:456–60. doi:10.1203/01.pdr.0000238379.67720.19.

[250] Kissack CM, Garr R, Wardle SP, Weindling AM. Postnatal changes in cerebral oxygen

extraction in the preterm infant are associated with intraventricular hemorrhage and hemorrhagic parenchymal infarction but not periventricular leukomalacia. Pediatr Res 2004;56:111–6. doi:10.1203/01.PDR.0000128984.03461.42.

[251] Wardle SP, Yoxall CW, Weindling AM. Determinants of cerebral fractional oxygen extraction using near infrared spectroscopy in preterm neonates. J Cereb Blood Flow Metab 2000;20:272–9. doi:10.1097/00004647-200002000-00008.

[252] Roberts D, Brown J, Medley N, Dalziel SR. Antenatal corticosteroids for accelerating fetal lung maturation for women at risk of preterm birth. Cochrane Database Syst Rev 2017;2017. doi:10.1002/14651858.CD004454.pub3.

[253] Schwab M, Roedel M, Akhtar Anwar M, Müller T, Schubert H, Buchwalder LF, et al. Effects of betamethasone administration to the fetal sheep in late gestation on fetal cerebral blood flow. J Physiol 2000;528:619–32. doi:10.1111/j.1469-7793.2000.00619.x.

[254] McCallum J, Smith N, Schwab M, Coksaygan T, Reinhardt B, Nathanielsz P, et al. Effects of antenatal glucocorticoids on cerebral substrate metabolism in the preterm ovine fetus. Am J Obstet Gynecol 2008;198:105.e1-105.e9. doi:10.1016/j.ajog.2007.05.007.

[255] Jellyman JK, Fletcher AJW, Fowden AL, Giussani DA. Glucocorticoid Maturation of Fetal Cardiovascular Function. Trends Mol Med 2020;26:170–84. doi:10.1016/j.molmed.2019.09.005.

[256] Yoshimura S, Masuzaki H, Gotoh H, Ishimaru T. Fetal redistribution of blood flow and amniotic fluid volume in growth-retarded fetuses. Early Hum Dev 1997;47:297–304. doi:10.1016/S0378-3782(96)01798-7.

[257] Smal JC, Uiterwaal CSPM, Bruinse HW, Steendijk P, Van Bel F. Inverse relationship between birth weight and blood pressure in growth-retarded but not in appropriate for gestational age infants during the first week of life. Neonatology 2009;96:86–92. doi:10.1159/000203338.

[258] Cheung YF, Wong KY, Barbara CC, Lam BCC, Tsoi NS. Relation of arterial stiffness with gestational age and birth weight. Arch Dis Child 2004;89:217–21. doi:10.1136/adc.2003.025999.

[259] Barker DJP, Osmond C, Golding J, Kuh D, Wadsworth MEJ. Growth in utero, blood pressure in childhood and adult life, and mortality from cardiovascular disease. Br Med J 1989;298:564–7. doi:10.1136/bmj.298.6673.564.

[260] Lurbe E, Torro MI, Carvajal E, Alvarez V, Redón J. Birth weight impacts on wave reflections in children and adolescents. Hypertension, vol. 41, Hypertension; 2003, p. 646–50. doi:10.1161/01.HYP.0000048341.52293.7C.

[261] te Velde SJ, Ferreira I, Twisk JWR, Stehouwer CDA, van Mechelen W, Kemper HCG. Birthweight and arterial stiffness and blood pressure in adulthood - Results from the Amsterdam growth and health longitudinal study. Int J Epidemiol 2004;33:154–61. doi:10.1093/ije/dyh011.

[262] Crispi F, Miranda J, Gratacós E. Long-term cardiovascular consequences of fetal growth restriction: biology, clinical implications, and opportunities for prevention of adult disease. Am J Obstet Gynecol 2018;218:S869–79. doi:10.1016/j.ajog.2017.12.012.

[263] Law CM, Shiell AW. Is blood pressure inversely related to birth weight? The strength of evidence from a systematic review of the literature. J Hypertens 1996;14:935–41.

[264] Tsyvian P, Malkin K, Artemieva O, Blyakhman F, Wladimiroff JW. Cardiac ventricular performance in the for-gestational age and small-for-gestational age fetus: Relation to regional cardiac non-uniformity and peripheral resistace. Ultrasound Obstet Gynecol 2002;20:35–41. doi:10.1046/j.1469-0705.2002.00734.x.

[265] Alsolai AA, Bligh LN, Greer RM, Kumar S. Correlation between fetoplacental Doppler indices and measurements of cardiac function in term fetuses. Ultrasound Obs Gynecol 2019;53:358–

66. doi:10.1002/uog.19056.

[266]   Hutter D, Kingdom J, Jaeggi E. Causes and Mechanisms of Intrauterine Hypoxia and Its Impact on the Fetal Cardiovascular System: A Review. Int J Pediatr 2010;2010:1–9. doi:10.1155/2010/401323.

[267]   Polglase GR, Allison BJ, Coia E, Li A, Jenkin G, Malhotra A, et al. Altered cardiovascular function at birth in growth-restricted preterm lambs. Pediatr Res 2016;80:538–46. doi:10.1038/pr.2016.104.

[268]   Fouzas S, Karatza AA, Davlouros PA, Chrysis D, Alexopoulos D, Mantagos S, et al. Neonatal cardiac dysfunction in intrauterine growth restriction. Pediatr Res 2014;75:651–7. doi:10.1038/pr.2014.22.

[269]   Sehgal A, Doctor T, Menahem S. Cardiac function and arterial indices in infants born small for gestational age: Analysis by speckle tracking. Acta Paediatr Int J Paediatr 2014;103. doi:10.1111/apa.12465.

[270]   Cohen E, Baerts W, Alderliesten T, Derks J, Lemmers P, Bel F Van, et al. Growth restriction and gender influence cerebral oxygenation in preterm neonates. Arch Dis Child - Fetal Neonatal Ed 2016;101:F156–61. doi:10.1136/archdischild-2015-308843.

[271]   Arduini D, Rizzo G, Romanini C, Mancuso S. Fetal haemodynamic response to acute maternal hyperoxygenation as predictor of fetal distress in intrauterine growth retardation. Br Med J 1989;298:1561–2. doi:10.1136/bmj.298.6687.1561.

[272]   Castillo-Melendez M, Yawno T, Allison BJ, Jenkin G, Wallace EM, Miller SL. Cerebrovascular adaptations to chronic hypoxia in the growth restricted lamb. Int J Dev Neurosci 2015;45:55–65. doi:10.1016/j.ijdevneu.2015.01.004.

[273]   Pearce WJ, Butler SM, Abrassart JM, Williams JM. Fetal cerebral oxygenation: The homeostatic role of vascular adaptations to hypoxic stress. Adv. Exp. Med. Biol., vol. 701,

Springer New York LLC; 2011, p. 225–32. doi:10.1007/978-1-4419-7756-4_30.

[274] Martyn CN, Barker DJP, Osmond C. Mothers' pelvic size, fetal growth, and death from stroke and coronary heart disease in men in the UK. Lancet 1996;348:1264–8. doi:10.1016/S0140-6736(96)04257-2.

[275] Sekar KC. Iatrogenic complications in the neonatal intensive care unit. J Perinatol 2010;30:S51–6. doi:10.1038/jp.2010.102.

[276] Stoll BJ, Hansen NI, Bell EF, Walsh MC, Carlo WA, Shankaran S, et al. Trends in Care Practices, Morbidity, and Mortality of Extremely Preterm Neonates, 1993-2012. JAMA 2015;314:1039–51. doi:10.1001/jama.2015.10244.

[277] Kugelman A, Borenstein-Levin L, Jubran H, Dinur G, Ben-David S, Segal E, et al. Less is More: Modern Neonatology. Rambam Maimonides Med J 2018;9:e0023. doi:10.5041/rmmj.10344.

[278] Norozi K, Beck C, Osthaus WA, Wille I, Wessel A, Bertram H. Electrical velocimetry for measuring cardiac output in children with congenital heart disease. Br J Anaesth 2008;100:88–94. doi:10.1093/bja/aem320.

[279] Noori S, Drabu B, Soleymani S, Seri I. Continuous non-invasive cardiac output measurements in the neonate by electrical velocimetry: A comparison with echocardiography. Arch Dis Child Fetal Neonatal Ed 2012;97. doi:10.1136/fetalneonatal-2011-301090.

[280] Torigoe T, Sato S, Nagayama Y, Sato T, Yamazaki H. Influence of patent ductus arteriosus and ventilators on electrical velocimetry for measuring cardiac output in very-low/low birth weight infants. J Perinatol 2015;35:485–9. doi:10.1038/jp.2014.245.

[281] Song R, Rich W, Kim JH, Finer NN, Katheria AC. The use of electrical cardiometry for continuous cardiac output monitoring in preterm neonates: a validation study. Am J Perinatol 2014;31:1105–10. doi:10.1055/s-0034-1371707.

[282] Noori S, Drabu B, Soleymani S, Seri I. Continuous non-invasive cardiac output measurements in the neonate by electrical velocimetry: a comparison with echocardiography. Arch Dis Child - Fetal Neonatal Ed 2012;97:F340–3. doi:10.1136/fetalneonatal-2011-301090.

[283] Blohm ME, Hartwich J, Obrecht D, Kersten JF, Singer D. Effect of patent ductus arteriosus and patent foramen ovale on left ventricular stroke volume measurement by electrical velocimetry in comparison to transthoracic echocardiography in neonates. J Clin Monit Comput 2017;31:589–98. doi:10.1007/s10877-016-9878-9.

[284] Di Fiore JM, Poets CF, Gauda E, Martin RJ, Macfarlane P. Cardiorespiratory events in preterm infants: Etiology and monitoring technologies. J Perinatol 2016;36:165–71. doi:10.1038/jp.2015.164.

[285] Di Fiore JM, MacFarlane PM, Martin RJ. Intermittent Hypoxemia in Preterm Infants. Clin Perinatol 2019;46:553–65. doi:10.1016/j.clp.2019.05.006.

[286] Schmid MB, Hopfner RJ, Lenhof S, Hummler HD, Fuchs H, Poets CF, et al. Intermittent hypoxemia/bradycardia and the developing brain: How Much is Too Much? Neonatology 2015;107:147–9. doi:10.1016/j.earlhumdev.2018.08.008.

[287] Garvey A, Kooi E, Smith A, Dempsey E. Interpretation of Cerebral Oxygenation Changes in the Preterm Infant. Children 2018;5:94. doi:10.3390/children5070094.

[288] Walter LM, Ahmed B, Odoi A, Cooney H, Horne RSC, Wong FY. Bradycardias are associated with more severe effects on cerebral oxygenation in very preterm infants than in late preterm infants. Early Hum Dev 2018;127:33–41. doi:10.1016/j.earlhumdev.2018.08.008.

[289] Schmid MB, Hopfner RJ, Lenhof S, Hummler HD, Fuchs H. Cerebral Oxygenation during Intermittent Hypoxemia and Bradycardia in Preterm Infants. Neonatology 2015;107:137–46. doi:10.1159/000368294.

[290] Juliano C, Sosunov S, Niatsetskaya Z, Isler JA, Utkina-Sosunova I, Jang I, et al. Mild

intermittent hypoxemia in neonatal mice causes permanent neurofunctional deficit and white matter hypomyelination. Exp Neurol 2015;264:33–42. doi:10.1016/j.expneurol.2014.11.010.

[291] Pillekamp F, Hermann C, Keller T, Von Gontard A, Kribs A, Roth B. Factors influencing apnea and bradycardia of prematurity - Implications for neurodevelopment. Neonatology 2007;91:155–61. doi:10.1159/000097446.

[292] Greene MM, Patra K, Khan S, Karst JS, Nelson MN, Silvestri JM. Cardiorespiratory events in extremely low birth weight infants: Neurodevelopmental outcome at 1 and 2 years. J Perinatol 2014;34:562–5. doi:10.1038/jp.2014.44.

[293] Poets CF, Roberts RS, Schmidt B, Whyte RK, Asztalos E V., Bader D, et al. Association between intermittent hypoxemia or bradycardia and late death or disability in extremely preterm infants. JAMA - J Am Med Assoc 2015;314:595–603. doi:10.1001/jama.2015.8841.

[294] Vesoulis ZA, Bank RL, Lake D, Wallman-Stokes A, Sahni R, Moorman JR, et al. Early hypoxemia burden is strongly associated with severe intracranial hemorrhage in preterm infants. J Perinatol 2019;39:48–53. doi:10.1038/s41372-018-0236-2.

[295] de Waal K, Phad N, Collins N, Boyle A. Myocardial function during bradycardia events in preterm infants. Early Hum Dev 2016;98:17–21. doi:10.1016/j.earlhumdev.2016.05.002.

[296] Finer NN, Higgins R, Kattwinkel J, Martin RJ. Summary proceedings from the apnea-of-prematurity group. Pediatrics, vol. 117, 2006. doi:10.1542/peds.2005-0620H.

[297] Corvaglia L, Martini S, Aceti A, Capretti MG, Galletti S, Faldella G. Cardiorespiratory events with bolus versus continuous enteral feeding in healthy preterm infants. J Pediatr 2014;165:1255–7. doi:10.1016/j.jpeds.2014.07.043.

[298] Henderson-Smart DJ, Butcher-Puech MC, Edwards DA. Incidence and mechanism of bradycardia during apnoea in preterm infants. Arch Dis Child 1986;61:227–32. doi:10.1136/adc.61.3.227.

[299] Eichenwald EC. Apnea of Prematurity. Pediatrics 2016;137. doi:10.1542/peds.2015-3757.

[300] Poets CF, Stebbens VA, Samuels MP, Southall DP. The relationship between bradycardia, apnea, and hypoxemia in preterm infants. Pediatr Res 1993;34:144–7. doi:10.1203/00006450-199308000-00007.

[301] Zeger SL, Liang K-Y. Longitudinal Data Analysis for Discrete and Continuous Outcomes. Biometrics 1986;42:121. doi:10.2307/2531248.

[302] Martini S, Frabboni G, Rucci P, Czosnyka M, Smielewski P, Galletti S, et al. Cardiovascular and cerebrovascular responses to cardio-respiratory events in preterm infants during the transitional period. J Physiol 2020;598:4107–19. doi:10.1113/JP279730.

[303] Perlman JM, Volpe JJ. Episodes of apnea and bradycardia in the preterm newborn: Impact on cerebral circulation. Pediatrics 1985;76:333–8.

[304] Pichler G, Urlesberger B, Müller W. Impact of bradycardia on cerebral oxygenation and cerebral blood volume during apnoea in preterm infants. Physiol Meas 2003;24:671–80. doi:10.1088/0967-3334/24/3/304.

[305] Miyamoto Y, Higuchi J, Abe Y, Hiura T, Nakazono Y, Mikami T. Dynamics of cardiac output and systolic time intervals in supine and upright exercise. J Appl Physiol Respir Environ Exerc Physiol 1983;55:1674–81. doi:10.1152/jappl.1983.55.6.1674.

[306] Lemmers PMAA, Toet MC, van Bel F. Impact of patent ductus arteriosus and subsequent therapy with indomethacin on cerebral oxygenation in preterm infants. Pediatrics 2008;121:142–7. doi:10.1542/peds.2007-0925.

[307] Chock VY, Rose LA, Mante J V., Punn R. Near-infrared spectroscopy for detection of a significant patent ductus arteriosus. Pediatr Res 2016;80:675–80. doi:10.1038/pr.2016.148.

[308] Dix L, Molenschot M, Breur J, de Vries W, Vijlbrief D, Groenendaal F, et al. Cerebral oxygenation and echocardiographic parameters in preterm neonates with a patent ductus

arteriosus: an observational study. Arch Dis Child Fetal Neonatal Ed 2016;101:F520–6. doi:10.1136/archdischild-2015-309192.

[309] Poon WB, Tagamolila V. Cerebral perfusion and assessing hemodynamic significance for patent ductus arteriosus using near infrared red spectroscopy in very low birth weight infants. J Matern Neonatal Med 2019:1–6. doi:10.1080/14767058.2019.1644313.

[310] Kluckow M, Lemmers P. Hemodynamic assessment of the patent ductus arteriosus: Beyond ultrasound. Semin Fetal Neonatal Med 2018;23:239–44. doi:10.1016/j.siny.2018.04.002.

[311] Shortland DB, Gibson NA, Levene MI, Archer LNJ, Evans DH, Shaw DE. Patent ductus arteriosus and cerebral circulation in preterm infants. Dev Med Child Neurol 1990;32:386–93. doi:10.1111/j.1469-8749.1990.tb16957.x.

[312] Darnall RA, Chen X, Nemani K V., Sirieix CM, Gimi B, Knoblach S, et al. Early postnatal exposure to intermittent hypoxia in rodents is proinflammatory, impairs white matter integrity, and alters brain metabolism. Pediatr Res 2017;82:164–72. doi:10.1038/pr.2017.102.

[313] Baschat AA, Harman CR. Antenatal assessment of the growth restricted fetus. Curr Opin Obstet Gynecol 2001;13:161–8. doi:10.1097/00001703-200104000-00011.

[314] Leipälä JA, Boldt T, Turpeinen U, Vuolteenaho O, Fellman V. Cardiac hypertrophy and altered hemodynamic adaptation in growth-restricted preterm infants. Pediatr Res 2003;53:989–93. doi:10.1203/01.PDR.0000061564.86797.78.

[315] Hirose A, Khoo NS, Aziz K, Al-Rajaa N, Van Boom J Den, Savard W, et al. Evolution of left ventricular function in the preterm infant. J Am Soc Echocardiogr 2015;28:302–8. doi:10.1016/j.echo.2014.10.017.

[316] Lara-Cantón I, Solaz A, Parra-Llorca A, García-Robles A, Vento M. Optimal Inspired Fraction of Oxygen in the Delivery Room for Preterm Infants. Children 2019;6:29. doi:10.3390/children6020029.